Reinforcing Concrete Structures with Fibre Reinforced Polymers

Design Manual No. 3
September 2007

ISIS CANADA RESEARCH NETWORK
The Canadian Network of Centres of Excellence on Intelligent Sensing for Innovative Structures
Le réseau canadien de Centres d'excellence sur les innovations en structures avec systèmes de détection intégrés

Design Manual No. 3
September 2007

ISIS CANADA RESEARCH NETWORK
The Canadian Network of Centres of Excellence on Intelligent Sensing for Innovative Structures
Le réseau canadien de Centres d'excellence sur les innovations en structures avec systèmes de détection intégrés

Acknowledgements

Technical Committee:

Author: **John Newhook**   **Dalhousie University**

Co-Author: **Dagmar Svecova**   **University of Manitoba**

TABLE OF CONTENTS

List of Figures

1.1 Preface

In Canada, more than 40 percent of the bridges currently in use were built more than 30 years ago. A significant number of these structures are in urgent need of strengthening, rehabilitation or replacement. Many bridges, as well as other types of structures, are deficient due to the corrosion of steel reinforcement and consequent break down of the concrete - a result of Canada's adverse climate and extensive use of de-icing salts. In addition, many structures are functionally obsolete because they no longer meet current standards. The expensive cycle of maintaining, repairing and rebuilding infrastructure has led owners to seek more efficient and affordable solutions in the use of fibre-reinforced polymers (FRPs). These lightweight, high-strength composite materials are resistant to corrosion, durable and easy to install. Glass and carbon FRPs are already increasing infrastructure service life and reducing maintenance costs.

Infrastructure owners can no longer afford to upgrade and replace existing infrastructure using 20th century materials and methodologies. They are looking for emerging new technologies such as FRPs that will increase the service life of infrastructure and reduce maintenance costs. Fibre-reinforced polymers contain high-resistance fibres embedded in a polymer resin matrix. They are rapidly becoming the materials of choice over steel for reinforced concrete structures. Despite their relatively recent entry into civil engineering construction, FRP-reinforced concrete structures are gaining wide acceptance as effective and economical infrastructure technologies. Indeed, the most remarkable development over the past few years in the field of FRPs has been the rapidly growing acceptance worldwide of these new technologies for an enormous range of practical applications.

Within the *ISIS Canada Network of Centres of Excellence*, much research has been conducted to develop advanced technologies for creative new FRP-reinforced concrete structures. ISIS Canada's approach takes into account aspects such as strength requirements, serviceability, performance, and durability. Glass and carbon FRPs can be used where longer, unsupported spans are desirable, or where a reduced overall weight, combined with increased strength, could mean greater seismic resistance. A lightweight, FRP-reinforced structure can reduce the size and cost of columns and foundations whilst accommodating increasing demands of heavier traffic loads. The goal is to optimize the use of FRP materials so that stronger, longer-lasting structures can be realized for minimum cost.

Many of these innovative designs for new structures incorporate remote monitoring systems using the latest generation of fibre-optic sensors. In the past, structures were monitored by transporting measuring devices to the site each time a set of readings was required. By using fibre-optic sensors for remote structural health monitoring, an extensive amount of data can be collected and processed without ever visiting the site. The ability to monitor and assess the behaviour of concrete structures reinforced with carbon and/or glass FRPs will hasten the material's widespread acceptance. Accurate monitoring is key to securing industry's confidence in fibre-reinforced polymers.

The content of this design manual focuses on reinforcing new concrete structures with fibre-reinforced polymers. It is one in a series of manuals that cover the use of fibre-optic sensors for monitoring structures, guidelines for structural health monitoring, and strengthening concrete structures with externally-bonded fibre-reinforced polymers. This design manual will be expanded and updated as other design procedures are developed and validated.

1.2   Preface to Version 2

Since the production of the original version of this document in 2001, research has continued into the use of FRP as reinforcement for concrete. As well, the number and variety of field applications has increased. Equally significant is the fact that CSA S806-02 *Design and Construction of Building Components with Fibre Reinforced Polymers* has been formally accepted as a code and Section 16 of CSA S6-06 Canadian Highway Bridge Design Code (referred to throughout the manual as CHBDC) has been revised. Finally, the members of ISIS Canada have received many useful comments and suggestions for improvement from the users of the original document.

Version 2 attempts to capture the state-of-the-art and the state-of-the-practice in 2006 to provide an up-to-date guide for engineers and designers seeking to use FRP reinforcement. While consistency with existing codes has been and is an important consideration, the version may differ from the code documents on certain clauses where recent research and studies indicate that better criteria or equations exist. Engineers should use this document in conjunction with relevant codes, standards and best practices in reinforced concrete and bridge design.

2.1 Overview

Intelligent Sensing for Innovative Structures (ISIS Canada) was launched in 1995 under the Networks of Centres of Excellence (NCE) program. As part of this now ongoing federal program, ISIS Canada adheres to the overall objectives of supporting excellent research, training highly-qualified personnel, managing complex interdisciplinary and multi-sectored programs, and accelerating the transfer of technology from the laboratory to the marketplace. ISIS Canada is a collaborative research and development process linking numerous universities with public and private sector organizations that provide matching contributions to the funding supplied by the NCE. By weaving the efforts of several universities into one cohesive program, this research gains all the advantages of sharing world-class scientists and facilities. A close relationship with industry ensures that all research is commercially-viable.

ISIS Canada researchers work closely with public and private sector organizations that have a vested interest in innovative solutions for constructing, maintaining and repairing bridges, roads, buildings, dams and other structures. This solution-oriented research is deemed critical to Canada's future because of the massive problems associated with deterioration of steel-reinforced concrete infrastructure. The Canadian Construction Association estimates that the investment required to rehabilitate global infrastructure hovers in the vicinity of $900 billion dollars.

2.2 Research Program

ISIS Canada is developing ways to use high-strength fibre-reinforced polymer (FRP) components to reinforce and strengthen concrete structures. The use of FRP is being combined with fibre-optic sensor (FOS) systems for structural health monitoring.

Demonstration projects across the country further research and foster an environment in which ISIS technologies are adopted as common practice. The projects are always carried out on, or result in, functional operating structures. While there are many different applications of ISIS Canada technologies, three general attributes remain constant:

- FRP products are up to six times stronger than steel, one fifth the weight, non-corrosive, and immune to natural and man-made electro-magnetic environments;

- Fibre-optic sensors (FOSs) are attached to the reinforcement and imbedded in structures to gather real-time information;

- Remote monitoring processes are used, whereby structural information can be interpreted using an expert system and then transmitted to a computer anywhere in the world.

Fibre-Optic Sensing

The ultimate goal is to ensure that FOSs become as user-friendly to install as conventional strain gauges, but with increased sophistication.

The research program is based on a new sensing device formed within an optical fibre called a Bragg Grating. ISIS has already installed short-gauge length Fibre Bragg Grating (FBG) sensors in new bridges to monitor slow changes over time as well as the bridge response to passing traffic.

This technology provides a new, unintrusive way of monitoring the impact of traffic and excess loads, long-term structural health, structural components rehabilitated with FRP wraps, and vibration frequency and seismic responses of structures. Notable benefits include reducing the tendency to over-design structures, monitoring actual load history, and detecting internal weak spots before deterioration becomes critical.

Remote Monitoring

Remote monitoring projects cover designing economical data acquisition and communication systems for monitoring structures remotely. This includes developing a system whereby the data can be processed intelligently in order to assess its significance. By modelling new structural systems, service life predictions can be made using the collected sensing data.

To date, several bridges and structures across Canada have been equipped with fibre-optic remote monitoring devices. A combination of commercially-available and ISIS developed components have been used in the measurement configurations. Both new and rehabilitated structures are currently being monitored. One of the major challenges is to develop a standardized intelligent processing framework for use with data records obtained from various ISIS field applications.

Smart reinforcement is another development in remote monitoring. Using pultrusion technology, FOSs can be built into FRP reinforcements. Smart reinforcements and connectors eliminate the need for meticulous installation procedures at the work site, resulting in construction savings.

New Structures

Creative approaches to new FRP-reinforced structures are also being developed. Aspects such as strength requirements, serviceability, performance, and durability are examined. The experimental program includes building and testing full-scale or scaled-down models in order to examine behaviour, and providing design guidelines for construction details for field applications.

Glass fibre-reinforced polymer (GFRP) and carbon fibre-reinforced polymer (CFRP) can be used for reinforcing cast-in-place and precast concrete. The reinforcement can take the shape of rebars, stirrups, gratings, pavement joint dowels, tendons, anchors, etc. In bridge design, this material is used where longer, unsupported spans are desirable, or where a reduced overall weight combined with increased strength could mean greater seismic resistance. A

lightweight, FRP-reinforced structure can reduce the cost of columns and foundations, and can accommodate the increasing demands of heavier traffic loads.

Research has led to field applications outfitted with the newest generation of FOS systems for remote monitoring. Accurate monitoring of internal strain is key to securing infrastructure owners' confidence in the material and design configuration.

The practical significance of monitoring a structure is that changes which could affect structural behaviour and load capacity are detected as they occur, thereby enabling important engineering decisions to be made regarding safety and maintenance considerations.

Rehabilitated Structures

The high strength and light weight of FRP and the fact that the material is now available in the form of very thin sheets makes it an attractive and economical solution for strengthening existing concrete bridges and structures. In rehabilitation projects, FRP serves to confine concrete subjected to compression, or improve flexural and/or shear strength, as an externally-bonded reinforcement.

There are numerous opportunities to apply this research because existing steel-reinforced concrete structures are in a continuous state of decay. This is due to the corrosive effects of de-icing, marine salt, and environmental pollutants, as well as the long-term effects of traffic loads that exceed design limits.

FRP patching and wrapping is the state-of-the-art method for repair and strengthening of structures. This new technology will lead to the optimum maintenance and repair of infrastructure. Research projects include developing smart repair technologies whereby FOSs are embedded in FRP wraps. Field applications cover a diverse range of structures under corrosive and cold climatic conditions.

2.3 Teaching and Educational Activities

More than 250 researchers are involved in ISIS Canada research activities. A substantial commitment is made to preparing students to enter a highly-specialized workforce in Canada's knowledge-based economy. Feedback from previous students who are now employed in the field of their choice, as well as from employers who invest substantial resources in seeking out potential employees, indicates that through the participating universities, ISIS Canada is providing an enriched multidisciplinary, learning environment. Field demonstration projects across the country involve on-site installations that provide a unique experience for students to work with industry partners, and gain hands-on multidisciplinary training.

In an effort to increase technology transfer of FRP technology, the ISIS Canada network has created a series, *Educational Modules,* for use by university professors and technical college instructors to facilitate the adoption of this material into the

education of new engineers and technicians. Since 2004, ISIS Canada has conducted an annual professors' and instructors' workshop to assist in this process.

There are currently 10 modules dealing with various aspects of FRP, structural health monitoring and life cycle engineering. The modules include presentations, notes, examples and case studies. These modules are available for download from the ISIS Canada website (www.isiscanada.com). These modules have become popular with professors, students and industry personnel from around the world.

3.1   General Requirements

The objective of this manual is to provide designers with guidelines and design equations that can be used for the design of FRP-reinforced concrete structures. This document is not part of a national or international code, but is mainly based on experimental results of research carried out in Canadian and other international university laboratories and institutions, and verified through field demonstration projects on functional structures.

Where possible, the document seeks to be consistent with either CSA S806 (2002) or CSA S6 (2006), for building and bridge applications, respectively. However, the guide may differ from both of these documents where the results of more research suggest an alternate approach is warranted.

For the most part, the suggested design methodologies of this manual have been validated by the research and testing carried out to date, or are a reflection of field experience with FRP-reinforced structures. A comparison of results of tests performed around the world and published in scientific papers was performed. The comparison results have been used to validate the proposed equations. The proposed design equations are representative of the tested models and are conservative when compared to available results. Since each reinforcing project is unique in its construction, loading history, and requirements, no generalizations should be allowed in the design process.

Users of this manual should be aware that research is ongoing around the world in this field. The document presents guidelines based on the consensus opinion of the Technical Committee of this document. Users of the manual should familiarize themselves with the relevant CSA or other appropriate codes as well as available literature before designing with FRP reinforcement. The document provides guidance to facilitate the users' understanding of this topic; however, it is not exhaustive and should be used with caution.

Readers of this manual should also be aware of the document on *Specifications for Product Certification of Fibre Reinforced Polymers (FRPs) as Internal Reinforcement in Concrete Structures*, ISIS Product Certification #1 (2006). The document responds to the fact that the use of FRPs (fibre-reinforced polymers) in civil structures becomes more widespread, a growing need for quality assurance of the FRP materials becomes imperative. These specifications deal with FRPs as internal reinforcement in concrete components of structures such as bridges, buildings and marine structures. They encompass information on FRPs in the form of bars and grids. Such a manual provides much needed information for owners of infrastructure, consulting engineers, FRP manufacturers, and the construction industry, all of whom need confidence and assurance that their materials being purchased and used have the quality envisioned during the design process.

3.2 Drawings and Related Documents

The engineer must prepare the various drawings and technical documents required for reinforced concrete structures using FRPs. These documents must identify all the requirements of existing standards (National Building Code, CSA-A23.3 Standard, CSA-S6 Standard etc.), as well as the following additional information related to the FRP systems:

- Identification of the FRP to be used;
- Required FRP mechanical properties;
- Mechanical properties of the existing materials;
- Summary of the considered design loads, allowable stresses, etc.;
- Quality control, supervision and field testing; and,
- Load testing when required.

3.3 Code References

ACI Standards:
- ACI-318-05, Building Code Requirements for Structural Concrete
- ACI-421 (2000), Design of Reinforced Concrete Slabs
- ACI-440.1R-06, Guide For the Design and Construction of Structural Concrete with FRP Bars
- ACI-440.3-04, Guide Test Methods for Fiber-Reinforced Polymers (FRPs) for Reinforcing or Strengthening Concrete Structures
- ACI-435 (2000), A General Approach to Calculation of Displacements of Concrete Structures

ASTM Standards:
- C234-86, Standard Test Method for Comparing Concretes on the Basis of the Bond Developed with Reinforcing Steel
- D792-86, Standard Test Methods for Density and Specific Gravity (Relative Density) of Plastics by Displacement
- D696-91, Standard Test Method for Coefficient of Linear Thermal Expansion of Plastics Between -30°C and 30°C
- D638-86, Standard Test Method for Tensile Properties of Plastics

CSA Standards:
- A23.3-05, Design of Concrete Structures
- S806-02, Design and Construction of Building Components with Fibre Reinforced Polymers (2002)
- S6-06, Canadian Highway Bridge Design Code (CHBDC), 2006

National Research Council of Canada:
- National Building Code of Canada, 2005

Other:

- CEB-FIP Model Code (1990), Model Code for Concrete Structures, Thomas Telford, London, 1993
- ISIS Product Certification #1 (2006), Specifications for Product Certification of Fibre Reinforced Polymers (FRPs) as Internal Reinforcement in Concrete Structures, ISIS Administrative Centre, University of Manitoba, Winnipeg, Manitoba, 27 p.
- ISIS Monograph - Durability of Fiber Reinforced Polymers in Civil Infrastructure, N. Banthia, B. Benmokrane, and V. Karbhari (eds), ISIS Administrative Centre, University of Manitoba, Winnipeg, Manitoba, 243 p.

4.1   Definitions

f_{frpu}	tensile strength of FRP, MPa
T_g	glass transition temperature
α_{frpL}	longitudinal thermal expansion coefficient of FRP
α_{frpT}	transverse thermal expansion coefficient of FRP

4.2   General

FRPs have been used for decades in the aeronautical, aerospace, automotive and other fields. Their use in civil engineering works dates back to the 1950s when GFRP bars were first investigated for structural use. However, it was not until the 1970s that FRP was finally considered for structural engineering applications, and its superior performance over epoxy-coated steel recognized. The first applications of glass fibre FRP were not successful due to its poor performance within thermosetting resins cured at high moulding pressures (Parkyn, 1970).
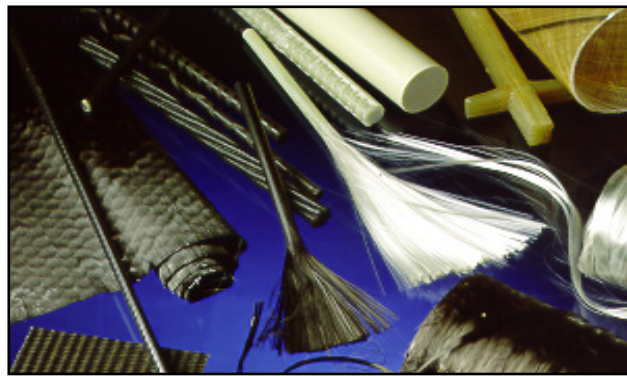
Figure 4.1: Available shapes of FRP products.

Since their early application, many FRP materials with different types of fibres have been developed. The fibres include aramid, polyvinyl, carbon and improved glass fibres. FRP products are manufactured in many different forms such as bars, fabric, 2D grids, 3D grids or standard structural shapes, as shown in Figure 4.1. In this Section, the two major components of FRP materials, namely the fibres and the matrices (or resins), and their properties, as well as the mechanical properties of the final product, i.e. the FRP materials, are discussed.

4.3   FRP Constituents

FRP products are composite materials consisting of a matrix (resin) and reinforcing fibres. As shown in Figure 4.2, the fibres are stronger than the matrix. In order to provide the reinforcing function, the fibre-volume fraction should be more than 55 percent for FRP bars and rods and 35 percent for FRP grids (ISIS Product Certification #1, 2006). The mechanical properties of the final FRP product depend on the fibre quality, orientation, shape, volumetric ratio, adhesion to the matrix, and on the manufacturing process. The latter is an

important consideration because simply mixing superior fibres and matrix does not guarantee a quality product. Accordingly, in FRP products with nominally the same fibres, matrix and fibre-volume ratio can differ significantly in their final properties. Additives and fillers appropriate for the fibre and resin systems are added for curing or other reasons. Diluents, such as styrene, and low-profile (shrink) additives shall not exceed 10 and 20 percent by weight of the specified base resin, respectively. Inorganic fillers may be used but shall not exceed 20 percent by weight of the specified base resin. Other additives, such as coupling agents, release agents, initiators, hardeners, promoters, catalysts, UV agents, fire retardants, wetting agent, foaming agents and pigments may be added (ISIS Product Certification #1, 2006).
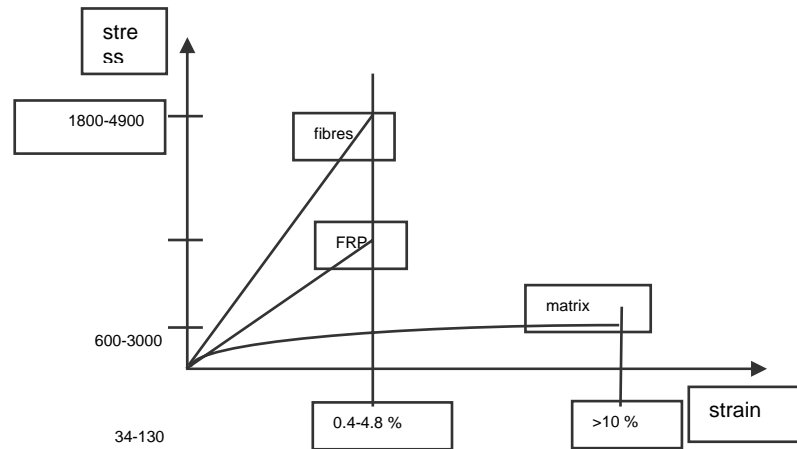
Figure 4.2: Stress-strain relationships for fibrous reinforcement and matrix.

4.3.1   Fibres

Fibres used for manufacturing composite materials must have high strength and stiffness, toughness, durability and preferably low cost. The performance of fibres is affected by their length, cross-sectional shape and chemical composition. Fibres are available in different cross-sectional shapes and sizes. The most commonly used fibres for FRPs are carbon, glass, and aramid. Typical mechanical properties of these fibres can be found in Table 4.1. The coefficient of thermal expansion of fibres in the longitudinal direction is denoted as α_{frpl}, and in the radial direction as α_{frpt}. Fibres must be treated with coupling agents to promote/enhance the bonding with the resin matrix.

Table 4.1 - Typical Mechanical Properties of Fibres					
FIBRE TYPE		Tensile Strength [MPa]	Modulus of Elasticity [GPa]	Elongation [%]	Coefficient of Thermal Expansion [x10⁻⁶]	Poisson's Ratio
CARBON						
PAN	High Strength	3500	200-240	1.3-1.8	(-1.2) to (-0.1) (α_{frpL}) 7 to 12 (α_{frpT})	-0.2
PAN	High Modulus	2500-4000	350-650	0.4-0.8		-0.2
Pitch	Ordinary	780-1000	38-40	2.1-2.5	(-1.6) to (-0.9) (α_{frpL})	N/A
Pitch	High Modulus	3000-3500	400-800	0.4-1.5		N/A
ARAMID						
Kevlar 29		3620	82.7	4.4	N/A	0.35
Kevlar 49		2800	130	2.3	-2.0 (α_{frpL}), 59 (α_{frpT})	0.35
Kevlar 129		4210 (est.)	110 (est.)	--	N/A	0.35
Kevlar 149		3450	172-179	1.9	N/A	0.35
Twaron		2800	130	2.3	(-2.0) (α_{frpL}), 59 (α_{frpT})	0.35
Technora		3500	74	4.6	N/A	0.35
GLASS						
E-Glass		3500-3600	74-75	4.8	5.0	0.2
S-Glass		4900	87	5.6	2.9	0.22
Alkali Resistant Glass		1800-3500	70-76	2.0-3.0	N/A	N/A

Table 4.2 (JSCE 1993; Banthia and MacDonald, 1996) gives the performance of fibres in damaging environments, such as acids (hydrochloric acid, sulphuric acid, and nitric acid), alkalis (sodium hydroxide and brine) and organic solutions (acetone, benzene, and gasoline). Carbon fibres were found to have the best performance. More information on the durability of composites can be found in Benmokrane and Rahman (1998).

Table 4.2 - Chemical Resistance of Fibres (JSCE 1993; Banthia and McDonald, 1996)				
FIBRE TYPE		Acid Resistance	Alkali Resistance	Organic Solvent Resistance
CARBON				
PAN	High Strength	Good	Excellent	Excellent
	High Modulus	Excellent	Excellent	Excellent
Pitch	Ordinary	Excellent	Excellent	Excellent
	High Modulus	Excellent	Excellent	Excellent
ARAMID				
Kevlar 49		Poor	Good	Excellent
Technora		Good	Good	Good
GLASS				
E-Glass		Poor	Fair	Excellent
S-Glass		Good	Poor	N/A
Alkali Resistant Glass		Good	Good	N/A
OTHERS				
EC-Polyethylene		Excellent	Excellent	Excellent
Polyvinyl Alcohol Fibre		Good	Good	Good
Steel Fibre		Poor	Excellent to Sodium Poor to Brine	Excellent

4.3.2   Resins

A very important issue in the manufacture of composites is the selection of the proper matrix because the physical and thermal properties of the matrix significantly affect the final mechanical properties as well as the manufacturing process. In order to be able to exploit the full strength of the fibres, the matrix should be able to develop a higher ultimate strain than the fibres (Phillips, 1989). The matrix not only coats the fibres and protects them from mechanical abrasion, but also transfers stresses between the fibres. Other very important roles of the matrix are transfer of inter-laminar and in-plane shear in the composite, and provision of lateral support to fibres against buckling when subjected to compressive loads (ACI 1995). There are two types of polymeric matrices widely used for FRP composites; namely, thermosetting and thermoplastic.

Thermosetting polymers are used more often than thermoplastic. They are low molecular-weight liquids with very low viscosity (ACI 1995), and their molecules are joined together by chemical cross-links. Hence, they form a rigid three-dimensional structure that once set, cannot be reshaped by applying heat or pressure. Thermosetting polymers are processed in a liquid state to obtain good wet-out of fibres. Some commonly used thermosetting polymers are polyesters, vinyl esters and epoxies. These materials have good thermal stability and chemical resistance and undergo low creep and stress relaxation. The FRP reinforcing bars should be produced and properly cured with a degree of curing above 95 percent (ISIS Product Certification #1, 2006). However, these polymers have relatively low strain to failure, resulting in low impact strength. Two major disadvantages are their short shelf life and long manufacturing time. Mechanical properties of some thermoset resins are provided in Table 4.3.

Table 4.3 — Typical Properties of Thermosetting Resins				
Resin	Specific Gravity	Tensile Strength [MPa]	Tensile Modulus [GPa]	Cure Shrinkage [%]
Epoxy	1.20-1.30	55.00-130.00	2.75-4.10	1.00-5.00
Polyester	1.10-1.40	34.50-103.50	2.10-3.45	5.00-12.00
Vinyl Ester	1.12-1.32	73.00-81.00	3.00-3.35	5.40-10.30

Thermoplastic matrix polymers are made from molecules in a linear structural form. These are held in place by weak secondary bonds, which can be destroyed by heat or pressure. After cooling, these matrices gain a solid shape. Although it can degrade their mechanical properties, thermoplastic polymers can be reshaped by heating as many times as necessary.

4.4   FRP Reinforcing Products and Material Properties

FRP reinforcing bars are manufactured from continuous fibres (such as carbon, glass, and aramid) embedded in matrices (thermosetting or thermoplastic). Similar to steel reinforcement, FRP bars are produced in different diameters, depending on the manufacturing process. The surface of the rods can be spiral, straight, sanded-straight, sanded-braided, and deformed. The bond of these bars with concrete is equal to, or better than, the bond of steel bars. The mechanical properties of some commercially available FRP reinforcing bars are given in Table 4.4 and durability aspects are discussed in Section 4.5. Appendix A contains addresses of the manufacturers.

Table 4.4 — Typical Mechanical Properties of FRP Reinforcing Bars			
Trade Name	Tensile Strength [MPa]	Modulus of Elasticity [GPa]	Ultimate Tensile Strain
CARBON FIBRE			
V-ROD	1596	120.0	0.013
Aslan	2068	124.0	0.017
Leadline	2250	147.0	0.015
NEFMAC	1200	100.0	0.012
GLASS FIBRE			
V-ROD	710	46.4	0.015
Aslan	690	40.8	0.017
NEFMAC	600	30.0	0.020

4.4.1   Manufacturing Process

There are three common manufacturing processes for FRP materials: pultrusion, braiding, and filament winding.

Pultrusion is a common technique for manufacturing continuous lengths of FRP bars that are of constant or nearly constant profile. A schematic representation of this technique is shown in Figure 4.3. Continuous strands of reinforcing

material are drawn from creels, through a resin tank, where they are saturated with resin, and then through a number of wiper rings into the mouth of a heated die. The speed of pulling through the die is predetermined by the curing time needed. To ensure good bond with concrete, the surface of the bars is usually braided or sand-coated.
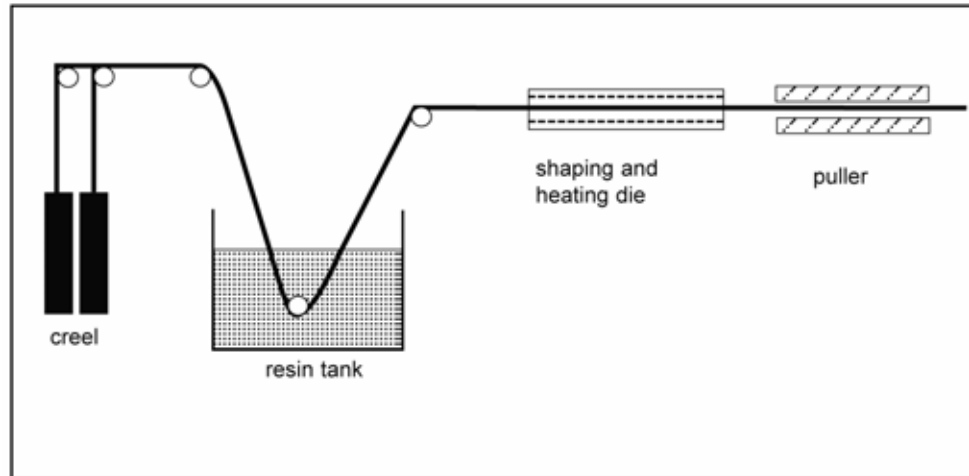
Figure 4.3: Pultrusion process.

Braiding is a term used for interlocking two or more yarns to form an integrated structure. Filament winding is a process whereby continuous fibres are impregnated with matrix resin and wrapped around a mandrel. During the latter process, the thickness, wind angle, and fibre-volume fraction are controlled. The final product is then cured using heat lamps. The most common products manufactured using this process are pipes, tubes, and storage tanks.

4.4.2   Coefficient of Thermal Expansion of FRP

Thermal properties of fibres are substantially different in the longitudinal and transverse directions, as shown in Table 4.5. Therefore, FRP reinforcing bars manufactured from these fibres have different thermal expansion in these two directions.

Thermal characteristics vary between products, depending on the fibre and matrix type and the fibre-volume ratio. CFRP has a coefficient of thermal expansion in the longitudinal direction close to zero (Erki and Rizkalla, 1993; Sayed and Shrive, 1998). Aramid fibre-reinforced polymer (AFRP) has a negative coefficient of longitudinal thermal expansion, indicating that AFRP contracts with increased temperature and expands with decreased temperature. GFRP has a longitudinal coefficient of thermal expansion comparable to concrete; however, the transverse coefficient is more than five times greater (Challal and Benmokrane, 1993). Coefficients of thermal expansion for some FRP reinforcing bars are shown in Table 4.5 (ACI 2000).

Table 4.5 — Typical Coefficients of Thermal Expansion for FRP Reinforcing Bars[1]				
Coefficient of Thermal Expansion (x 10^{-6}/°C)				
Direction	Steel	GFRP	CFRP	AFRP
Longitudinal	11.7	6 to 10	-1 to 0	-6 to –2
Transverse	11.7	21 to 23	22 to 23	60 to 80

4.4.3 Effect of High Temperature

High temperatures may have a negative effect on the performance of FRP. Therefore, special precaution should be taken when FRP is used for structures where fire resistance is a significant design factor. Even though FRP cannot burn when embedded in concrete, due to a lack of oxygen, the epoxy will soften. The temperature at which this occurs is referred to as the glass transition temperature, T_g. The value of the glass transition temperature is a function of resin type and generally reaches values of 110°C (230°F). At this temperature, both the flexural and bond strength of FRP will be affected. The effect of T_g is much more dramatic for thermoplastics than for thermosets, such as vinyl ester resin because the molecular chains of thermoplastics, being not cross-linked, are more mobile than those of thermoset resins, which are mobile between two cross-linked points only. For example, the flexural modulus of a thermoset-containing rebar will be equal to 50 and 20 GPa before and after T_g, respectively, whereas it will be equal to 40 and 0.4 GPa for a thermoplastic resin. A limited number of experiments are reported in the literature to date. According to Katz et al. (1998 and 1999), bond strength of FRP can be reduced up to 40 percent at 100°C (210°F) and up to 90 percent at 200°C (390°F). For GFRP, CFRP and AFRP fibres, these temperatures are 980°C (1800°F), 1650°C (3000°F), and 175°C (350°F), respectively (ACI 2000).

Limited information is available related to the effect of very high temperatures. Sayed-Ahmed and Shrive (1999) note that after 24 hours at 200C° and 300°C, the surface of Leadline had become darker, indicating some resin loss. Twenty-four hours of exposure at 400°C caused some of the fibres on the surface to become loose. Exposure to 500°C caused evaporation of the resin mainly within the first hour of exposure, reducing the tendon to a bundle of loose fibres. The effect of temperature on the strength of Leadline can be clearly seen in Figure 4.4. This study is applicable only to the Leadline product tested; other products may exhibit distinctly different behaviour and specific product testing should be conducted.

---

[1] Typical values for fibre-volume fraction ranging from 0.5 to 0.7.
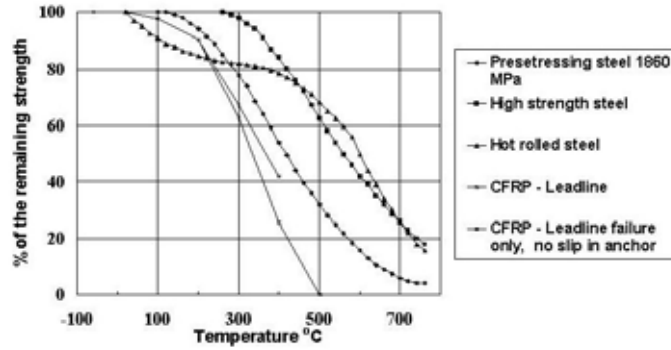
Figure 4.4: Effect of temperature on strength of Leadline
(Sayed-Ahmed and Shrive, 1999).

4.4.4   Bond Properties of FRP Reinforcing Bars

Bond properties of FRP bars depend on the surface preparation of the bar, which may be sand-coated, ribbed, helically wrapped, or braided. Mechanical properties of the bar, as well as environmental conditions, influence bond of FRP bars (Nanni et al., 1997).

Friction, adhesion, and mechanical interlock transfer bond forces to concrete. Unlike the case of steel-reinforced concrete, the compressive strength of concrete has no influence on the bond of FRP bars (Benmokrane et al., 1996). Detailed information regarding the development length is presented in Section 8.

4.4.5   Fatigue of FRP Reinforcing Bars

Tensile fatigue of FRP reinforcing bars has not yet been thoroughly investigated. At present, there is no universally-accepted testing technique for FRP products; hence, each test result must be accompanied by a description of the testing technique used.

Tanigaki et al. (1989) reported tests of AFRP bar FiBRA, which were performed as partial pulsating tensile fatigue tests. The lower limit of the stress was equal to 50 percent of the actual tensile strength and the upper limit was varied. Table 4.6 contains results from this test, which was performed at room temperature. The typical tensile strength of this bar is 1255 MPa and, if the upper limit does not exceed 80 percent of the ultimate strength, rupture does not occur even under two million cycles, as can be seen from Table 4.6.

Test	Lower Limit		Upper Limit		Stress Range [MPa]	Cycles to Rupture x 10³
	Load [kN]	Stress [MPa]	Load [kN]	Stress [MPa]		
1	32.26	645.3	46.97	939.5	294.2	>2090
2	32.26	645.3	42.52	990.5	345.2	>3577
3	32.26	645.3	50.99	1019.9	374.6	>2063
4	32.26	645.3	54.43	1088.5	443.3	305

Table 4.6 - Tensile Fatigue Strength Results for FiBRA (f_{frpu}=1255 MPa, Tanigaki et al.1989)

CFRP has excellent resistance to fatigue. For 2×10^6 cycles, Leadline (Mitsubishi Chemical Corporation) has an endurance limit of 1100 MPa at a stress ratio of 0.1. Yagi et al. (1997) tested pultruded CFRP at a stress ratio of 0.1, finding an endurance limit of 1400 MPa for one million cycles and 1200 MPa for 10 million cycles.

4.4.6 Creep and Relaxation of FRP Reinforcing Bars

The creep behaviour of most FRP materials is characterised by an initial elastic response, followed by non-linear creep behaviour towards failure. When FRP materials are subjected to a constant stress, they can fail suddenly. This phenomenon is referred to as creep rupture. The larger the ratio of sustained load stresses to live load stresses, the smaller the endurance of FRP. Creep rupture is also affected by ultraviolet radiation, high temperature, alkalinity, and weathering.

CFRP reinforcing bars are least susceptible to creep rupture, followed by AFRP, and then by GFRP which has the highest risk of failure due to creep rupture. To avoid creep rupture, the sustained service stress in the FRP reinforcing element is limited to a fraction of its ultimate strength. In general, CFRP is permitted to have higher service stresses followed by AFRP with GFRP being the lowest. In code documents, this limit on allowable service stress is partially achieved through the use of load and resistance factors; however, some codes such as CSA S6-00 and CSA S806-02 provide specific limits which the designer should check during the design process. These limits will be discussed under the design section of this document.

4.5 Durability of FRP Reinforcing Bars

One of the main reasons for considering FRP bars for concrete reinforcement is that steel bars can corrode in concrete subjected to harsh environments, resulting in a loss of strength and structural integrity (ACI 2000). Concrete exposed to chlorides through marine or de-icing salts is particularly prone to corrosion of reinforcing steel. Concrete is highly alkaline, having a pH of about 12.5 to 13.5, and the alkalinity decreases with carbonation (Coomarasamy and Goodman, 1997). Durability tests are conducted to determine the strength and stiffness reduction due to natural ageing of FRP bars under service environments during 50 to 100 years of service life. Many researchers are establishing these reduction factors. Additional work is being conducted to establish calibration factors based on field results.

Simple extrapolation of results from weathering exposure programs, although extremely valuable, is not sufficient to support the rapid increase in the use of FRP reinforcement. Some form of an accelerated ageing test procedure and predictive method is needed in order to provide appropriate long-term strength estimates. The designer is referred to existing literature for information on the conditioning environment for accelerated testing (Coomarasamy and Goodman, 1997; Porter et al., 1997; Porter and Barnes, 1998; Benmokrane et al., 1998).

Research on the effects of temperature on the durability of FRP bars in a concrete alkaline environment indicates that an acceleration factor for each

temperature difference can be defined by using Arrhenius laws. These factors differ for each product, depending on the type of fibre, type of resin, and bar size. In addition, the factors are affected by the environmental condition, such as surrounding solution media, temperature, pH, moisture, and freeze-thaw conditions (Gerritse, 1992; Coomarasamy and Goodman, 1997; Porter et al., 1997; and Porter and Barnes, 1998).

In another set of tests (Coomarasamy and Goodman, 1997), the mass uptake results and morphological studies on samples indicated a similar pattern qualitatively and, therefore, the simple test method could be used as a screening procedure to eliminate poor quality products without conducting extensive testing on them. The results of the mass uptake show an average increase of 0.6 percent after seven weeks for samples that retained 75 percent of their structural integrity versus up to 2.4 percent for samples that lost their structural integrity.

In another set of tests, an increase in average moisture uptake of the GFRP samples made of low-viscosity, urethane-modified vinyl ester, was measured for a year under tap water, salt solutions, and alkaline solutions. Maximum moisture uptake was observed to be under 0.6 percent at room temperature. For tap and salt water immersion, moisture uptake was under 0.3 percent. Alkaline conditioning produced about twice the moisture absorption rate in GFRP as compared to tap water and salt solution conditioning. This is an indication of the rate and magnitude of strength and stiffness degradation in GFRP bars caused by an alkaline environment compared to plain water and salt solution (Vijay et al., 1998).

With regard to the durability characteristics of FRP bars, one is referred to the provisional standard test methods (Benmokrane et al., 1998). The designer should always consult with the bar manufacturer before finalizing the design.

It is noted that the results from these accelerated test methods should be interpreted cautiously. The conditioning environments to promote accelerated deterioration are often unrealistic when compared with the actual environment in the field (Debaiky et al., 2006). Most accelerated tests lack correlation with actual field results over many years. To address this gap, ISIS recently undertook a field evaluation of existing structures with GFRP reinforcement (Mufti et al., 2005). Experienced contractors were employed to extract cores from five structures in service under supervision of senior engineers. The extracted core samples were found to be in excellent condition. The specimens with GFRP were sent for analysis to three independent research teams comprised of expert material scientists at the University of Manitoba, the Université de Sherbrooke, and the University of British Columbia in collaboration with the University of Saskatchewan.

Five field demonstration projects were chosen in this study:

- Hall's Harbor Wharf;
- Joffre Bridge;
- Chatham Bridge;
- Crowchild Trail Bridge; and,
- Waterloo Creek Bridge.

These structures are located across Canada from Atlantic to Pacific coasts. The demonstration structures perform in a wide range of environmental conditions, and were designed for normal use (i.e., heavy truck traffic) (Newhook et al., 2000; Benmokrane et al., 2000; Tadros et al., 1998; Aly et al., 1997).

The GFRP reinforcement rods or grids in all of the selected demonstration structures were made of E-glass and vinyl ester matrix. The structure type from which the core samples were taken, the age, GFRP type and general environmental conditions for each demonstration structure included in this study are shown in Table 4.7.

Table 4.7- Field Demonstration Structures' Age and Environmental Conditions				
Demonstration Project (year of construction)	Structure (Type)	Age at Testing (year)	GFRP (type)	Environmental Conditions
1) Hall's Harbor, Nova Scotia (1999)	Wharf	5	GFRP V-ROD™	Thermal range +35°C and -35°C; wet-dry cycles (splash and tidal; salt water); Freeze-thaw cycles.
2) Joffre Bridge, Quebec (1997)	Sidewalk Barrier Walls	7	GFRP C-BAR™	Thermal range +35°C and -35°C; Wet-dry and Freeze-thaw cycles; De-icing salt.
3) Chatham Bridge, Ontario (1996)	Barrier Walls	8	GFRP NEFMAC™	Thermal range +35°C and -35°C; Wet-dry and Freeze-thaw cycles; De-icing salt.
4) Crowchild Trail Bridge, Alberta (1996)	Barrier Walls and Bridge Deck	8	GFRP C-BAR™	Thermal range +35°C and -35°C; Freeze-thaw cycles; De-icing salt.
5) Waterloo Creek Bridge, British Columbia (1998)	Barrier Walls	6	GFRP NEFMAC™	Thermal range +35°C and -35°C; Wet-dry and Freeze-thaw cycles

From each field demonstration structure, at least 10 specimens of GFRP-reinforced concrete were removed from various areas of the structure. The cores were cylinders with 75 mm diameter and 140 mm to 180 mm length. A set of analytical methods was used to evaluate the state of degradation of the GFRP materials. This included Optical Microscopy (OM), Scanning Electron Microscopy (SEM) and Energy Dispersive X-ray (EDX), Differential Scanning Calorimetry (DSC) and Fourier Transformed Infrared Spectroscopy (FTIS).

Based on the results of the analyses described above, the study stated that there was no visible degradation of the GFRP reinforcement (rods and grids) in the concrete environment in real-life engineering structures exposed to natural environmental conditions for a duration of five to eight years. GFRP reinforcement is durable and highly compatible with the concrete material and should be allowed as the primary reinforcement in the concrete structures. Users of this manual are encouraged to obtain the detailed report of this study available through ISIS Canada for more details on the procedures and specific conclusions.

4.6   Commercially-Available Reinforcing Bars

Unlike steel reinforcement, there does not yet exist any governing standard for the production of FRP reinforcement or the required mechanical properties. ISIS Canada, working with industry, has developed a draft standard (ISIS Canada, 2006); however, its adoption by CSA or other regulatory bodies may still take several years. The range of material properties in commercially-available FRP products can be quite large, particularly for CFRP. This is one of its inherent advantages in that the designer may select different commercial products depending on the needs of the design for strength versus stiffness. The user is encouraged to consult commercial suppliers for the most up-to-date mechanical properties of their products as they can change when new versions of the product are produced. The designer should also request sufficient information from the supplier to be satisfied that the properties listed by the supplier were obtained through suitable tests. Both CSA S6-06 and CSA S806-02, as well as many other international guides, provide suggested test procedures.

This document will not attempt to list all suppliers or commercially-available products, nor will it seek to endorse any particular product. The ones selected for inclusion were chosen based on availability at the time of production of this document and experience of ISIS researchers in using these products in test or in field applications. Designers should always verify the latest product information with manufacturers prior to proceeding with design. For illustration, some typical FRP bars properties are listed below for the GFRP V-ROD product. More details on this and other FRP products can be found in Appendix A. An example of reinforcement for a concrete beam illustrating the availability of GFRP bars as both straight and bent bars is shown in Figure 4.5.

Table 4.8 – Properties of V-ROD GFRP bars				
Soft Metric Size	Nominal Diameter (mm)	Area, (mm^2)	Tensile Modulus of Elasticity (MPa)	Guaranteed Tensile Strength (MPa)
#6	6.35	31	46100	788
#10	9.53	71	46200	765
#13	12.70	127	46400	710
#16	15.88	198	48200	683
#19	19.05	285	47600	656
#25	25.40	507	51000	611

Figure 4.5: Inverted reinforced concrete T-beam reinforced with GFRP bars
(courtesy of Pultrall Inc.).

5.1   Definitions

–

E_c	modulus of elasticity of concrete, MPa
f'_c	compressive strength of concrete, MPa
f_r	modulus of rupture, MPa
F_{SLS}	service stress limit factor
k	stress decay factor
n	curve fitting factor
R_n	nominal resistance
S_n	nominal load effect
α	load factor
γ_c	density of concrete, kg/m^3
ε_c	strain in concrete
ε_o	strain in concrete at peak stress
ϕ	resistance factor
λ	modification factor for density of concrete
Ψ	load combination factor

5.2   General

There are currently two design codes in Canada which permit the use of FRP as internal reinforcement for concrete structures. CSA S806-02 deals with FRP reinforcement in building components and uses the load factors specified by the National Building Code of Canada (1995). CHBDC (CSA S6-06) deals with FRP reinforcement for bridge components. It contains both load factors and resistance factors. The user should be familiar with these documents before attempting a design using FRP and should take great care not to mix load factors or resistance factors from each document in an inappropriate way. A brief overview of the respective factors is given below.

5.3   Limit States Design

Canadian codes are based on a unified limit state design philosophy. To reduce the failure probability of a structure, either its resistance (R) is underestimated and/or the effects of specified loads (D and S) are overestimated. For any load combination, the general form can be written as follows:

$$\phi R_n \geq \alpha_D D + \alpha_i S_i + \sum \alpha_k S_k \qquad \text{Equation 5.1}$$

ϕ	material resistance factor
R_n	nominal resistance
α_D	load factor for dead load
α_i	load factor for principal load
α_k	load factor for for companion load
D	dead load
S_i	principal load (dominant specified variable load)
S_k	companion load (accompanying specified variable load)

The material resistance factor ϕ is always less than unity to reflect uncertainties in determining the nominal resistance R_n. The load factor α_i reflects uncertainties in determining the nominal load effect S_i. α_k reflects uncertainties in determining the nominal load effect S_k, and is determined in accordance with load combinations listed in the National Building Code of Canada (2005). Both the material resistance factor and the load combination factor will be discussed in greater detail in the following sections.

5.4   Load Factors and Loading Combinations for Buildings

This section will discuss load factors and loading combinations for design of concrete members reinforced with FRP. Loads considered in the design process follow the National Building Code of Canada (2005) and are denoted as follows:

D	dead load
E	earthquake load and effects
L	live load
S	snow load
T	temperature variations, creep, shrinkage and differential settlement
W	wind load

Effects of factored loads are considered in the design of a structure. Factored loads are obtained by multiplying the specified loads by load factors. The following factors are considered:

α_D	dead load factor
α_i	principal load factor
α_k	companion load factor

These load factors account for load combination effects described in the National Building Code of Canada (2005). The five possible load cases are listed in Table 5.1 along with the corresponding load factors.

Table 5.1 — Load Combinations for Ultimate Limit States		
Case	Load Combination	
	Principal Loads	Companion Loads[1]
1	1.4D	
2	$(1.25D^{(2)}$ or $0.9D^{(3)}) + 1.5L^{(4)}$	$0.5S^{(5)}$ or 0.4W
3	$(1.25D^{(2)}$ or $0.9D^{(3)}) + 1.5S$	$0.5L^{(5)(6)}$ or 0.4W
4	$(1.25D^{(2)}$ or $0.9D^{(3)}) + 1.4W$	$0.5L^{(6)}$ or 0.5S
5	$1.0D^{(3)} + 1.0E^{(7)}$	$0.5L^{(5)(6)}$ or $0.25S^{(5)}$

Notes to Table 5.1:

[1] Refer to Appendix A of NBCC (2005).
[2] The load factor of 1.25 for dead load **D** in the case of soil, superimposed earth, plants and trees should be increased to 1.5 except that when the soil depth exceeds 1.2 m, the factor can be reduced to $1+0.6/h_s$ but not less than 1.25 where h_s is the depth of soil in metres supported by the structure.

(3) The counteracting dead load 0.9**D** in load combination cases 2, 3 and 4 as well as 1.0**D** in case 5 should be used when the dead load acts to resist overturning, uplift, sliding, failure due to stress reversal and to determine anchorage requirements and the factored resistance of members.
(4) The principal load factor of 1.5 for live load **L** may be reduced to 1.25 for liquids in tanks.
(5) Refer to Section 4.1.5.5 of NBCC (2005).
(6) The companion load factor of 0.5 for live load **L** should be increased to 1.0 for storage areas as well as equipment areas and service rooms in Table 4.1.5.3 of NBCC (2005).
(7) The earthquake load **E** in load combination case 5 includes horizontal earth pressure due to earthquake determined in accordance with Sentence 4.1.8.16(4) of NBCC (2005).

5.4.1 Resistance Factors

The material resistance factor for concrete is $\phi_c = 0.65$. The material resistance factor for FRP is based on variability of the material characteristics, the effect of sustained load and the type of fibres. Table 5.2 shows resistance factors from CSA S806-02.

Table 5.2 — Resistance Factors From CSA S806-02		
Material	Notation	Factor
Concrete-Cast-In-Situ	ϕ_c	0.6
Concrete-Precast	ϕ_c	0.65
Steel reinforcement	ϕ_s	0.85
CFRP	ϕ_f	0.75
AFRP	ϕ_f	0.75
GFRP	ϕ_f	0.75

5.4.2 Service Stress Limit for Glass FRP S806-02

Clause 7.1.2.3, CSA S806-02 states:

"When GFRP is used for structural purposes, the tensile stress in the fibre under sustained factored loads shall not exceed 30% of its tensile failure stress."

Considering magnitude of load factors, this effectively limits the sustained stress under specified loads to 20 to 25 percent of the tensile strength.

5.5 Load Factors and Loading Combinations for Bridges

This Section denotes the load factors and load combinations to be used in bridge design, as specified in the Canadian Highway Bridge Design Code. The following loads are considered:

A	ice accretion load
D	dead load
E	loads due to earth pressure and hydrostatic pressure other than dead load; surcharges shall be considered as earth pressure even when caused by other loads
F	loads due to stream flow and ice pressure
H	collision load
K	all strains, deformations, displacements and their effects, including the effects of their restraint and those of friction or stiffness in bearings; strains and deformation include those due to temperature change and temperature differential, concrete shrinkage, differential shrinkage and creep, but not elastic strains
L	live load, including dynamic allowance when applicable
Q	earthquake load
S	load due to foundation deformation
V	wind load on live load
W	wind load on structure

5.5.1   Load Combinations

All combinations of factored loads specified in Table 5.3, using the dead load factor α_D, and earth load factor α_E, as given in Table 5.4.

Table 5.3 – Load Combinations for Bridges (Canadian Highway Bridge Design Code)											
	Permanent Loads[1]		Transitory Loads					Exceptional Loads (use one only)			
Loads	D	E	L	K	W	V	S	Q	F	A	H
FATIGUE LIMIT STATES											
Combination 1	1.00	1.00	0.80	0	1.00[2]	0	0	0	0	0	0
SERVICEABILITY LIMIT STATES											
Combination 1	1.00	1.00	0.75	0.80	0.70[2]	0	1.00	0	0	0	0
ULTIMATE LIMIT STATES											
Combination 1	α_D	α_E	1.40	0	0	0	0	0	0	0	0
Combination 2	α_D	α_E	1.25	1.15	0	0	0	0	0	0	0
Combination 3	α_D	α_E	1.15	1.00	0.40	0.40	0	0	0	0	0
Combination 4	α_D	α_E	0	1.25	1.30	0	0	0	0	0	0
Combination 5	α_D	α_E	0	0	0.70[2]	0	0	1.30	1.30	1.30	1.40

---

[1] Use Table 5.4 for values of α_D and α_E.

[2] For luminary sign, traffic signal supports, barriers and slender structure elements.

Table 5.4 — Load Factors for Bridges (Canadian Highway Bridge Design Code)		
DEAD LOAD	Maximum α_D	Minimum α_D
Factory-produced components excluding wood	1.10	0.95
Cast-in-place concrete, wood and all non-structural components	1.20	0.90
Wearing surfaces, based on nominal or specified thickness	1.50	0.65
Earth fill, negative skin friction on piles	1.25	0.80
Water	1.10	0.90
EARTH PRESSURE AND HYDROSTATIC PRESSURE	Maximum α_E	Minimum α_E
Passive earth pressure (when considered as load)	1.25	0.50
At-rest earth pressure	1.25	0.80
Active earth pressure	1.25	0.80
Backfill pressure	1.25	0.80
Hydrostatic pressure	1.25	0.90

5.5.2   Resistance Factors

The material resistance factors which were revised in 2006 for Section 16 of CHBDC are given in Table 5.5.

Table 5.5 — Resistance Factors From CHBDC (2006)		
Material	Notation	Factor
Concrete	ϕ_c	0.75
CFRP	ϕ_f	0.75
AFRP	ϕ_f	0.6
GFRP	ϕ_f	0.5

5.5.3   Service Stress Limits States – CHBDC

For FRP reinforcement in bridges, the allowable stress in the FRP at service limit state (SLS) shall not be more than $F_{SLS} \times f_{FRPu}$ where F_{SLS} is given in Table 5.6.

TABLE 5.6 – SLS STRESS LIMIT FACTORS FOR FRP-CHBDC (2006)	
Material	F_{SLS}
CFRP	0.65
AFRP	0.35
GFRP	0.25

5.6   Constitutive Relationships for Concrete

5.6.1   Tensile Strength

Before cracking, concrete is assumed to behave as an elastic material. The modulus of rupture, f_r, MPa, can be found from the following equation:

$$f_r = 0.6\lambda\sqrt{f_c'}$$

<div align="right">Equation 5.2</div>

λ modification factor for density of concrete (1.0 for normal density concrete)
f_c' compressive strength of concrete, MPa

5.6.2   Compressive Behaviour

The behaviour of concrete in compression may be calculated by the model proposed by Collins and Mitchell (1997). The expression relates the stress, f_c, and the strain at that stress, ε_c, as also shown in Figure 5.1

$$\frac{f_c}{f_c'} = \frac{n\left(\dfrac{\varepsilon_c}{\varepsilon_o}\right)}{n-1+\left(\dfrac{\varepsilon_c}{\varepsilon_o}\right)^{nk}}$$

<div align="right">Equation 5.3</div>

ε_o concrete strain at f_c'
n curve fitting factor
E_c $= f_c/\varepsilon_o$
E_o tangent stiffness at zero strain (Equation 5.8), MPa
k stress decay factor, taken as 1.0 for ($\varepsilon_c/\varepsilon_o < 1.0$) and as a number greater than 1.0 for ($\varepsilon_c/\varepsilon_o > 1.0$)

These factors are given in Table 5.7, or can be calculated using Equations 5.5 to 5.7.
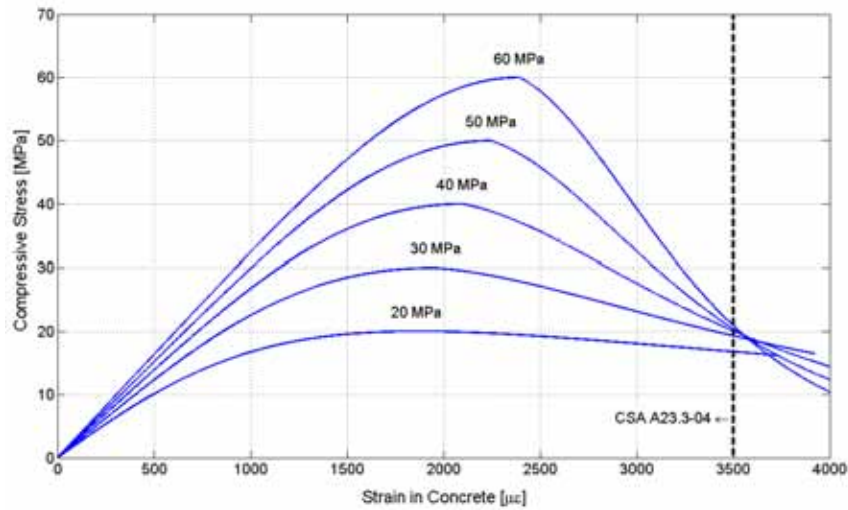
Figure 5.1: Stress-strain relationship for concrete.

Table 5.7 — Compressive Stress-Strain Coefficients for Normal-Density Concrete									
f_c [MPa]	20	25	30	35	40	45	50	55	60	65
E_c [GPa]	21.75	23.50	25.08	26.54	27.90	29.17	30.38	31.52	32.62	33.67
$\varepsilon_0 \times 10^{-6}$	1860	1900	1960	2030	2100	2170	2250	2320	2390	2460
n	1.97	2.27	2.56	2.85	3.15	3.45	3.74	4.04	4.33	4.62
k	0.99	1.07	1.15	1.23	1.31	1.39	1.48	1.56	1.64	1.72

Curve-fitting factor n

For normal density concrete, the following equation is used to estimate the value of n (all units are MPa):

$$n = 0.8 + \frac{f_c'}{17}$$

Equation 5.4

Strain ε_o at peak stress

$$\varepsilon_o = \frac{f_c'}{E_c} \frac{n}{n-1}$$

Equation 5.5

E_c can be calculated according to Equations 5.7 and 5.8.

Stress decay factor, k
The value of the decay factor k is calculated according to the following equation where f'_c is in MPa:

$$k = 0.67 + \frac{f'_c}{62} > 1.0$$

Equation 5.6

This factor is taken as 1.0 for $(\varepsilon_c/\varepsilon_o < 1.0)$ and as a number greater than 1.0 for $(\varepsilon_c/\varepsilon_o > 1.0)$.

5.6.3 Modulus of Elasticity

For concrete with density γ between 1500 and 2500 kg/m³, the modulus of elasticity may be taken as either of:

$$E_c = (3300\sqrt{f'_c} + 6900)\left(\frac{\gamma_c}{2300}\right)^{1.5}$$

Equation 5.7
CSA A23.3-94

The modulus of elasticity of normal density concrete with compressive strength between 20 to 40 MPa may be taken as either of:

$$E_c = 4500\sqrt{f'_c}$$

Equation 5.8
CSA A23.3-94

5.7 Constitutive Relationship for FRP

5.7.1 Tensile Strength and Modulus of Elasticity

The stress-strain relationship for FRP in tension is linear up to failure. The ultimate tensile strength of FRP, f_{frpu}, used in design calculations may be obtained from the manufacturer or from tests in accordance with ACI 440, CHBDC, or CSA.

Due to shear lag, fibres near the outer surface are stressed more than those near the centre of the bar (Faza, 1991). Therefore, tensile strength is dependent on bar diameter. Smaller diameter bars are more efficient.

The values of tensile strength vary with fibre type, fibre-volume ratio, manufacturing process, etc. Generally, glass fibre polymers achieve the lowest strength, and carbon fibre polymers and aramid fibre polymers achieve the highest strength. Figure 5.2 illustrates the strength and modulus of elasticity of various FRP materials. Table 4.4 includes typical values of tensile strength of FRP materials. Detailed information on mechanical properties based on manufacturer-supplied data for several FRP reinforcing bars currently available can be found in Appendix A.
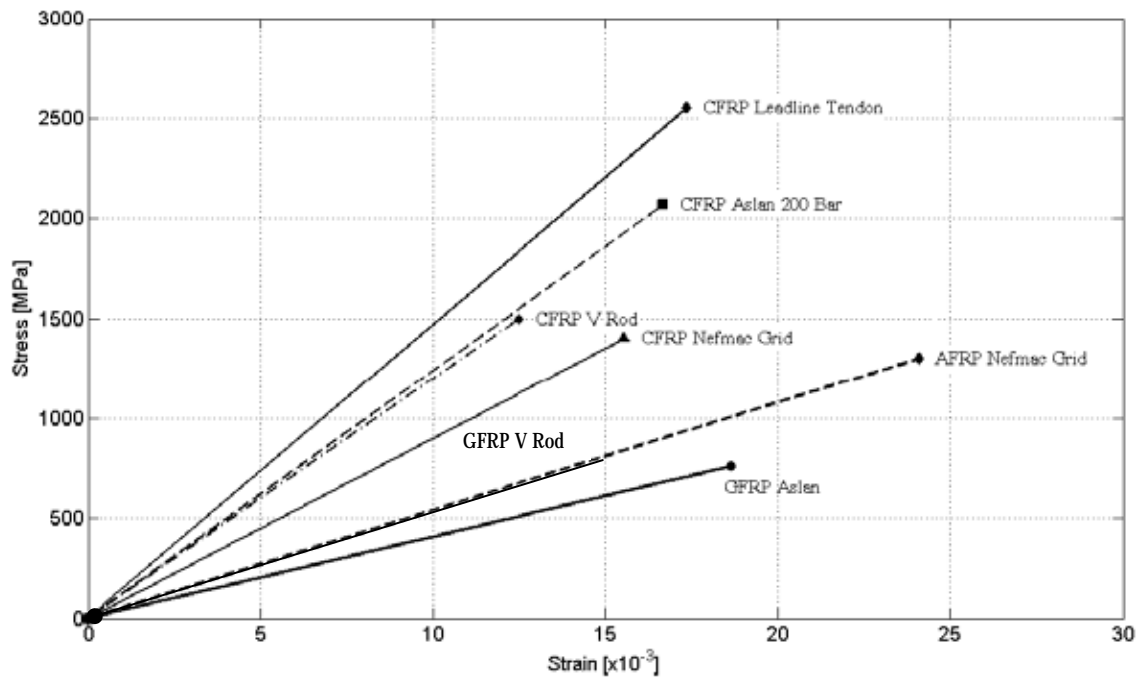
Figure 5.2: Stress-strain relationship of FRP materials.

Modulus of elasticity of FRP is dependent on the type of fibre. It can vary from 30 GPa for GFRP to 300 GPa for CFRP. Modulus of elasticity of FRP can be obtained directly from tensile tests. Most manufacturers provide this information in their specifications. Typical values of the modulus of elasticity can be found in Section 4.

5.7.2   Compressive Strength and Modulus of Elasticity

The compressive strength of FRP is relatively low compared to its tensile strength. Compressive strength is dependent on the fibre type, the fibre-volume ratio, manufacturing process, etc. It has been reported that aramid bars do not behave well in compression (Bedard, 1992; Chaallal and Benmokrane, 1993). Higher compressive strengths are expected for bars with higher tensile strength (ACI 1995).

The compressive modulus of elasticity depends on length-to-diameter ratio, bar size and type, as well as on other factors, such as boundary conditions. In the reported results from compression tests, it is generally agreed that the compressive stiffness ranges from 77 to 97 percent of the tensile stiffness (Bedard, 1992; Chaallal and Benmokrane, 1993).

According to Kobayashi and Fujisaki (1995), the compressive strength of AFRP bars is in the range of 10 percent of their tensile strength, for CFRP bars 30 to 50 percent of their tensile strength, and for GFRP bars 30 to 40 percent of their tensile strength. Chaallal and Benmokrane's (1993) tests on GFRP bar with 73 to

78 percent E-glass fibre showed the compressive strength of GFRP bars to be approximately 80 percent of their tensile strength. This appears to be rather high and is not in accordance with previous findings. This type of disparity is quite usual for FRP because there are many types of products differing in volumetric ratio of fibres, matrix type, and manufacturing process. A testing method for FRP materials is given in Benmokrane et al., 1998.

6 DESIGN FOR FLEXURE

6.1   Definitions

A_{frp}	area of FRP reinforcement, mm²
A_{frpb}	area of FRP reinforcement for balanced conditions, mm²
A_{frpmin}	minimum area of FRP reinforcement, mm²
b	width of compression face of member, mm
b_w	width of web, mm
C	resultant of compressive stresses in concrete, N
C_n	nominal resultant of stresses in concrete, N
c	depth of neutral axis, mm
c_b	depth of neutral axis at balanced failure conditions, mm
d	effective depth, mm
E_{frp}	modulus of elasticity of FRP, MPa
f'_c	compressive strength of concrete, MPa
f_{frp}	stress in FRP, MPa
f_{frpu}	ultimate tensile strength of FRP, MPa
f_r	modulus of rupture of concrete, MPa
I_t	second moment of area of the uncracked section transformed to concrete, mm⁴
M_{cr}	cracking moment, N·mm
M_f	moment due to factored loads, N·mm
M_r	moment resistance, N·mm
n_{frp}	modular ratio
T	internal force due to tension in FRP reinforcement, N
T_n	nominal internal force due to tension in FRP reinforcement, N
α, β	stress-block factors for concrete
α_1, β_1	stress-block factors for concrete based on CSA A23.3-94
ε_c	strain in concrete
ε_{cu}	ultimate strain in concrete in compression
ε_{frp}	strain in FRP
ϕ_c	material resistance factor for concrete
ϕ_{frp}	material resistance factor for FRP
ρ_{frp}	reinforcement ratio
ρ_{frpb}	balanced reinforcement ratio
Ψ_u	curvature at ultimate

6.2   General

Failure of a section in flexure can be caused by rupture of the FRP or by crushing of the concrete. Research has established that the ultimate flexural strength for both types of failure can be calculated using the same approach whether the reinforcement technique utilizes steel or FRP bars. Relevant equations for steel, given in several textbooks, are revised here and used in this manual.

Assumptions used in designing FRP-reinforced sections[1] are summarized below:

- Maximum strain at the concrete compression fibre is 3500×10^{-6}.
- Tensile strength of concrete is ignored for cracked sections.
- The strain in concrete and FRP at any level is proportional to the distance from the neutral axis.
- The stress-strain relationship for FRP is linear up to failure.
- Perfect bond exists between the concrete and the FRP reinforcement.

6.3   Strain Compatibility

The design philosophy is based on the assumption that a plane cross-section before deformation remains plane after deformation, leading to linear strain distribution over the cross-section.

Strain compatibility analysis is used for the analysis of FRP-reinforced members. If it is shown by material testing that the maximum compressive strain in concrete is higher than 3500×10^{-6}, the higher value should be used for analysis. The value of maximum compressive strain is important when calculating the balanced failure reinforcement ratio, ρ_{frpb}, and assessing the failure mode of the member.

6.4   Modes of Failure

There are three possible modes of flexural failure of a concrete section reinforced with FRP bars:

- **Balanced failure** - simultaneous rupture of FRP and crushing of concrete;
- **Compression failure** - concrete crushing while FRP remains in the elastic range with a strain level smaller than the ultimate strain; and,
- **Tension failure** - rupture of FRP before crushing of concrete.

Compression failure is less violent and more desirable than tension failure and is similar to that of an over-reinforced concrete beam with steel reinforcing bars.

Tension failure, due to rupture of FRP while the strain in the extreme fibres of the compression zone is less than the ultimate compressive strain of the concrete, is sudden. It will occur when the reinforcement ratio is smaller than the balanced failure reinforcement ratio, discussed in Section 6.4.1.

---

[1] Throughout this Section, the term FRP reinforcement refers to a single layer of tensile FRP reinforcement, unless stated otherwise.

Both failure modes are permitted in Section 16 of CHBDC which imposes an additional safety requirement of $M_r \geq 1.5 M_f$ when the failure mode is tensile rupture of the FRP. It is recommended in this manual that this approach be adopted for both building and bridge components.

6.4.1   Balanced Failure Reinforcement Ratio

The balanced failure strain condition occurs when the concrete strain reaches its ultimate value ε_{cu}, while the outer layer of FRP reaches its ultimate strain ε_{frpu}, as shown in Figure 6.1. No lumping of FRP reinforcement is allowed. The term "balanced failure strain" has a very different meaning for FRP-reinforced concrete than does the term "balanced strain condition" for steel-reinforced concrete. Since the FRP does not yield at the balanced failure strain condition, an FRP-reinforced member will fail suddenly, without warning. This phenomenon will subsequently be referred to as "balanced failure". At this condition, the strain in concrete reaches its ultimate value $\varepsilon_{cu} = 3500 \times 10^{-6}$ while the FRP reinforcement simultaneously reaches its ultimate strain ε_{frpu}. From the strain compatibility in the cross-section (Figure 6.1), the ratio of the neutral axis to the effective depth is:

$$\frac{c_b}{d} = \frac{\varepsilon_{cu}}{\varepsilon_{cu} + \varepsilon_{frpu}}$$

Equation 6.1

c_b depth of neutral axis at balanced failure condition, mm
d effective depth, mm
ε_{cu} ultimate strain in concrete in compression
ε_{frpu} ultimate strain in FRP in tension

The stress distribution in the compressive zone of concrete is non-linear, as indicated by the shaded diagram in Figure 6.1. According to CSA A23.3-05, this stress distribution may be replaced by an equivalent rectangular stress block with parameters α_1 and β_1.
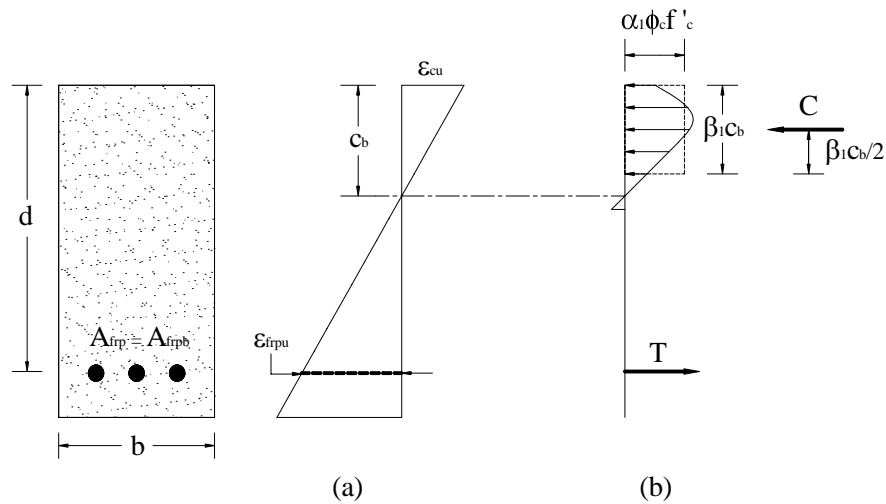
Figure 6.1: (a) Strain, and (b) Stress distribution at ultimate (balanced condition).

The force equilibrium in the cross-section, without including the material resistance factors, is given as follows:

$$C_n = T_n$$

<div align="right">Equation 6.2</div>

The stress resultants are calculated as follows:

$$C_n = \alpha_1 \phi_c f'_c \beta_1 c_b b$$

<div align="right">Equation 6.3</div>

$$T_n = \phi_f \varepsilon_{frpu} E_{frp} A_{frpb} = \phi_f f_{frpu} A_{frpb}$$

<div align="right">Equation 6.4</div>

α_1 ratio of average concrete strength in rectangular compression block to the specified concrete strength, given by the following, in which

$$\alpha_1 = 0.85 - 0.0015\, f'_c \geq 0.67$$

f'_c compressive strength of concrete, MPa

β_1 ratio of depth of rectangular compression block to the depth of the neutral axis, given as

$$\beta_1 = 0.97 - 0.0025 f'_c \geq 0.67$$

b   width of compression face of a member, mm

A_{frpb} area of FRP reinforcement for balanced conditions, mm²

E_{frp} modulus of elasticity of FRP, MPa

f_{frpu} ultimate tensile strength of FRP, MPa

ε_{frpu} ultimate tensile strain of FRP

Thus, $\alpha_1 \phi_c f'_c \beta_1 c_b b = \phi_f f_{frpu} A_{frpb}$

Substituting Equations 6.1 into 6.2 and solving for the balanced failure reinforcement ratio ρ_{frpb}:

$$\rho_{frpb} = A_{frpb} \Big/ (bd)$$

<div align="right">Equation 6.5</div>

$$\rho_{frpb} = \alpha_1 \beta_1 \frac{\phi_c}{\phi_f} \frac{f'_c}{f_{frpu}} \left(\frac{\varepsilon_{cu}}{\varepsilon_{cu} + \varepsilon_{frpu}} \right)$$

<div align="right">Equation 6.6</div>

Table 6.1 gives balanced reinforcement ratios for a variety of FPR-reinforced concretes. For some products, the value of f_{frpu} varies with cross-section size. Due to shear lag between the individual fibres at the core of the bars and those on the outer diameter, larger diameter bars can have lower values of f_{frpu} which will effect the value of ρ_{frpb}. The values provided in Table 6.1 should be considered nominal

for reference purposes only. The engineer should calculate the value of ρ_{frpb} for the actual product and bar size being used in design.

Table 6.1 — Balanced Reinforcement Ratio for FRP-Reinforced Concrete					
Fibre Type (f_{frpu} [MPa], E_{frp} [GPa])		Concrete Strength [MPa]			
		30	40	50	60
GFRP					
	ASLAN (655, 40.8)	0.0051	0.0065	0.0078	0.0088
	V-ROD (710, 46.4)	0.0047	0.006	0.0071	0.0082
	NEFMAC (600, 30)	0.0046	0.0059	0.007	0.008
CFRP					
	LEADLINE (2255, 147)	0.0015	0.002	0.0023	0.0027
	ASLAN (2400, 131)	0.0013	0.0045	0.0053	0.0061
	NEFMAC (1200, 100)	0.0035	0.0045	0.0053	0.0061
AFRP					
	NEFMAC (1300, 54)	0.0018	0.0023	0.0028	0.0032

6.4.2   Failure Due to Crushing of Concrete

When flexural failure is induced by crushing of concrete without rupture of the reinforcement, the section is said to be over-reinforced. For a T-section to be over-reinforced it must have a large amount of reinforcement, which is considered to be impractical. Thus, only rectangular cross-sections are considered in this case.

The strain profile with the top fibre strain equal to the ultimate compressive strain of concrete in compression, 3500×10^{-6}, is constructed as shown in Figure 6.2 (a). Under this strain distribution, the cross-section fails due to concrete crushing. The non-linear distribution of concrete stresses in the compression zone is replaced by an equivalent uniform stress over a part of the compression zone, as shown in Figure 6.2 (b), according to CSA 23.3-05.
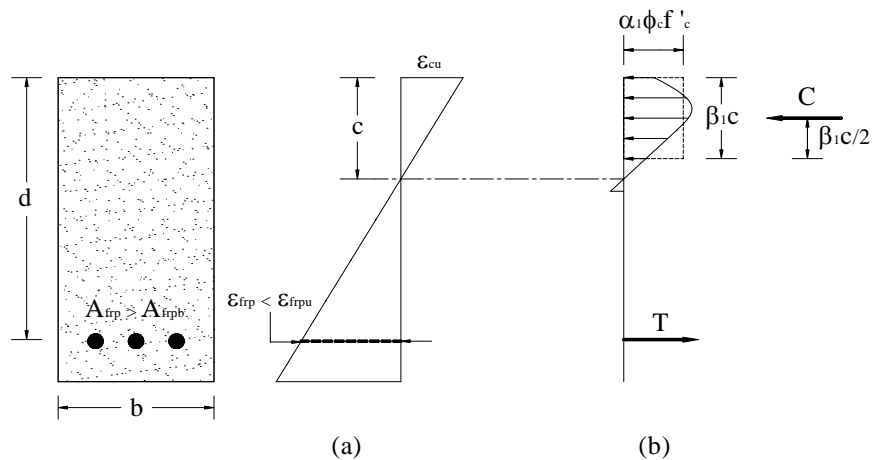
Figure 6.2: (a) Strain, and (b) Stress distribution at ultimate (concrete crushing).

The ultimate moment resistance for such an over-reinforced section can be calculated as follows:

$$C = \alpha_1 \phi_c f_c' \beta_1 c b$$

Equation 6.7

c depth of neutral axis, mm
ϕ_c material resistance factor for concrete

The tensile force in reinforcement is calculated as:

$$T = A_{frp} \phi_{frp} f_{frp}$$

Equation 6.8

A_{frp} area of FRP reinforcement, mm²
ϕ_{frp} material resistance factor of FRP reinforcement
f_{frp} stress in the FRP reinforcement at failure, which is smaller than the tensile strength, MPa

Whence,

$$f_{frp} = 0.5 E_{frp} \varepsilon_{cu} \left[\left(1 + \frac{4\alpha_1 \beta_1 \phi_c f_c'}{\rho_{frp} \phi_{frp} E_{frp} \varepsilon_{cu}} \right)^{1/2} - 1 \right]$$

Equation 6.9

where reinforcement ratio $\rho_{frp} = \dfrac{A_{frp}}{bd}$

According to CSA A23.3-94, failure of concrete due to crushing is considered to have occurred when $\varepsilon_{cu} = 3500 \times 10^{-6}$ and the values of α_1 and β_1 are as defined in the balanced failure case.

Alternatively, an iteration process may be used. For each iteration for an assumed depth of neutral axis, the forces in the concrete and in the reinforcement are calculated and their equilibrium is checked as follows:

$$\alpha_1 \phi_c f_c' \beta_1 c b = A_{frp} \phi_{frp} \varepsilon_{frp} E_{frp}$$

If this equilibrium is not satisfied, a new value of depth of neutral axis, c, is chosen and C and T are recalculated using the new values of c and ε_{frp}.

When the equilibrium between Equations 6.7 and 6.8 is satisfied, as a means of verifying the assumed value of c, the moment of resistance of the section is given by:

$$M_r = C \left(d - \frac{\beta_1 c}{2} \right)$$

Equation 6.10

The curvature at ultimate is:

$$\psi_u = \frac{\varepsilon_{cu} + f_{frp}/E_{frp}}{d}$$

Equation 6.11

6.4.3   Tension Failure

The theory for sections under-reinforced with steel bars is well-documented in textbooks. Before failure, the steel yields and the curvature increases rapidly until the strain in concrete in the extreme compressive surface reaches an ultimate value of 3500 x 10^{-6}, when failure occurs. The rectangular stress block typically idealises the stress in concrete. However, when a section is under-reinforced with FRP, no yield occurs. Rather, the failure is caused by rupture of the FRP. The strain in the reinforcement will be:

$$\varepsilon_{frpu} = \frac{f_{frpu}}{E_{frp}}$$

Equation 6.12

The corresponding strain ε_c at the extreme compressive fibre will be less than ε_{cu} as shown in Figure 6.3(a). Thus the traditional rectangular block cannot idealize the distribution of compressive stress in the concrete zone. In the following section, α and β as shown in Figure 6.3 (b) will be derived for ε_c varying up to 3500 x 10^{-6} because the coefficients α_1 and β_1, are valid only for $\varepsilon_c = \varepsilon_{cu}$.
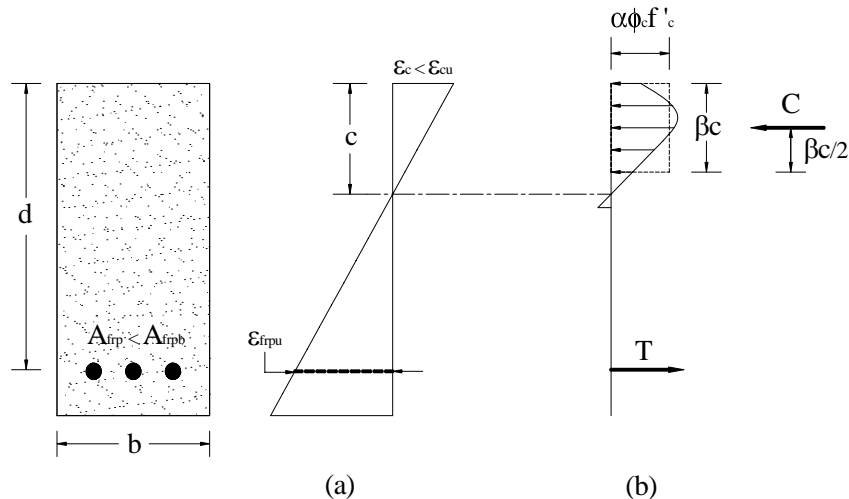
Figure 6.3: (a) Strain, and (b) Stress distribution at ultimate (rupture of FRP).

The process will start by specifying the strain in the reinforcement equal to the ultimate tensile strain, ε_{frpu}. An iterative approach will be used and an assumed value of the depth of neutral axis, c, will be used for every iteration. The strain in the top fibres, ε_c, will be calculated using strain compatibility, and must be less than the ultimate strain of concrete in compression, ε_{cu}. The stress-block parameters α and β will be found for the strain ε_c using the tables in Appendix B, or using Figures 6.4 and 6.5. These parameters depend on the strain in concrete; when this strain reaches 3500 x 10^{-6} they are identical to parameters α_1 and β_1 of CSA A23.3-05. The resultant of the compressive stresses in concrete, C, is then calculated as:

$$C = \alpha \, \phi_c f_c' \beta \, cb \qquad\qquad \text{Equation 6.13}$$

α stress-block factor for concrete (Figure 6.4 and Tables B.1 to B.3)
β stress-block factor for concrete (Figure 6.5 and Tables B.1 to B.3)

The equivalent stress block parameters α and β are tabulated in Appendix B for different ratios of $\varepsilon_c/\varepsilon_o$ and different concrete strengths. Figures 6.4 and 6.5 show the stress block parameters α and β versus the strain in concrete for concrete strengths from 20 to 60 MPa. Using the factors α_1 and β_1 specified by CSA A23.3-05 for given material values will provide moment resistance values within 5 to 10 percent.
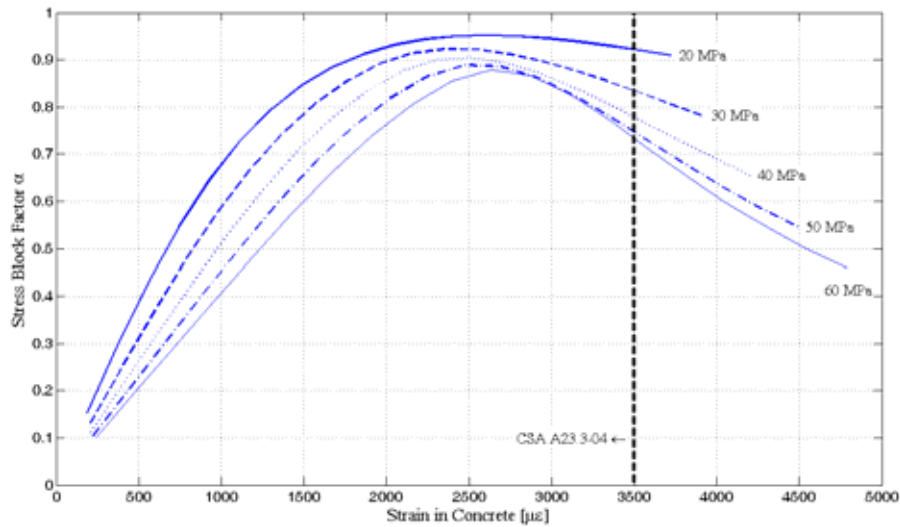
Figure 6.4: Equivalent stress-block parameter α
for concrete strengths of 20 to 60 MPa.
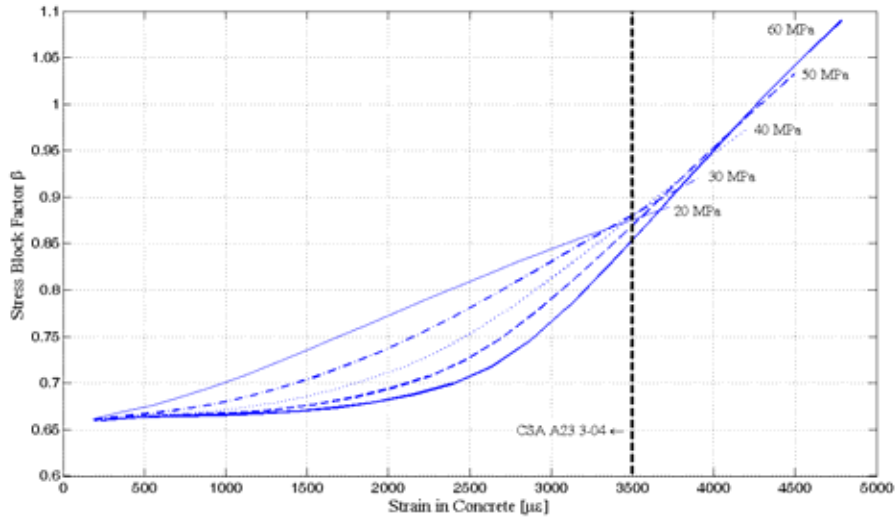
Figure 6.5: Equivalent stress-block Parameter β
for Concrete Strengths of 20 to 60 MPa.

The tensile force in reinforcement is calculated as:

$$T = A_{frp}\phi_{frp}\varepsilon_{frpu}E_{frp}$$

Equation 6.14

Equilibrium in a cross-section is found by equating Equations 6.13 and 6.14

$$\alpha\,\phi_c f_c'\beta\,cb = A_{frp}\phi_{frp}\varepsilon_{frpu}E_{frp}$$

If these two forces are not in equilibrium, another iteration is made using a different value of the depth of neutral axis, c, while the strain in FRP remains equal to ε_{frpu}, until force equilibrium is satisfied.

The moment of resistance of the member can be found using the following equation:

$$M_r = T\left(d - \frac{\beta\,c}{2}\right)$$

Equation 6.15

For this type of failure, serviceability requirements will typically control the design.

The curvature in this case can be determined as:

$$\psi_u = \frac{\varepsilon_c + \varepsilon_{frpu}}{d}$$

Equation 6.16

6.5 Cracking Moment

Cracking occurs when the stress in concrete at the extreme tension surface reaches the tensile strength of concrete in tension, f_r. The cracking moment value, M_{cr}, at which cracking occurs is:

$$M_{cr} = \frac{f_r I_t}{y_t}$$

Equation 6.17

f_r	modulus of rupture, MPa
I_t	second moment of area of the transformed uncracked section about its centroidal axis, mm^4
y_t	distance from the centroid of uncracked section to extreme surface in tension, mm

The transformed uncracked section is composed of the area of concrete plus $(n_{frp}-1)A_{frp}$. To avoid sudden failure by rupture, the amount of FRP reinforcement must be sufficient to have a moment resistance M_r greater than M_{cr}.

Both CSA S6-06 and CHBDC permit the use of gross section properties in this calculation.

6.6 Minimum Flexural Resistance

Failure of a member immediately after cracking should be avoided, and therefore the moment of resistance, M_r, should be at least 50 percent greater than the cracking moment $M_{cr.}$

$$M_r \geq 1.5 M_{cr}$$

Equation 6.18

If the above condition is not satisfied, the moment of resistance, M_r, should be at least 50 percent greater than the moment due to factored loads, $M_{f.}$

6.7 Additional Criteria for Tension Failure

In keeping with the provisions of CHBDC, it is recommended that, when ULS is governed by tension failure of the FRP, Equation 6.19 also be satisfied:

$$M_r \geq 1.5 M_f$$

Equation 6.19

6.8   Beams with FRP Reinforcement in Multiple Layers

Design of FRP-reinforced T-sections usually leads to the use of FRP reinforcement in layers as shown in Figure 6.6. The strain in the outer layer of the FRP reinforcement is the critical strain, and it may not exceed the ultimate tensile strain at the ultimate load, or the maximum strain for serviceability requirements, as discussed in Section 7.
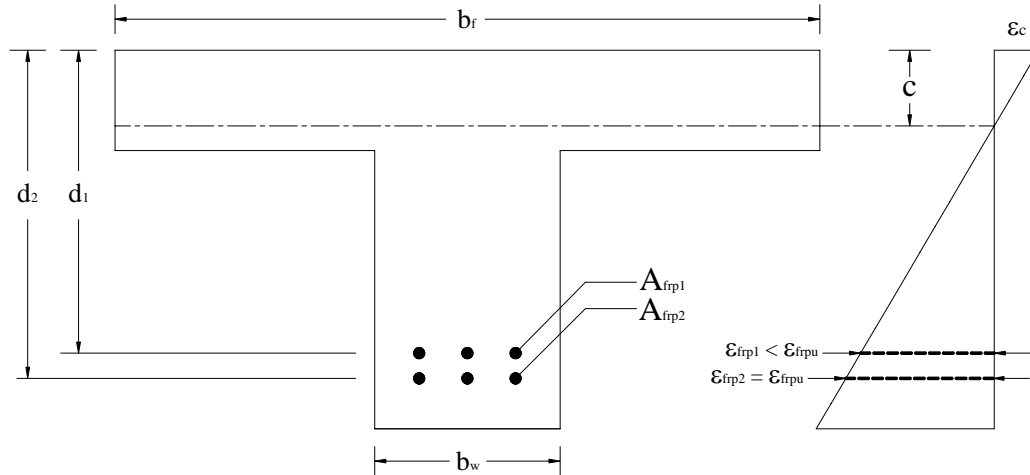
Figure 6.6: Strain compatibility for section with multiple layers of FRP.

6.9   Beams with Compression Reinforcement

FRP reinforcement can be placed in the compression zone in continuous beams and slabs. The compressive strength of such reinforcement should not, however, be accounted for in the design. Therefore, the compressive reinforcement shall be ignored when calculating flexural capacity of FRP-reinforced members (Almusallam et al., 1997).

6.10   Beams with Multiple Reinforcement Types

In developing a design solution for a particular application, the designer may choose to use more than one type of reinforcement in the structure. If the different reinforcement types are in separate tension zones (e.g. CFRP bars used as top transverse reinforcement in a bridge deck cantilever and GFRP bars used as bottom bars), then the design can be easily accomplished using appropriate reinforcement properties in each section analysis. If the different types are used in the same tension zone (e.g. an inner layer of steel and an outer layer of GFRP bars where used in the web of a T-beam for the Hall's Harbor Wharf Project) (Newhook et al., 2000), then strain compatibility as shown in Figure 6.6 must be employed. At SLS, the design must ensure that stress limits for each reinforcement type are not exceeded. At ULS the ultimate stress for each layer must be evaluated to determine the failure mode.

6.11   Examples

These examples were selected to illustrate the computation of moment resistance for flexural sections reinforced with FRP.

6.11.1   Rectangular Beam Example

Determine the moment resistance of the rectangular beam section shown below. The concrete compressive strength is 35 MPa. The beam is reinforced with four 12 mm-diameter GFRP bars with the following properties:

d_b , diameter = 12 mm
A_b , area = 120 mm²
f_{frpu} , ultimate strength= 630 MPa
ε_{frpu} , ultimate strain= 0.01575
E_{frp} , Modulus of Elasticity = 40000 MPa
concrete cover = 30 mm
diameter of stirrups = 10 mm
$\phi_c = 0.65$
$\phi_{frp} = 0.75$
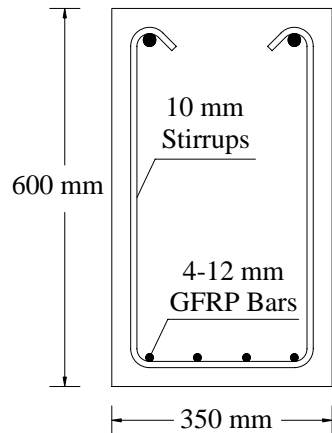
1. Compute effective depth
$$d = 600 - 30 - 10 - 12/2 = 554 mm$$

2. Calculate reinforcement ratios
$$\rho_{frp} = \frac{A_{frp}}{bd} = \frac{4 \times 120}{350 \times 554} = 0.00248$$

3. Compare with balanced reinforcement ratio
$$\rho_{frp} = \alpha_1 \beta_1 \frac{\phi_c}{\phi_f} \frac{f'_c}{f_{frpu}} \frac{\varepsilon_{cu}}{\varepsilon_{cu} + \varepsilon_{frpu}}$$
where

$$\alpha_1 = 0.85 - 0.0015 f_c'$$

$$= 0.85 - 0.0015(35)$$

$$= 0.7975$$

$$\beta_1 = 0.97 - 0.0025 f_c'$$

$$= 0.97 - 0.0025(35)$$

$$= 0.8825$$

$$\rho_{frpb} = 0.7975 \times 0.8825 \frac{0.65}{0.75} \frac{35}{630} \frac{0.0035}{0.0035 + 0.01575}$$

$$= 0.00616$$

$$\rho_{frp} < \rho_{frpb} \rightarrow \quad Tension \quad failure$$

4. Find the neutral axis location which gives equilibrium of forces in the section.

At ultimate limit states, the strain in the FRP is equal to ε_{frpu} and the strain in the extreme compression fibre in the concrete is less than ε_{cu} (Refer to Figure 6.3).

Process:
- Assume a value of neutral axis location, c
- Calculate value of concrete strain, ε_c
- Compute resultant compressive and tensile forces and compare (If T=C then equilibrium condition has been found; if T≠C then assume new value of c and iterate).

Assume value of c:

$$\frac{\rho_{frp}}{\rho_{frpb}} = \frac{0.00248}{0.00616} = 0.403$$

Assume c = 0.40×c$_b$ as initial value.

$$c_b = \frac{\varepsilon_{cu}}{\varepsilon_{cu} + \varepsilon_{frpu}} \times d = \frac{0.0035}{0.0035 + 0.01575} \times 554 = 100mm$$

$$c = 0.40 \times 100 = 40mm$$

Calculate ε_c

$$\frac{c}{d} = \frac{\varepsilon_c}{\varepsilon_c + \varepsilon_{frpu}} \implies \varepsilon_c = \frac{c}{d-c} \times \varepsilon_{frpu}$$

$$= \frac{40}{554-40} \times 0.01575$$

$$= 0.00123$$

Find α and β from Table B.2 or Figures 6.4 and 6.5, respectively.

$\alpha = 0.68$
$\beta = 0.67$

Compute resultant tension force.

$$T = A_{frp} \phi_f f_{frpu} = 4 \times 120 \times 0.75 \times 630 = 226800N = 226.8kN$$

Compute resultant compression force.

$$C = \alpha\varphi_c f'_c \beta cb = 0.68 \times 0.65 \times 35 \times 0.67 \times 40 \times 350 = 145109 \text{ N} = 145.1 \text{ kN}$$

$C \neq T$ Iterate.

Assume c=50mm

$$\varepsilon_c = \frac{50}{554-50} \times 0.01575 = 0.00156$$

$\alpha = 0.81$
$\beta = 0.68$

$$C = 0.81 \times 0.65 \times 35 \times 0.68 \times 50 \times 350 = 219287 \quad N = 219.3 \quad kN$$

$$T \approx C$$

5. Compute M_r:

c=50
$\beta = 0.68$

$$M_r = A_{frpu} \phi_f f_{frpu} \left(d - \frac{\beta c}{2} \right)$$

$$= 4 \times 120 \times 0.75 \times 630 \left(554 - \frac{0.69 \times 50}{2} \right) = 121734900 \, N \cdot mm = 121.7 \, kN \cdot m$$

6.11.2 Slab Example

Determine the moment resistance of a 30 MPa concrete slab with 9mm diameter CFRP bars at a spacing of 125 mm. The slab is 150 mm thick and the concrete cover is 35 mm. The properties of the CFRP bars are:

> d_b , diameter = 9 mm
> A_b , area   = 65 mm²
> F_{frpu} , ultimate strength = 2200 MPa
> ε_{frpu} , ultimate strain   = 0.01467
> E_{frp} , Modulus of Elasticity = 150000 MPa

A 1,000 mm wide strip of slab is used in analysis.

> $\varphi_c = 0.65$
> $\varphi_{frp} = 0.75$
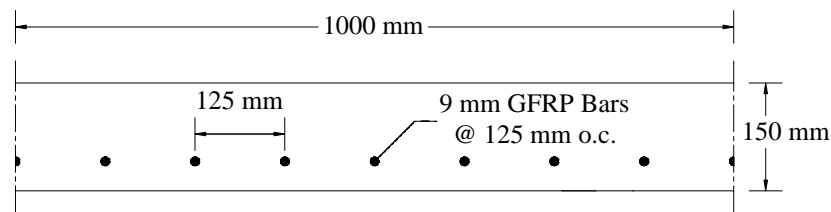
1. Compute effective depth

$$d = 150 - 35 - 9/2 = 110.5 \, mm$$

2. Calculate reinforcement ratio

$$A_{frp} = A_b \times \frac{1000}{125} = 65 \times \frac{1000}{125} = 520 mm^2$$

$$\rho_{frp} = \frac{520}{1000 \times 110.5} = 0.00471$$

3. Compare with balanced reinforcement ratio

$$\rho_{frp} = \alpha_1 \beta_1 \frac{\phi_c}{\phi_f} \frac{f'_c}{f_{frpu}} \frac{\varepsilon_{cu}}{\varepsilon_{cu} + \varepsilon_{frpu}}$$

$$\alpha_1 = 0.85 - 0.0015(30) = 0.81$$
$$\beta_1 = 0.97 - 0.0025(30) = 0.90$$

$$\rho_{frpb} = 0.81 \times 0.90 \frac{0.65}{0.75} \frac{30}{2200} \frac{0.0035}{0.0035 + 0.01467}$$

$$= 0.00163$$

$$\rho_{frp} > \rho_{frpb} \rightarrow \quad Compression \quad failure$$

4. Compute stress in CFRP at ULS

$$f_{frp} = 0.5 E_{frp} \varepsilon_{cu} \left[\left(1 + \frac{4\alpha_1 \beta_1 \phi_c f_c'}{\rho_{frp} \phi_{frp} E_{frp} \varepsilon_{cu}} \right)^{1/2} - 1 \right]$$

$$= 0.5 \times 150000 \times 0.0035 \left[\left(1 + \frac{4 \times 0.81 \times 0.90 \times 0.65 \times 30}{0.00471 \times 0.75 \times 15000 \times 0.0035} \right)^{1/2} - 1 \right]$$

$$= 1215 \quad MPa$$

5. Find neutral axis, c

$$\varepsilon_{frp} = \frac{f_{frp}}{E_{frp}} = \frac{1215}{150000} = 0.0081$$

$$c = \frac{\varepsilon_{cu}}{\varepsilon_{cu} + \varepsilon_{frp}} \times d = \frac{0.0035}{0.0035 + 0.0081} \times 110.5 = 33.3 \quad mm$$

6. Compute M$_r$

$$M_r = A_{frp} \phi_{frp} f_{frp} \left(d - \frac{\beta c}{2} \right)$$

$$= 520 \times 0.75 \times 1215 \times \left(110.5 - \frac{0.90 \times 33.3}{2} \right) = 42259283 \quad N.mm / m = 42.3 \quad kN.m / m$$

6.12   Concrete Slab-On-Girder Bridge Decks

CHBDC (2006) provides two methods for designing FRP-reinforced concrete deck slabs. Furthermore, CHBDC provides a method for designing externally-restrained concrete bridge deck slabs in which GFRP bars are used for crack control.

6.12.1   Flexural Method – FRP-Reinforced Deck Slabs

Decks may be designed for flexure in accordance with the provisions of CHBDC for determination of design moments. If FRP reinforcement is used then the flexural method outlined in the previous section is employed. Standard detailing requirements for distribution of reinforcement in bridge deck should be followed.

This flexural design method is always used for the cantilever section of the deck.

6.12.2   Internally Restrained Bridge Deck Design – FRP-Reinforced

A method for selecting steel reinforcement for a deck slab is specified in CHBDC in Clause 8.18.4. This approach has been adapted for use with FRP reinforcement in a deck slab. The designer should review the appropriate conditions and limitations on the use of empirical design method in the relevant clauses of Section 8 and 16 of CHBDC. If use of the method is applicable, then the amount of FRP reinforcement may be selected according to the following:

(a) The deck slab shall contain two orthogonal assemblies of FRP bars with the clear distance between top and bottom bars being a minimum of 55 mm.

(b) For the transverse FRP bars in the bottom assembly, the minimum cross-sectional area of the FRP shall be 500 d_s / E_{frp} mm^2 / mm where d_s is the distance from the top of the slab to the centroid of the bottom transverse FRP bars.

(c) Longitudinal bars in the bottom assembly and both transverse and longitudinal bars in the top assembly are GFRP with a minimum ρ of 0.0035.

In addition, the transverse edges of the slab shall be stiffened in accordance with CHBDC requirements.

The criteria are schematically shown in Figure 6.7.
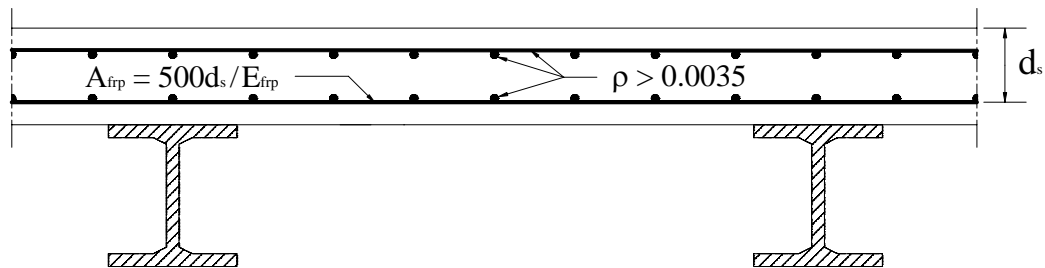
Figure 6.7: Empirical Method for FRP-Reinforced Bridge Decks.

6.12.3 Example: GFRP-Reinforced Deck Slab

Design the reinforcing for a concrete bridge deck slab with 200 mm thickness and supported on steel girders at a spacing of 3150 mm. The bridge is a simply supported right bridge. Use the following material properties:

Concrete: $f_c' = 40$ MPa , clear cover to bars = 35 mm

GFRP: 13 mm bars - diameter = 13 mm , Area = 130 mm² , $E_{frp} = 41$ GPa , $f_{frpu} = 600$ MPa

16 mm bars - diameter = 16 mm, Area = 200 mm² , $E_{frp} = 41$ GPa , $f_{frpu} = 650$ MPa

19 mm bars - diameter = 19 mm, Area= 285 mm² , $E_{frp} = 41$ GPa , $f_{frpu}= 620$ MPa

Bottom transverse bars (19 mm diameter)

$$d_s = 200 - 35 - (19/2) = 155 mm$$

$$A_{frp} = \frac{500 d_s}{E_{frp}} = \frac{500 \times 155}{41} = 1890 mm^2 / m$$

# of bars = 1890/285 = 6.63

$$Spacing = \frac{1000}{6.68} = 151 \ mm \rightarrow 19 \ mm \ bars @ 150 \ mm$$

Option 1

All others (16 mm diameter)

$$\rho = 0.0035$$

$$A_{frp} = 0.0035 \times 1000 \times 155 = 542.5 \ mm^2 / m$$

# of bars = 542.5/200 = 2.71

$$Spacing = \frac{1000}{2.71} = 368 \ mm \rightarrow Use \ 300 mm \ \max imum \ spacing$$

Option 2

All other bars (13 mm diameter)

# of bars = 542.5/130 = 4.17

$$Spacing = \frac{1000}{4.17} = 240 \quad mm \rightarrow Use \quad 13 \quad mm \quad bars \, @ \, 225 \quad mm$$

Use Option #2 for efficiency of bar usage and cost.
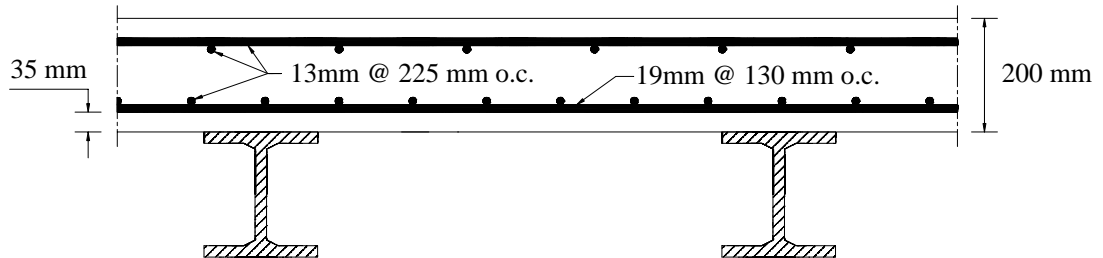
Figure 6.8: FRP Reinforcement for GFRP-Reinforced Bridge Deck Slab Example.

7.1 Definitions

A	effective tension area of concrete surrounding the flexural tension reinforcement and bearing the same centroid as that reinforcement, divided by the number of rebars, mm^2
b	width of cross-section, mm
c	depth of neutral axis, mm
d	distance from extreme compression surface to the tension reinforcement, mm
d_c	concrete cover measured from the centroid of tension reinforcement to the extreme tension surface, mm
E_c	modulus of elasticity of concrete, MPa
E_{frp}	modulus of elasticity of FRP, MPa
E_s	modulus of elasticity of steel, $200x10^3$ MPa
f_{frp}	stress in FRP reinforcement, MPa
f_{frps}	stress in FRP at service load, MPa
f_r	modulus of rupture of concrete, MPa
f_y	yield stress of steel, MPa
h	member thickness, mm
h_1	distance from the centroid of tension reinforcement to the neutral axis, mm
h_2	distance from the extreme tension surface to the neutral axis, mm
I_{cr}	moment of inertia of cracked section, mm^4
I_e	effective moment of intertia, mm^4
I_g	gross moment of inertia, mm^4
I_t	moment of inertia of uncracked section transformed to concrete, mm^4
k_b	bond dependent coefficient
ℓ	length of member, mm
ℓ_n	clear span, mm
M_a	applied moment, N·mm
M_{cr}	cracking moment, N·mm
n_{frp}	modular ratio
w	crack width, mm
α_b	bond dependent coefficient
α_d	coefficient equal to 0.55 for T-section and 0.40 for rectangular section reinforced with FRP
β_b	bond reduction coefficient
δ	deflection, mm
ε_{frp}	strain in FRP
ε_{frps}	strain in FRP at service load
ε_s	strain in steel
Ψ	curvature
ρ_{frp}	reinforcement ratio

7.2   General

FRP bars have higher strength, f_{frpu}, than the specified yield strength, f_y, of commonly-used steel reinforcing bars. However, because the modulus of elasticity of FRP bars, E_{frp}, is typically lower than that for steel, E_s, the higher strength cannot be fully utilized in reinforced concrete structures. Hence, the design is mainly to control deflection and crack width. In addition, the stress in the FRP reinforcement must be checked against allowable SLS stresses given in Section 5.

The concept of a transformed section applies for FRP-reinforced concrete with the transformed section being used for all calculations related to crack width and deflection. No lower limit is superimposed on the modular ratio, n_{frp} (E_{frp}/E_c). The value obtained from the actual material properties should be used.

Steel-reinforced concrete structures are generally designed for ultimate moment capacity and checked for limiting deflection or crack width. This is not the case for FRP-reinforced concrete. Requirements for limiting crack width and deflection are crucial in these types of members since the large curvatures subsequent to cracking lead to large strain in the reinforcement. The following sections discuss different serviceability limits.

7.3   Calculation of Service Stresses

As with steel-reinforced members, it is generally assumed that the concrete is still approximately linear elastic. As well, the general assumptions of no bond slip and plane sections remain plane are also used leading to the situation shown in Figure 7.1. The service stress calculation for the FRP-reinforced section follows the approach shown below. If desired, the designer may choose a more rigorous approach using the non-linear concrete compression model given in Section 5 and use the tension failure approach without any material resistance factors.
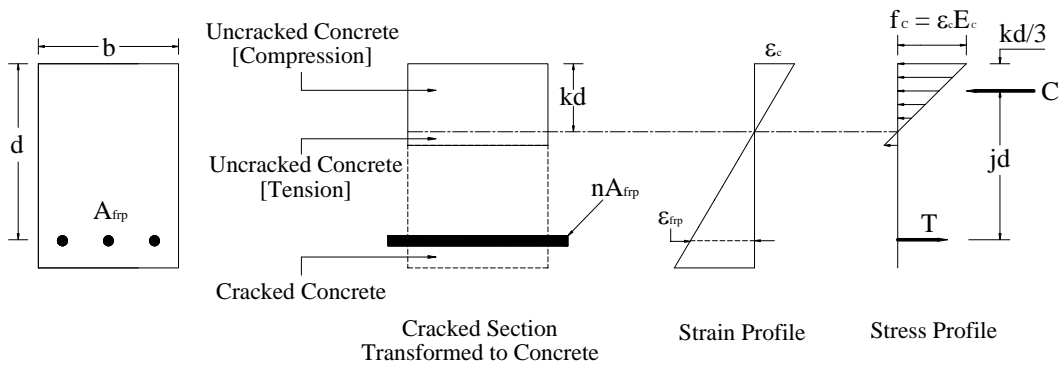
Figure 7.1: Service Stress Condition.

$$n_{frp} = \frac{E_{frp}}{E_c}$$

Equation 7.1

$$\rho = \frac{A_{frp}}{bd}$$

Equation 7.2

$$k = \sqrt{(\rho n_{frp})^2 + 2\rho n_{frp}} - \rho n_{frp}$$

Equation 7.3

$$j = 1 - \frac{k}{3}$$

Equation 7.4

$$f_{frp} = \frac{M_s}{A_{frp} \cdot j \cdot d}$$

Equation 7.5

The value of the f_{frp} can then be compared against allowable limits given in Section 5.

7.4 Cracking

To address the issue of cracking of FRP-reinforced sections, the designer may choose one of two approaches: limiting the service strain (Section 7.4.2) or checking crack width directly (Section 7.4.3). Where specific crack width limits are to be satisfied, the latter approach is preferred. The strain limit approach may be very effective in initial design to limit iterations. The crack width may then be specifically checked as part of the final design.

The issue of limiting crack width is discussed in Section 7.4.1.

7.4.1 Permissible Crack Width

In steel-reinforced concrete, it is necessary to reduce the crack width in order to inhibit the corrosion of steel reinforcement. This is not a requirement for FRP-reinforced concrete due to the excellent corrosion resistance of FRP materials. Crack width limitations may arise for aesthetic reasons and to provide an environment that will not initiate concerns about personal safety. Crack width must also be limited where leakage is concerned.

When maximum crack width is considered, the following issues need to be addressed:
- Exposure type (internal or external)
- Aggressiveness of the environment for GFRP
- Type of structure (whether the intended use of the structure may be affected by cracking)
- Visibility of concrete surfaces
- Anticipated life of the structure

If the structure is not occupied, as would be the case for a culvert structure, the crack limit does not need to be considered; however, the maximum stress limits for the reinforcement must be satisfied.

CHBDC (2006) specifically limits crack width for FRP-reinforced components to 0.5 mm.

7.4.2 Strain Limit Approach

The parameters that influence crack width are the crack spacing, the quality of bond between the concrete and reinforcing bars and, above all, the strain in the bars. To control the width of cracks, ACI 318-99 (1999) limits the stress in steel reinforcement at service to 60 percent of f_y. When $f_y = 400$ MPa, the allowable strain in steel bars in service, ε_s, is:

$$\varepsilon_s = \frac{0.6 \times 400}{200000} = 1200 \times 10^{-6}$$
<div align="right">Equation 7.6</div>

The deterring of corrosion of steel is one motive for controlling the width of cracks. When steel reinforcing bars are used, allowable crack widths of 0.4 mm and 0.3 mm for interior and exterior exposure, respectively, are normally used. When FRP bars are employed, there is no risk of corrosion. It is recommended that limiting the crack width to 0.7 mm and 0.5 mm for interior and exterior exposure, respectively, is acceptable for FRP-reinforced components. From this, it is seen that the width of cracks allowed for FRP-reinforced members is 1.7 or 1.5 times the value allowed for steel-reinforced members.   In the following discussion, it is assumed that the ratio between crack widths of FRP and steel-reinforced beams is 5/3. Furthermore, it is assumed that the width of cracks is proportional to the strain in the reinforcement. Thus, the allowable strain and stress in the FRP reinforcement at service may be assumed as:

$$\varepsilon_{frps} = \frac{5}{3}\varepsilon_s = 2000 \times 10^{-6}$$
<div align="right">Equation 7.7</div>

$$f_{frps} = E_{frp}\varepsilon_{frps}$$
<div align="right">Equation 7.8</div>

ε_{frps} strain in FRP at service load
E_{frp} modulus of elasticity of FRP, MPa
f_{frps} stress in FRP at service load, MPa

This is significantly lower than the service stress limits given in Section 5. If applicable, the designer may choose to increase limiting strain value and calculate the crack width directly in Section 7.4.3.

7.4.3 Crack Width Calculation

If there is a need to calculate the crack width for special applications, the calculation can be performed based on revised coefficients for the Gergely-Lutz equation (Gergely and Lutz, 1968), widely used for steel-reinforced concrete. These modifications have been developed for a specific type of FRP reinforcement and therefore, their use is limited. The original work by Gergely

and Lutz (1968) reported problems in developing a formula to fit all available data for steel-reinforced concrete. Nevertheless, the Gergely-Lutz equation includes the most important parameters: the effective area of concrete in tension, the number of bars, the reinforcement cover, the strain gradient from the level of the reinforcement to the tensile face, and the stress in the flexural reinforcement.

For FRP-reinforced members, it is necessary to consider the bond properties of the bar when calculating crack width. The following equation can be used when the bond properties of the bar are known:

$$w = 2.2k_b \frac{f_{frp}}{E_{frp}} \frac{h_2}{h_1} (d_c A)^{1/3}$$

Equation 7.9

w	crack width at the tensile face of the beam, mm
E_{frp}	modulus of elasticity of FRP, MPa
k_b	bond dependent coefficient. For FRP bars having bond properties similar to concrete, $k_b=1.0$. For FRP bars with inferior bond behaviour, $k_b>1.0$. For FRP bars with superior bond behaviour, $k_b<1.0$. In the absence of significant test data $k_b =1.2$ is recommended.
f_{frp}	stress in the tension FRP reinforcement at location of the crack, MPa
h_2	distance from the extreme tension surface to the neutral axis, mm
h_1	distance from the centroid of tension reinforcement to the neutral axis, mm
d_c	concrete cover measured from the centroid of tension reinforcement to the extreme tension surface, mm
A	effective tension area of concrete surrounding the flexural tension reinforcement and having the same centroid as that reinforcement, divided by the number of rebars, mm²

CHBDC (2006) presents an alternative equation for determining crack width in bridge applications which may also be used.

7.5   Deflection

The modulus of elasticity of FRP is generally smaller than that of steel. Therefore, members having the same concrete cross-section and the same loading typically exhibit larger deflection when FRP is used. However, by appropriate choice of the minimum thickness and by adopting an allowable stress in the FRP at service, the ratio of the span to the deflection can be the same as with steel-reinforced members.

The designer may also choose to calculate deflection directly using the moment of inertia given in Section 7.5.2 or the curvature approach given in Section 7.5.3.

Until an engineer is experienced in the design of FRP-reinforced components, it is recommended that the initial member thickness be selected by the method given in Section 7.5.1 and then checked by direct calculation of deflection. This direct check of deflection is especially important in applications where controlling serviceability deflection is critical. The engineer must also check

deflections under sustained loads, including additional deflection due to creep of the concrete.

7.5.1   Minimum Thickness of Members Reinforced with FRP

Reinforced concrete design codes specify span-to-thickness ratios in order to avoid excessive deflection. For example, for simply-supported one-way slabs and T-beams reinforced with steel:

$$h = \frac{\lambda}{20} \qquad\qquad (for\,slabs);$$
$$h = \frac{\lambda}{16} \qquad\qquad (for\,T-beams);$$

Equation 7.10

The codes specify other ℓ/h ratios for other end conditions.

FRP bars have relatively low modulus of elasticity, E_{frp}, compared to steel. Thus, members reinforced with FRP are relatively more vulnerable to excessive deflection. Different FRPs have different E_{frp}. Thus, the ℓ/h ratio to be used in design will depend upon the type of FRP. Experience has shown that the values of $(\ell/h)_s$ specified by codes give satisfactory ratios of span to deflection (ℓ/δ) when the reinforcement is steel. The $(\ell/h)_{frp}$ for use with FRP should give the same (ℓ/δ) ratios.

Equation for span to depth ratio for members reinforced with FRP of any type:

$$\left(\frac{\lambda_n}{h} \right)_{frp} = \left(\frac{\lambda_n}{h} \right)_s \left(\frac{\varepsilon_s}{\varepsilon_{frp}} \right)^{\alpha_d}$$

Equation 7.11

Subscripts *frp* and *s* refer to FRP and steel, respectively.

ℓ_n	clear span between faces of support, mm
h	member thickness, mm
ε	maximum strain allowed in the reinforcement in service
α_d	dimensionless coefficient, 0.50 for rectangular section, $0.50 + 0.03$ (b/b_w) - $b/(80h_s)$ for T-section, where b and b_w are width of flange and width of the web, respectively; h_s is the hypothetical minimum thickness required by CSA A23. 3-05 if steel is used as reinforcement.
$(\ell_n/h)_{frp}$	ratio of span to depth for FRP reinforced member
(ℓ_n/h)	ratio of span to depth for steel reinforced member
$(\varepsilon_s/\varepsilon_{frp})$	ratio of service strain in steel to service strain in FRP

When the ratio $(\ell_n/h)_{frp}$ of length to thickness of a member reinforced with FRP satisfies Equation 7.11, its length to deflection ratio $(\ell_n/\delta)_{frp}$ will be approximately the same as that of a conjugate member having its length to thickness equal to $(\ell_n/h)_s$. Equation 7.11 has been developed and verified by parametric studies (Hall and Ghali, 2000). The ratio of length to minimum

thickness $(\ell_n/h)_s$ for members reinforced with steel bars is specified in CSA A23.3-05 to control deflection. Table 7.1 is a copy from this code.

Table 7.1 — Minimum Thickness of Steel-Reinforced Concrete (CSA-A 23.3-05)			
Thickness Below Which Deflections Must be Computed for Non-prestressed Beams or One-way Slabs Not Supporting or Attached to Partitions or Other Construction Likely to be Damaged by Large Deflections (See Clauses 9.8.2.1 and 9.8.5)			
	Minimum Thickness, h		
	Simply Supported	One End Continuous	Both Ends Continuous	Cantilever
Solid one-way slabs	$\ell_n/20$	$\ell_n/24$	$\ell_n/28$	$\ell_n/10$
Beams or ribbed one-way slabs	$\ell_n/16$	$\ell_n/18.5$	$\ell_n/21$	$\ell_n/8$
Note: Values given shall be used directly for members with normal density concrete, where $\gamma_c > 2150$ kg/m^3, and Grade 400 reinforcement. For other conditions, the values shall be modified as follows: (a) for structural low-density concrete and structural semi-low-density concrete, the values shall be multiplied by $(1.65 - 0.0003\,\gamma_c)$, but not less than 1.00, where γc is the density in kg/m^3; and (b) for f_y other than 400 MPa, the values shall be multiplied by $(0.4 + f_y/670)$.			

The values $(\ell_n/h)_s$ given by CSA A23.3-04 are intended for steel-reinforced members (Table 7.1). To control width of cracks, the same standard requires that the strain in steel at a cracked section does not exceed 60 percent of the specified yield stress f_y corresponding to $\varepsilon_s = 1200 \times 10^{-6}$ with $f_y = 400$ MPa. Thus, the value $\varepsilon_s = 1200 \times 10^{-6}$ should be used in Equation 7.11 and ε_{frp} selected by the designer. It is recommended here to take $\varepsilon_{frp} \leq 2000 \times 10^{-6}$. The cracks to be expected with this strain are $(\varepsilon_{frp}/\varepsilon_s)$ times wider. When ε_{frp} is chosen greater than ε_s, the minimum thickness h_{frp} should be greater than h_s for members of the same span.

7.5.2   Effective Moment of Inertia Approach

This section is concerned only with reinforced concrete members without prestressing that are subjected to bending without axial force. If the service load level is less than the cracking moment, M_{cr}, the immediate deflection can be accurately evaluated using the transformed moment of inertia, I_t. If the service moment exceeds the cracking moment, CSA A23.3-04 recommends the use of the effective moment of inertia, I_e, to calculate the deflection of cracked steel-reinforced concrete members. The procedure entails the calculation of a moment of inertia, which is assumed uniform throughout the beam. This value is used in deflection equations based on linear elastic analysis.

The effective moment of inertia I_e, is based on empirical considerations. It has yielded satisfactory results in applications when the maximum bending moment at service is greater than $2M_{cr}$, where M_{cr} is the value of the moment just sufficient to cause flexural cracking (Ghali and Azarnejad, 1999).

Investigators initially applied the code-based effective moment of inertia concept to FRP-reinforced concrete members, but they discovered that predictions of deflections based on this concept were not in agreement with experimental data. Accordingly, attempts were made to modify the I_e expression in order to make it applicable to FRP-reinforced concrete members. The modified expressions were

again based on the assumption that a uniform moment of inertia can be substituted for the actual variable moment of inertia of the beam along its length.

Mota et al. (2006) examined a number of the suggested formulations for I_e and found that Equation 7.12 provided the most consistently conservative results over the entire range of test specimens. In lieu of experimental results or specific expertise of the designer in this field, it is recommended that this equation be used in design.

$$I_e = \frac{I_t I_{cr}}{I_{cr} + \left(1 - 0.5\left(\frac{M_{cr}}{M_a}\right)^2\right)(I_t - I_{cr})}$$

Equation 7.12

where I_t is moment of inertia of a non-cracked section transformed to concrete.

Moment of Inertia of Transformed Cracked Section

The cracked moment of inertia, I_{cr}, for rectangular sections is given by:

$$I_{cr} = \frac{b(kd)^3}{3} + n_{frp} A_{frp} (d - kd)^2$$

Equation 7.13

b	width of cross-section, mm
d	depth to FRP layer , mm
k	given by Equation 7.3

7.5.3   Curvature Approach

CSA S806-02 recommends the integration of curvature along the span to determine deflection. When curvature Ψ is known, the virtual work method can be used to calculate deflection of concrete frames under any load level with the integral being for all members of the structure:

$$\delta = \int m\psi dx$$

Equation 7.14

For a cracked reinforced concrete member without prestressing and subjected to bending moment M without axial force, the curvature at any section can be calculated by:

$$\psi = \frac{M}{E_c I_e}$$

Equation 7.15

The transverse deflection at mid-length of a member, measured from the chord joining its ends can be calculated by Equation 7.16, which can be derived from Equation 7.14.
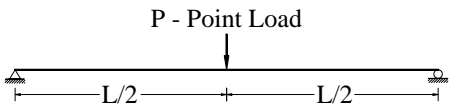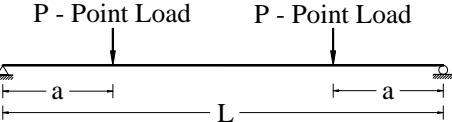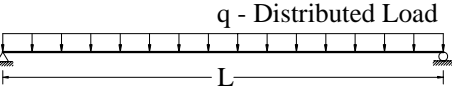
$$\delta = \frac{\lambda^2}{96}(\psi_{end1} + 10\psi_{mid} + \psi_{end2})$$

Equation 7.16

$\Psi_{end1}, \Psi_{end2}, \Psi_{mid}$ curvatures at two ends and at the middle

This equation implies the assumption of parabolic variation of Ψ. For simply supported beam:

$$\delta = \frac{10\psi_{mid}\lambda^2}{96}$$

Equation 7.17

Although this method also produces conservative predictions of deflection, it is generally more tedious to employ. As an aid, Table 7.2 provides formulas derived from this method for simply supported beam cases.

Table 7.2 — Maximum Deflection Formulas Using the Curvature Approach	
Load/Beam Type	Formula
P - Point Load, L/2 + L/2	$\delta_{max} = \frac{PL^3}{48E_cI_{cr}}\left[1 - 8\eta\left(\frac{L_g}{L}\right)^3\right]$
P - Point Load P - Point Load, a, L, a	$\delta_{max} = \frac{PL^3}{24E_cI_{cr}}\left[3\left(\frac{a}{L}\right) - 4\left(\frac{a}{L}\right)^2 - 8\eta\left(\frac{L_g}{L}\right)\right]^3$
q - Distributed Load, L	$\delta_{max} = \frac{5qL^4}{384E_cI_{cr}}\left[1 - \frac{192}{5}\eta\left[\frac{1}{3}\left(\frac{L_g}{L}\right)^3 - \frac{1}{4}\left(\frac{L_g}{L}\right)\right]\right]$

Where L_g = length of beam still uncracked, mm

$$\eta = (1 - \frac{I_{cr}}{I_g})$$

7.5.4   Deflection Under Sustained Load

Ghali and Favre (1994) and El-Badry and Ghali (1989) give a procedure for calculation of long-term curvature at a reinforced concrete cracked or uncracked section with or without prestressing. When the reinforcement is with FRP materials, the same procedure can be applied with appropriate values of elasticity modulus and relaxation of the reinforcements. Once the curvature at various sections is determined, the deflection can be calculated by Equation 7.15. Hall and Ghali (2000-2) have verified the validity of the procedure when FRP materials are used. Only limited experimental long-time deflection data are available in the literature. On the other hand, extensive test data on immediate deflection of simple beams are available. Using this data, Hall (2000) has shown that the procedure described in this section gives a more accurate prediction of deflection compared to the use of any of the methods which assume I_e to be constant over the member length.

The procedure described above is adopted in ACI 435 (2000) for concrete construction reinforced with steel or with FRP. The codes ACI 318-99 and CSA A23.3-05 allow the use of the effective moment of inertia approach for non-prestressed members in flexure (without axial force). The same codes also permit more comprehensive analysis. ACI 421 (2000) adopts the procedure described above as a comprehensive treatment for prediction of the displacements of reinforced concrete frames with or without prestressing.

In lieu of specific knowledge or investigation by the designer, it is recommended that the approached used in ACI 318 and CSA A23.3 be used to account for the influence of creep on long-term deflection. The deflection under sustained loads, Δ_s, can be calculated as $(1+\xi)$ times the immediate deflection, Δ_i, or $\Delta_s = (1+\xi)\Delta_i$. The creep parameter, ξ, is taken as:

> 1.0 after 3 months,
> 1.2 after 6 months,
> 1.4 after 12 months,
> 2.0 for 5 years or more.

7.5.5   Permissible Deflection

Based on CSA A23.3-05, the deflection calculated according to the effective moment of inertia, or the moment-curvature method must satisfy the following requirements. These are the same as the requirements for steel-reinforced concrete structures.

If the deflection calculated using the cracked moment of inertia satisfies the permissible deflection limit, there is no need to find the deflection using effective moment of inertia.

Table 7.3 — Maximum Permissible Deflections‡		
MEMBER TYPE	DEFLECTION TO BE CONSIDERED	DEFLECTION LIMITATION
Flat roofs not supporting or attached to non-structural elements likely to be damaged by large deflections	Immediate deflection due to specified live load	ℓ_n/180 *
Floors not supporting or attached to non-structural elements likely to be damaged by large deflections	Immediate deflection due to specified live load	ℓ_n/360
Roof or floor construction supporting or attached to non-structural elements likely to be damaged by large deflections	That part of the total deflection occurring after detachment of non-structural elements (sum of the long-time deflection due to all sustained loads and the immediate deflection due to any additional live load)‡	ℓ_n/480 †
Roof or floor construction supporting or attached to non-structural elements not likely to be damaged by large deflections		ℓ_n/240 §

‡ Long-time deflections shall be calculated under sustained load, but may be reduced by the amount of deflection calculated to occur before the attachment of non-structural elements.

* Limit not intended to safeguard against ponding. Ponding should be checked by suitable calculations of deflection, including added deflections due to ponded water, and considering long-time effects of all sustained loads, camber, construction tolerances, and reliability of provisions for drainage.

† Limit may be exceeded if adequate measures are taken to prevent damage to supported or attached elements.

§ But not greater than the tolerance provided for non-structural elements. Limit may be exceeded if camber is provided so that total deflection minus camber does not exceed the limit.

7.5.6 Example: Determining Minimum Thickness using Span-to-Deflection Ratio

Consider a one-way slab of clear span ℓ_n = 4000 mm. Determine the minimum thickness assuming GFRP with allowable strain at service ε_{frp} = 2000 x 10^{-6}.

For the case considered, CSA A23.3-05 specifies $(\ell_n/h)_s$ = 20. For the slab reinforced with FRP, (Equation 7.6):

$$\left(\frac{\lambda_n}{h}\right)_{frp} = 20\left(\frac{1200\times10^{-6}}{2000\times10^{-6}}\right)^{0.5}$$

$$\left(\frac{\lambda_n}{h}\right)_{frp} = 15.5$$

Minimum thickness for the considered slab:

$$h = \frac{4000}{15.5} = 258 \quad mm$$

7.6 Example of Service Stress, Crack Width and Deflection Calculations

A simply-supported one-way slab with 150 mm thickness and 3300 mm span is subjected to a specified live load of 4.8kPa and dead load of 1.0kPa. The concrete properties are $f_c' = 30$ MPa , $E_c = 24650$ MPa and $\gamma_{conc} = 23.5$ kN/m³ . The GFRP reinforcing bars are #16 bars at 100 mm spacing with diameter = 15.9 mm, Area= 198 mm² , $f_{frpu} = 680$ MPa, $E_{frp} = 48200$ MPa, bond quality $k_b = 1.2$. The concrete cover for reinforcement is 35mm.

Determine: 1) Service stress in FRP under dead load and live load
                      2) Crack width under dead load and live load
                      3) Immediate deflection under live load

1) Service stress in FRP:

$$d = 150 - 35 - 15.9/2 = 107 \text{ mm}$$
$$w_{DL+LL} = 23.5 \times 0.15 + 4.8 + 1.0 = 9.3\, kN/m^2 = 9.3 \times 10^{-3}\, N/mm^2$$

Maximum of the moment is:

$$M_s = \frac{wl^2}{8} = \frac{9.3 \times 10^{-3} \times (3300)^2}{8} = 12.7 \times 10^6 \quad N \cdot mm/m$$

Area of reinforcement per meter of width:

$$A_{frp} = 198 \times 1000/100 = 1980 \quad mm^2$$

$$n_{frp} = \frac{E_{frp}}{E_c} = \frac{48200}{24648} = 1.96$$

$$\rho = \frac{A_{frp}}{bd} = \frac{1980}{1000 \times 107} = 0.0185$$

$$k = \sqrt{(\rho n_{frp})^2 + 2\rho n_{frp}} - \rho n_{frp}$$

$$= \sqrt{(0.0185 \times 1.96)^2 + 2 \times 0.0185 \times 1.96} - (0.0185 \times 1.96) = 0.235$$

$$j = 1 - \frac{k}{3} = 1 - \frac{0.235}{3} = 0.92$$

$$f_{frp} = \frac{M_s}{A_{frp} \cdot j \cdot d} = \frac{12.7 \times 10^6}{1980 \times 0.92 \times 107} = 65 \quad MPa$$

Allowable tensile stress in GFRP is 30 percent of tensile failure stress. So:

$$f_{allowable} = 0.3 \times 680 = 204 \quad MPa > f_{frp} = 65 \quad MPa$$

2) Calculate crack width:

$$w = 2.2k_b \left(\frac{f_{frp}}{E_{frp}} \right) \frac{h_2}{h_1} \left(\sqrt[3]{d_c A} \right)$$

$$kd = 0.235 \times 107 = 25.2 \quad mm$$

$$d_c = 35 + 15.9 / 2 = 42.5 \quad mm$$

$$h_2 = 150 - 25.2 = 124.8 \quad mm$$

$$h_1 = 124.8 - 42.5 = 82.3 \quad mm$$

# of bars per m = 1000/100 = 10

$$A = 2bx \Big/ \text{\# of bars} = \frac{2(1000)(42.5)}{10} = 8590 \, mm^2$$

$$w = 2.2. \times 1.2 \times \left(\frac{65}{48200} \right) \times \left(\frac{124.8}{82.3} \right) \left(\sqrt[3]{(42.5)(8590)} \right) = 0.39 \, mm < 0.5 \, mm \quad O.K.$$

3) Calculate immediate live load deflection

A_{frp} = 10 bars per m x 198 = 1980 mm^2/m

$$y_t = \frac{1000 \times 150 \times (150 / 2) + (1.96 - 1) \times 1980 \times 42.5}{1000 \times 150 + (1.96 - 1) \times 1980} = 74.6 \quad mm$$

$$I_t = \frac{1000 \times 150^3}{12} + 1000 \times 150(74.6 - 150 / 2)^2 + (1.96 - 1)(1980)(74.6 - 42.5)^2 = 283.2 \times 10^6 \, mm^4$$

$$I_{cr} = \frac{b(kd)^3}{3} + nA_{frp}(d - kd)^2$$

$$= \frac{(1000)(25.2)^3}{3} + (1.96 \times 1980)(107 - 25.2)^2 = 31.3 x 10^6 \, mm^4 / m$$

$$M_{cr} = \frac{f_r I_t}{y_t} = \frac{(0.6 \times \sqrt{30}) \times 283.3 \times 10^6}{74.6} = 12.5 \times 10^6 \, N.mm / m$$

$$I_e = \frac{I_t I_{cr}}{I_{cr} + \left(1 - 0.5 \left(\frac{M_{cr}}{M_a} \right)^2 \right)(I_t - I_{cr})}$$

$$I_e = \frac{\left(283.2 \times 10^6\right) \times \left(31.3 \times 10^6\right)}{31.3 \times 10^6 + \left[1 - 0.5\left(\frac{12.5}{12.7}\right)^2\right] \times \left(282.3 \times 10^6 - 31.3 \times 10^6\right)} = 55.0 \times 10^6 \, mm^4 \, / \, m$$

$$\Delta_{LL} = \frac{5}{384} \frac{4.8(3300)^4}{24650 \times 55.0 \times 10^6} = 5.5 \quad mm < \Delta_{allowable} = \frac{1}{360} = \frac{3300}{360} = 9.2 \quad mm$$

8.1 Definitions

A_{frp} area of FRP bar, mm²
d_b bar diameter, mm
f_{cr} flexural cracking strength of concrete, MPa
f_{frp} stress in FRP reinforcement, MPa
f_{frpu} ultimate strength of FRP, MPa
ℓ_{frpd} development length, mm
ℓ_{frpdh} development length of a hooked bar, mm
μ_{frp} bond strength, MPa

8.2 General

In order for concrete to be FRP-reinforced, there must be bond (force transfer) between the FRP and concrete. Bond of FRP bars depends on the bar diameter, surface condition, embedment length, and shape. Bond of FRP bars is good compared to the bond of steel bars. However, it has been found by many researchers that bond failure of FRP bars is initiated by shearing off at the surface of the FRP bar. Steel bond failure was due to crushing of concrete in the vicinity of bar deformations. In contrast to steel bars, bond of FRP bars does not depend on the strength of concrete (Benmokrane et al., 1997).

8.3 Development Length and Anchorage

Development length is the shortest length of bar in which the stress can increase from the initial zero stress to the ultimate strength, $f_{frpu.}$ From mechanics, for a straight bar this can be expressed as follows:

$$\lambda_{frpd} \pi d_b \mu_{frp} = A_{frp} f_{frpu} \qquad \text{Equation 8.1}$$

ℓ_{frpd} development length, mm
d_b bar diameter, mm
μ_{frp} bond strength, MPa
A_{frp} area of FRP bar, mm²
f_{frpu} ultimate strength of FRP, MPa

Both CSA S806-02 and CHBDC (2006) provide different equations for determination of development length. The CHBDC approach is recommended and is presented below.

The development length of a FRP reinforcing bar in tensile shall be:

$$l_d = .45 \frac{k_1 k_4}{\left(d_{cs} + k_{tr} \dfrac{E_{frp}}{E_s}\right)} \left(\frac{f_{frp}}{f_{cr}}\right) A_{frp}$$

Equation 8.2

Where

k_1 is a bar location factor.
=1.3 for horizontal reinforcement placed so that more than 300 mm of fresh concrete is cast below the bar.
=1.0 for all other cases.

k_4 is a bar surface factor representing the ratio of bond strength of FRP to that of steel rebar having same cross-sectional area, but not greater than 1.0.
=0.8 in absence of manufacturer or test data.

d_{cs} is the smaller of the distance from the closest concrete surface to the centre of the bar being developed, or 2/3 of the centre-to-centre spacing of bars being developed, mm\

k_{tr} is a transverse reinforcement index specified in clause 8.15.2.2 of CHBDC (2006).

$$\left(d_{cs} + k_{tr} \frac{E_{frp}}{E}\right) \le 2.5 d_b$$

8.4   Splicing of FRP Reinforcement

Section 12 of CSA A23.3-05, distinguishes between two types of tension lap splices depending on the fraction of the bars spliced in a given length and on the reinforcement stress in the splice. Table 8.1 is a reproduction of the CSA A23.3-05 Table 12.2, with some modifications applicable to FRP reinforcement. For steel reinforcement, the splice length for a Class A splice is 1.0 ℓ_d and for a Class B splice is 1.3 ℓ_d.

Table 8.1 – Type of Tension Lap Splice Required			
$\dfrac{A_{frp,provided}}{A_{frp,required}}$	$\dfrac{f_{frp}}{f_{frpu}}$	Maximum percentage of A_{frp} spliced within required lap length	
		50 percent	100 percent
2 or more	0.5 or less	Class A	Class B
less than 2	more than 0.5	Class B	Class B

Research on FRP lap splices (Benmokrane et al., 1997) indicates the ultimate capacity of FRP is achieved at 1.6 ℓ_{frpd} for Class B FRP splices. Currently, data

are not available for the minimum development length for Class A FRP splices. Since the length of a splice is related to its strength and as the stress level in FRP bars is relatively low compared to its ultimate strength, the value of 1.3 ℓ_{frpd} is conservative for Class A FRP splices.

9.1 Definitions

A_{frp} area of FRP reinforcement, mm²
b   width of a cross-section, mm
d   effective depth of cross-section, mm
f_c' specified compressive strength of concrete, MPa
f_{frps} allowable stress in the FRP in service, MPa
M_s service load moment, N·mm
M_u ultimate moment, N·mm
Δ_u ultimate deflection, mm
Ψ_u ultimate curvature (ε_c/c)

9.2 Deformability

Ductility in steel-reinforced concrete is quantified by a ratio of values of displacements or curvatures at ultimate to those at yielding of steel. Despite the fact that FRP does not yield, concrete flexural components with FRP reinforcement also exhibit substantial deflection prior to failure. Jaeger et al. (1997) introduced the concept of deformability as means of quantifying this deformation characteristic and providing a means of comparison between the level of safety between ultimate and service states. CHBDC (2006) and Jaeger et al. (1997) assess the deformability of sections reinforced with FRP by a "deformability factor" presented in Equation 9.1. The values $\psi_u M_s$ correspond to the curvature and moment at service. Currently, CHBDC defines the service state as the strain state corresponding to a maximum compressive strain in concrete of 0.001. CHBDC requires that the deformability factor be greater than 4 or 6 for rectangular and T-sections, respectively. Newhook et al. (2000) have suggested that the values $\psi_u M_s$ should correspond to actual service limit state and presented a formulation for using the limiting service strain values in the FRP as a basis for deformability-based design.

$$Deformability \quad factor \quad = \quad \left(\frac{\psi_u M_u}{\psi_s M_s} \right)$$

Equation 9.1

$$Curvature \quad factor \quad = \frac{\psi_u}{\psi_s} \quad , \quad \psi_u = \frac{\varepsilon_c}{c} \quad , \quad \psi_s = \frac{\varepsilon_c}{kd} = \frac{0.001}{kd} \quad , \quad \varepsilon_c = stress \quad at \quad ultimate$$

Equation 9.2

Where M is the bending moment and Ψ is the curvature, the subscripts *u* and *s* refer to ultimate limit states and service limit states, respectively.

Unless the engineer has specific experience or expertise in this area, it is recommended that the CHBDC formulation be used in design. CSA S806-02 does not require a specific check of deformability; however, CHBDC does require checking this criterion when FRP reinforcement is used in flexural components for bridges.

The values of curvature are normally calculated using Equation 9.2. The values of moment can be calculated using the flexural analysis approaches outlined in Sections 6 and 7 for ultimate and service states, respectively.

9.2 Example of Deformability Calculation

Determine deformability factor for the slab in Example 7.6; use appropriate factors from CSA S806-02.

Service state values (ε_c=0.001).

$$M_s = f_c \cdot \frac{kj}{2} bd^2 \quad where \quad f_c = E_c \cdot \varepsilon_c = 24650 \times 0.001 = 24.7 \;\; MPa$$

$$= 24.7 \times \frac{0.235 \times 0.92}{2} \times 1000 \times 107^2 = 30.6 \times 10^6 \; N.mm$$

$$\psi_s = \frac{\varepsilon_c}{kd} = \frac{0.001}{25.2} = 39.7 \times 10^{-6}$$

Ultimate state values:

$$\rho_b = \alpha_1 \beta_1 \frac{\phi_c}{\phi_f} \frac{f_c'}{f_{frpu}} \left(\frac{\varepsilon_{cu}}{\varepsilon_{cu} + \varepsilon_{frpu}} \right)$$

$$\varepsilon_{frpu} = \frac{680}{48200} = 0.014$$

$$\varepsilon_{cu} = 0.0035$$

$$\alpha_1 = 0.85 - 0.0015(30) = 0.81$$

$$\beta_1 = 0.97 - 0.0025(30) = 0.90$$

$$\phi_c = 0.65$$

$$\phi_f = 0.75$$

$$\rho_b = 0.81 \times 0.90 \times \frac{0.65}{0.75} \times \frac{30}{680} \left(\frac{0.0035}{0.0035 + 0.014} \right) = 0.0056$$

$$\rho = 0.0185 > 0.0056 \;\; so \;\; compression \;\; failure$$

Using Equation 6.9 with Φ_c and Φ_f set equal 1.0 for the nominal condition.

$$f_{frp} = 0.5 \times 48200 \times 0.0035 \left[\left(1 + \frac{4(0.81)(0.90)1.0 \times 30}{0.0185 \times 1.0 \times 48200 \times 0.0035} \right)^{1/2} - 1 \right] = 367.5 \;\; MPa$$

$$\varepsilon_{frp} = \frac{367.5}{48200} = 0.0076$$

By strain compatibility:
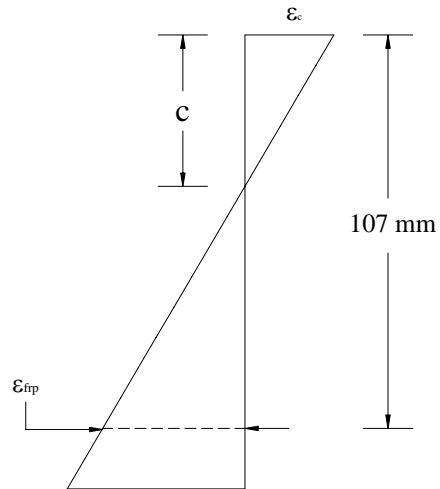
$$c = \frac{0.0035}{(0.0035 + 0.0076)} \times 107 = 33.7 \ mm$$

$$M_u = f_{frp} \times A_{frp}(d - \beta_1 c/2) = 367.5 \times 1980\ (107 - 0.9(33.7)/2) = 67 \times 10^6 \quad N.mm$$

$$\psi_u = \frac{\varepsilon_c}{c} = \frac{0.0035}{33.7} = 104.0 \times 10^{-6}$$

$$Deformability \quad factor = \frac{\psi_u M_u}{\psi_s M_s} = \frac{104.0 \times 10^{-6} \times 67 \times 10^6}{39.7 \times 10^{-6} \times 30.6 \times 10^6} = 5.7 > 4.0$$

10 SHEAR DESIGN

10.1 Definitions

A_b	area of FRP bar, mm²
A_{frpv}	area of shear reinforcement perpendicular to the axis of a member within a distance s, mm²
b_w	minimum effective web width within depth d, mm
d	distance from the extreme compression fibre to the centroid of the reinforcement, mm
d_{ct}, d_{cb}	clear cover to the stirrups at the top and bottom of the beam, respectively, mm
d_b	bar diameter, mm
d_e	effective diameter $d_e = \sqrt{4A_b/\pi}$, mm
d_v	effective depth of section in shear taken as 0.9d, mm
E_{frpl}	modulus of elasticity of flexural FRP reinforcement, MPa
E_{frpv}	modulus of elasticity of FRP stirrup, MPa
E_s	modulus of elasticity of steel, 200x10³ MPa
f_{frpv}	limiting value of tensile strength of stirrup to be used in design, MPa
f_{frpu}	ultimate tensile strength, MPa
l_d^*	tail length, mm
l_{frpd}	development length, mm
N	number of stirrups intersecting the shear plane
r_b	radius of bend, mm
s	spacing of shear reinforcement measured parallel to the longitudinal axis of the member, mm
V_c	factored shear resistance attributed to concrete, N
V_{frp}	factored shear resistance attributed to shear reinforcement, N
V_{ser}	shear force at service load level, N
$\varepsilon_{frpvser}$	strain in FRP stirrup at service load level
ε_v	limiting strain in FRP stirrup to be used in design
ϕ_{frp}	resistance factor for FRP stirrups
ϕ_c	resistance factor for concrete
λ	modification factor for density of concrete
θ	angle of inclination of shear plane
ρ_{frpv}	reinforcement ratio for shear reinforcement
ρ_{frpl}	reinforcement ratio for flexural (longitudinal) reinforcement

10.2 General

Shear design of concrete beams reinforced with FRP stirrups is, to a large extent, based on the results of extensive experimental work. The design should distinguish between beams entirely reinforced with FRP for both flexure and shear, and beams reinforced with steel for flexure and FRP stirrups for shear. Shear design of these types of structures can then take into account differences in material properties of these two reinforcement types.

During the shear design process, contributions of both concrete and stirrup reinforcement must be determined. This Section will discuss the process of calculation of the contributions from both concrete and stirrups, and determine the shear resistance of members reinforced with FRP shear reinforcement.

10.3   Beams with FRP Web Reinforcement

FRPs are widely used in round bars or rectangular shapes for flexural reinforcement and in sheet configuration for strengthening. As shear reinforcement, this material is still in a developmental stage. This section will only deal with members reinforced entirely with FRP for both flexure and shear.

Several issues need to be addressed in discussing a member reinforced with FRP for flexure and shear:
- lower dowel resistance of bars;
- lower modulus of elasticity of bars;
- high tensile strength of straight bars with sufficient embedment length; and,
- dramatic decrease in tensile strength of bent bars.

10.3.1   Types of FRP Stirrups

Two factors affecting the performance of FRP stirrups are the radius of the bend and the embedment length. Research indicates the strength of a stirrup can be reduced to 54 percent of the tensile strength of a straight bar due to stress concentrations at the bend (Morphy et al., 1997). These stress concentrations occur during manufacturing, and depend on the manufacturing process. All FRP stirrups are bent in the manufacturing plant and then shipped to the site.

According to Ehsani et al. (1995), the minimum ratio of radius of bend to the stirrup diameter is three, and FRP stirrups should be closed with 90-degree hooks. Shehata (1999) recommends using only 40 percent of the ultimate tensile strength of FRP when calculating the capacity of a stirrup.

The tensile force in the stirrup leg is transferred through the bond between the concrete and the tail of an FRP stirrup. The tail length has been investigated by Ehsani et al. (1995) and by Morphy et al. (1997). Noticeable differences have been found among different types of FRP, as well as different stirrup configurations. According to Ehsani et al. (1995), the tail length of GFRP stirrups should be at least 12 times the bar diameter. The tail length of CFRP stirrups was found to be 35 times the bar diameter for Leadline stirrups, and 15 and 20 times the bar diameter for CFCC stirrups with continuous anchorage and standard hook, respectively (Morphy et al., 1997).

10.3.2   Detailing of FRP Stirrups

The development length of hooked bars was studied by Morphy et al. (1997). Based on research on a number of bent stirrups with different embedment length and bend diameter for rectangular Leadline CFRP bar, the embedment

length to diameter ratio (l_{frpd}/d_e) sufficient to develop the full guaranteed strength is 40. For the embedment length to diameter ratio less than the limiting value, the strength can be found using the smaller value of the following:

$$f_{frpv} = \left(0.4 + 0.015 \frac{l_{frpd}}{d_e} \right) f_{frpu}$$

Equation 10.1

$$f_{frpv} = \left(0.05 \frac{r_b}{d_b} + 0.3 \right) f_{frpu}$$

f_{frpu} ultimate tensile strength, MPa
r_b radius of bend, mm
d_b bar diameter, mm

d_e effective diameter $d_e = \sqrt{4A_b/\pi}$ [mm]

l_{frpd} development length, mm

FRP stirrups may be designed using Figure 10.1 (Shehata, 1999).
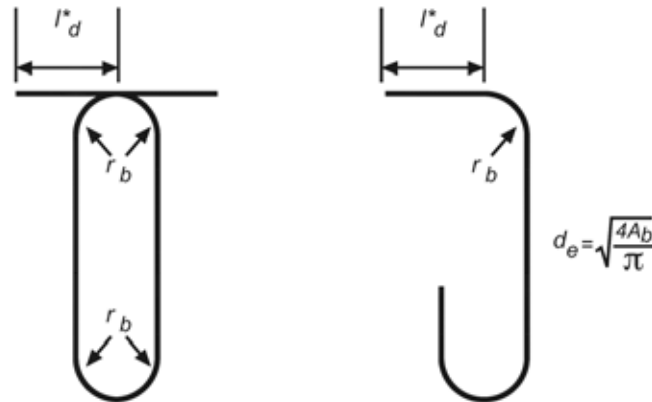
d_e= effective bar diameter
r_b= bend radius $r_b \geq$ max(4d_e,50 mm)
l_d^*= tail length $l_d^* \geq$ max(6d_e,70 mm)

Figure 10.1: Stirrup configurations (Shehata, 1999).

10.3.3   Shear Resistance Provided by FRP Stirrups

This approach is based on the criteria given in CHBDC (2006). For components with transverse FRP reinforcement perpendicular to the longitudinal axis:

$$V_{frp} = \phi_{frp} \frac{A_{frpv} \sigma_v d_v \cot \theta}{s}$$

Equation 10.2

Where

$$\sigma_v = \frac{(0.05\frac{r_b}{d_s}+0.3)f_{frpv}}{1.5}$$

Or

$$\sigma_v = E_{frpv}\varepsilon_v$$

where

$$\varepsilon_v = .0001(f_c'\frac{\rho_{frp}E_{frp}}{\rho_{frpv}E_{frpv}})^{0.5}\left\{1+2(\frac{\sigma_N}{f_c'})\right\} \le 0.0025$$

10.3.4   Maximum Strain in FRP Stirrups

To control the shear crack width in FRP-reinforced concrete beams, the strain in the stirrups at service load is limited to 0.002.

$$\varepsilon_{frpv_{ser}} = \frac{s(V_{ser}-V_c)}{A_{frpv}dE_{frpv}} \le 0.002 \qquad \text{Equation 10.3}$$

$\varepsilon_{frpv_{ser}}$	strain in FRP stirrup at service load level
V_{ser}	shear force at service load level, N
E_{frpv}	modulus of elasticity of FRP stirrup, MPa

10.4   Modes of Failure

Shear failures are brittle and, therefore, should be avoided. Due to the mechanical properties of FRP, the following issues need to be addressed in the design of FRP stirrups:

- tension capacity of FRP stirrup bent;
- required tail length for FRP stirrup; and,
- minimum radius of bend of FRP stirrup.

Shear failure is initiated by either reaching the tensile capacity of stirrups or by crushing of the web concrete. As a solution for the latter problem it is suggested to provide an upper limit on the total shear resistance of the member. For the former problem, only 40 percent of the strength of the FRP stirrup is considered. Since studies have not revealed enough information at this stage, it is appropriate to be conservative with the shear design of FRP-reinforced concrete members at this time.

As with steel-reinforced beams, the simplified shear design approach allows for calculation of the shear resistance provided by the concrete and stirrups separately.

10.5 Shear Resistance Provided by Concrete

For some members which do not contain shear reinforcement, such as slabs and footings, and beams with the effective depth not greater than 300 mm or members in which at least the minimum stirrups are provided, the factored shear resistance attributed to concrete, V_c, is calculated according to:

$$V_c = 0.2\lambda\phi_c \sqrt{f'_c}\, b_w d \sqrt{\frac{E_{frp}}{E_s}}$$

Equation 10.4

where $\sqrt{\dfrac{E_{frp}}{E_s}} \leq 1.0$

V_c factored shear resistance attributed to concrete, N
λ modification factor for density of concrete
ϕ_c resistance factor for concrete
b_w minimum effective web width within depth d, mm
d distance from the extreme compression surface to the centroid of the reinforcement, mm
E_{frp} modulus of elasticity of flexural FRP reinforcement, MPa
E_s modulus of elasticity of steel taken as 200 x 10³ MPa

For sections with an effective depth greater than 300 mm and not containing at least the minimum transverse reinforcement the concrete resistance, V_c, is taken as:

$$V_C = \left(\frac{260}{1000+d}\right)\lambda\phi_c \sqrt{f'_c}\, b_w d \sqrt{\frac{E_{frp}}{E_s}}$$

Equation 10.5

where $\sqrt{\dfrac{E_{frp}}{E_s}} \leq 1.0$

The reduction in V_c compared to steel-reinforced concrete is based on the use of longitudinal FRP reinforcement and should be used regardless of the type of transverse reinforcement used in the component.

10.6 Minimum Amount of Shear Reinforcement

Failure of a beam without shear reinforcement is sudden and brittle. Therefore, a minimum amount of shear reinforcement is required when the factored shear force, V_f, exceeds $0.5V_c$. This reinforcement is not necessary for slabs, footings, and beams with a total depth not greater than 300 mm. The minimum area of FRP shear reinforcement can be found from Equation 10.6 based on experimental work of Shehata (1999).

$$A_{frpv} = 0.06\sqrt{f'_c}\ \frac{b_w\ s}{0.0025\ E_{frpv}}$$

Equation 10.6

A_{frpv} area of shear reinforcement perpendicular to the axis of a member within a distance s, mm²

s   spacing of shear reinforcement measured parallel to the longitudinal axis of the member, mm

The minimum reinforcement ratio for shear reinforcement is derived directly from Equation 10.6 as:

$$\rho_{frpv\,min} = \frac{A_{frpv}}{b_w s} > \frac{0.06\sqrt{f'_c}}{0.0025E_{frpv}}$$

Equation 10.7

10.7 Maximum Spacing of FRP Stirrups

The spacing of transverse reinforcement, s, shall not exceed $0.7d_v$ or 600 mm.

10.8 Shear Design Example

A normal density concrete beam needs to carry a dead load of 17.5 N/mm and live load of 20 N/mm over a 6000 mm single span in addition to its own self-weight. Information on the beam cross-section and longitudinal reinforcement is provided below. Determine the required amount of shear reinforcement using GFRP ISOROD Stirrups.

GIVEN:

Dimensions: b = 350 mm   d = 515 mm   h = 600 mm   L = 6000 mm
Concrete Strength: f'_c = 40 MPa
Flexural Reinforcement: A_{frp} = 1131 mm² [2 Layers] E_{frp} = 147 GPa, d_v = 464 mm
Shear Reinforcement: f_{frpv} = 770 MPa E_{frpv} = 43.9 GPa
Section Properties: M_R = 418.9x10⁶ N·mm M_{ser} = 149x10⁶ N·mm w_{ser} = 33 N/mm
   V_{ser} = 99.3 x 10³ N [Support]

SOLUTION:

1. Design loads are calculated on the basis of factors presented for load case 2 in Table 5.1 of Section 5.4. The shear envelope is shown below and was obtained by placing the live load on half the beam length such that the design is optimized at midspan.

Factored Dead Load: w_{fDL} = 1.25[w_{DL} + w_{SW}] = 1.25[w_{DL} + $\gamma_c$bh]
   w_{fDL} = 1.25[17.5 + 23.5x10⁻⁶ x 350 x 600]
   w_{fDL} = 28.0 N/mm

Factored Live Load: $w_{fLL} = 1.5\,w_{LL}$
$w_{fLL} = 1.5 \times 20$
$w_{fLL} = 30.0 \text{ N/mm}$

Total Factored Load: $w_f = w_{fDL} + w_{fLL} = 28.0 + 30.0$
$w_f = 58 \text{ N/mm}$
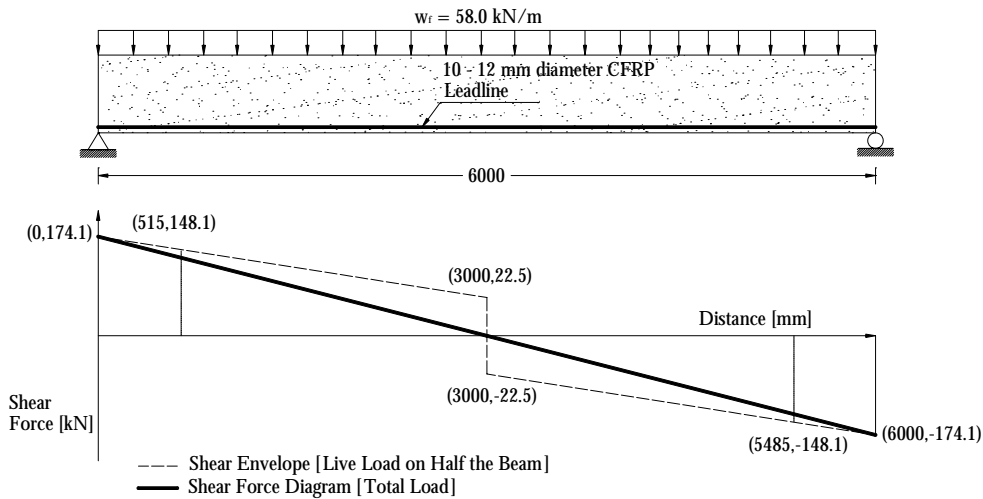
2. Contribution of concrete to shear resistance is calculated on the basis of a beam depth greater than 300 mm and the assumption that at least minimum transverse reinforcing area will be provided.

$$V_c = 0.2\lambda\phi_c\sqrt{f'_c}\,b_w d\sqrt{E_{frp}/E_s} \quad where \quad \sqrt{E_{frp}/E_s} = \sqrt{147/200} = 0.86 < 1.0$$

$$= 0.2 \times 1.0 \times 0.65 \times \sqrt{40} \times 350 \times 515 \times 0.86$$

$$= 127.5 \times 10^3\,N$$

3. For concrete beams reinforced with FRP reinforcement, stirrups are not required whenever the factored shear falls below half the shear contribution provided by the concrete.

ZONE I – No Shear Reinforcement: $V_f < \dfrac{V_c}{2} = 63.8 \times 10^3\ N$

On the basis of the shear envelope, this zone is found to extend 800 mm from each side of the beam centreline covering a total of 1600 mm within the central portion of the beam. For factored shear exceeding half the shear contribution of concrete, at least minimum transverse reinforcement should be provided.

ZONE II – Minimum Shear Reinforcement: $\qquad \dfrac{V_c}{2} \leq V_f < V_c + V_{frp\,min}$

Minimum shear contribution from the transverse reinforcement is obtained by limiting the stirrup strain to 2500×10^{-6}. Further assuming a stirrup diameter of 9.5 mm for a total transverse cross-sectional area of 70.9 mm² per leg gives the following:

$$
\begin{aligned}
V_{frp\,min} &= \varepsilon_{frpv} E_{frpv} A_{frpv} \\
&= 0.0025 \times 43900 \times 2(70.9) \\
&= 15.6 \times 10^3\,N
\end{aligned}
$$

$$V_{min} = V_c + V_{frp\,min} = 127.5 \times 10^3 + 15.6 \times 10^3 = 143.1 \times 10^3 \ N$$

$$\Rightarrow \quad 63.8 \times 10^3 \ N \leq V_f < 143.1 \times 10^3 \ N$$

The second zone therefore extends from 800 mm to 2350 mm on each side of the beam centre. Minimum shear reinforcement as that given by Equation 10.6 should be provided in this region. Continuing with the same geometrical properties for the stirrups gives an initial requirement for spacing in the second zone as well as for maximum spacing.

$$s \leq \frac{0.0025 E_{frpv} A_{frpv}}{0.06\sqrt{f'_c}\,b_w} = \frac{0.0025 \times 43900 \times 2(70.9)}{0.06\sqrt{40} \times 350} = 117.2 \ mm$$

A spacing of 100 mm should therefore be adopted in the second shear zone.

ZONE III – Shear Reinforcement Required:

$$V_c + V_{frp\,min} \leq V_f < V_{fd}$$
$$143.1 \times 10^3\,N \leq V_f < 148.1 \times 10^3\,N$$

The spacing in the third zone is calculated on the basis of criteria given in the CHBDC (2006). The shear contribution provided by the CFRP stirrups as well as that provided by the concrete is taken into account.

$$V_{frp} \geq V_{fd} - V_c \quad \Rightarrow \quad s \leq \frac{A_{frpv}\phi_f \sigma_v d_v \cot\theta}{V_{fd} - V_c}$$

Here, the stress in the stirrup ε_v is limited by equations accounting for the embedment length l_{fprd} as well as the bend radius r of the shear reinforcement without neglecting the effect of prestressing within the component. In this example, axial stresses σ_N arising from the prestressing effect are absent.

$$\sigma_v \; smallest \; of \; \begin{cases} \dfrac{\left(0.05\,^{r_b}\!\!\big/\!_{d_s} + 0.3\right)f_{frpv}}{1.5} \\[3em] \dfrac{\left(0.4 + 0.015\dfrac{l_{frpd}}{d_s}\right)f_{frpv}}{1.5} \; where \; \dfrac{l_{frpd}}{d_s} \le 40 \\[3em] 0.0001E_{frpv}\left(f'_c\,\dfrac{\rho_{frp}E_{frp}}{\rho_{frpv}E_{frpv}}\right)^{0.5} with \; \sigma_N = 0 \end{cases}$$

The bend radius r of the stirrup can be determined in conjunction with the tail length on the basis of requirements illustrated in Figure 10.1 and a stirrup bar diameter d_s of 9.5 mm. This gives us the first limiting value for stirrup stress:

Tail Length:
$$l_d^* \ge 6d_s \; or \; 70\,mm$$
$$\Rightarrow 70\,mm \; gorverns$$

Bend Radius:
$$r_b \ge 4d_s \; or \; 50\,mm$$
$$\Rightarrow 50\,mm \; gorverns$$
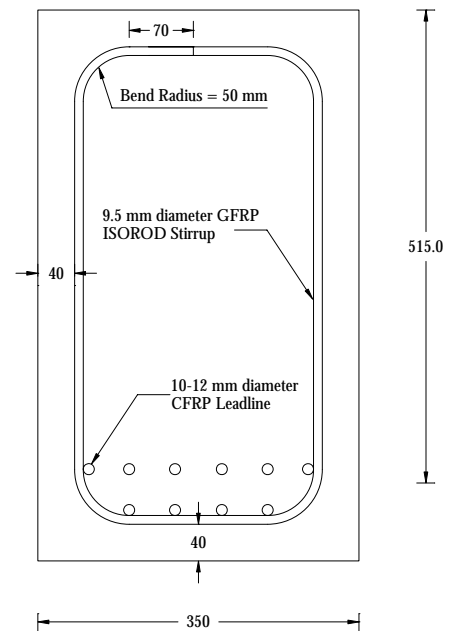
$$\sigma_v = \frac{\left(0.05\,^{r_b}\!\!\big/\!_{d_s} + 0.3\right)f_{frpv}}{1.5} = \frac{\left(0.05\cdot\,^{50}\!\!\big/\!_{9.5} + 0.3\right)\cdot 770}{1.5}$$
$$= 289.1 \; MPa$$

Using the tail length as the embedment length can be used to determine the second limitation on stirrup stresses:

$$\sigma_v = \frac{\left(0.4 + 0.015\dfrac{l_{frpd}}{d_s}\right)f_{frpv}}{1.5} \quad \text{with } l_{frpd} = 70mm$$

$$\Rightarrow \sigma_v = \frac{\left(0.4 + 0.015 \times \dfrac{70}{9.5}\right) \times 770}{1.5}$$

$$= 262.1 \; MPa$$

The third limitation on stirrup stress is obtained by iterating stirrup spacing. A trial stirrup spacing is used to determine an initial stirrup reinforcement ratio ρ_{fprv} on which the stirrup stress depends. A subsequent trial spacing as that required in the third zone is then determined on the basis of this stress and shear force at the critical section.

TRIAL #1 – Stirrup Spacing of 225 mm

$$\sigma_v = 0.0001 E_{frpv}\left(f'_c \frac{\rho_{frp}E_{frp}}{\rho_{frpv}E_{frpv}}\right)^{0.5} \quad \text{with } \rho_{frp} = \frac{A_{frp}}{bd} \; \& \; \rho_{frpv} = \frac{A_{frpv}}{bs}$$

$$\Rightarrow \sigma_v = 0.0001 \times 43900 \times \left(40 \times \frac{\dfrac{1131}{350 \times 515} \times 147000}{\dfrac{141.8}{350 \times 225} \times 43900}\right)^{0.5} = 94.8 \; MPa$$

REVISED SPACING:

$$s \le \frac{A_{frpv}\phi_f\sigma_v d_v}{V_{fd} - V_c} = \frac{141.8 \times 0.75 \times 94.8 \times 464}{(148.1 - 127.5) \times 10^3}$$

$$\Rightarrow s \le 227.1 \; mm$$

TRIAL #2 – Stirrup Spacing of 230 mm

$$\sigma_v = 0.0001 \times 43900 \times \left(40 \times \frac{\dfrac{1131}{350 \times 515} \times 147000}{\dfrac{141.8}{350 \times 230} \times 43900}\right)^{0.5} = 95.9 \; MPa$$

REVISED SPACING:

$$s \leq \frac{141.8 \times 0.75 \times 95.9 \times 464}{(148.1 - 127.5) \times 10^3} = 229.7\,mm$$

Based on results of the two previous iterations, it appears that the spacing converges to a value residing between 225 mm and 230 mm. A spacing of 200 mm can therefore be safely used in the third zone since the stress level corresponding to the third limitation on stirrup stress ($\sim$ 96 MPa) is the smallest of all calculated values. The stirrup strain ε_v (2037 x 10^{-6}) is also found to be below the 2500 x 10^{-6} requirement:

$$\varepsilon_v = 0.0001 \left(f'_c \frac{\rho_{frp} E_{frp}}{\rho_{frpv} E_{frpv}} \right)^{0.5} \leq 0.0025$$

$$= 0.0001 \times \left(40 \times \frac{1131/_{350 \times 515} \times 147000}{141.8/_{350 \times 200} \times 43900} \right)^{0.5}$$

$$= 0.002037 < 0.0025$$

Spacing from the third limitation on stirrup stress can also be obtained without the use of iteration. Substituting stirrup stress in the equation for spacing in the third zone gives the required expression for determining stirrup spacing. The spacing obtained from this method is similar to that achieved through iteration, assuming $\theta = 45°$.

$$s \leq \left(\frac{0.0001 \phi_f d_v}{V_{fd} - V_c} \right)^2 f'_c \, \rho_{frp} E_{frp} b A_{frpv} E_{frpv} \; with \; \rho_{frp} = \frac{A_{frp}}{bd}$$

$$\leq \left(\frac{0.0001 \times 0.75 \times 464}{(148.1 - 127.5) \times 10^3} \right)^2 40 \times \frac{1131}{350 \times 515} \times 147000 \times 350 \times 141.8 \times 43900 = 229.4\,mm$$

4. Finally, stirrups are placed in accordance with spacing and zone delimitations obtained during the design process. To follow maximum spacing requirements, stirrup spacing of 100 mm was adopted in zones II and III.

ZONE I
No Shear Reinforcement

Center Line

500

1600

800

ZONE III
6 @ 100 mm o.c.

ZONE II
17 @ 100 mm o.c.

3000

3000
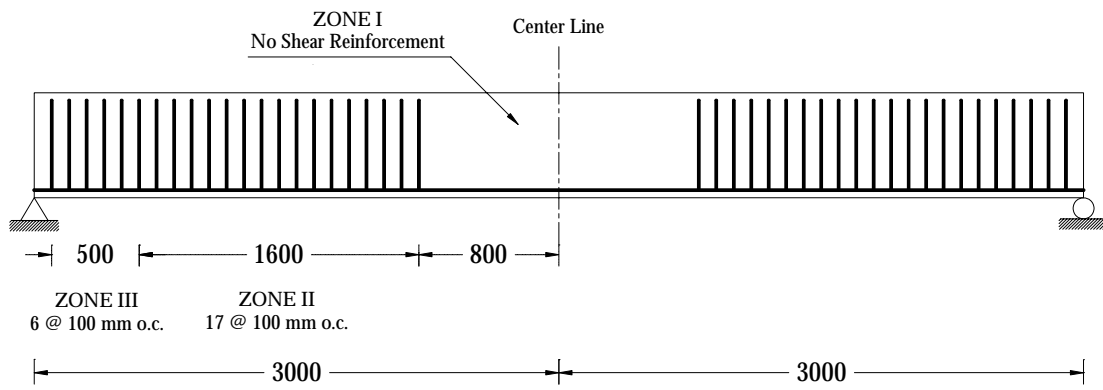
11.1   General

From a handling and application point of view, construction and installation practices required when using FRP reinforcing bars are similar to those used with conventional steel bars. In most cases, the lightweight properties of FRP bars actually make the placement of reinforcement in formwork less time-consuming. The following sections very briefly outline some of the important issues that must be kept in mind when handling and installing FRP reinforcing bars.

11.2   Spacing of Longitudinal Reinforcement

The minimum spacing of longitudinal reinforcement in a beam should be the maximum of the following:
- $1.4\, d_b$
- 1.4 times the maximum aggregate size
- 30 mm

This maximum value will assure that concrete can be placed properly, and that temperature cracking will be avoided. The maximum spacing for minimum slab reinforcement is the smallest of three times the slab thickness or 300 mm for primary reinforcement and five times the slab thickness or 500 mm for secondary reinforcement (CSA A23.3-04).

11.3   Graders, Sizes, Bar Identification

Unlike conventional reinforcing steel, which has a relatively long history of use in construction projects, FRP reinforcement for concrete is still considered an emerging technology. Over the years, certain specific grades and sizes of steel reinforcement have emerged as industry standards, such that any engineer can easily specify the grade and size of bars required for a particular application. Because FRP reinforcing bars are a newer technology, and since slight variations in the composition and manufacturing processes of these bars can lead to significant differences in physical and mechanical properties, the same degree of standardization does not yet exist for FRP reinforcing bars. However, all FRP bars for use as reinforcement for concrete are manufactured to meet certain performance requirements and they are typically graded and marked accordingly.

11.4   Strength and Modulus Grades

The American Concrete Institute (ACI 2003) recommends that FRP bars be graded (using imperial units) according to both their ultimate tensile strength and their tensile modulus of elasticity. An FRP bar with a tensile strength of 60 ksi would be designated as "F60" in the ACI system, whereas a bar with a strength of 3000 ksi would be "F3000". Similarly, a bar with a tensile elastic modulus of 5.7 ksi would be graded as "E5.7". This grading system is recommended but has not yet been codified.

11.5   Surface Geometry

Various surface geometries currently exist for FRP bars, including spiral braids, sand-coatings, and surface ribs (Refer to Figure 4.1). There is currently no standard classification for these treatments. Manufacturers should be consulted if questions regarding surface treatments arise.

11.6   Bar Sizes

Various bar sizes are available from specific FRP bar manufacturers. No standard bar sizes currently exist, although ACI (2003) recommends the use of a system wherein bar size designations correspond to their nominal diameter in increments of an eighth of an inch, similar to the current bar designation system for steel reinforcing bars used in the United States.

11.7   Bar Identification

While the various FRP bar manufacturers are not currently bound by any identification requirements for their products, ACI (2003) has suggested the use of a designation system that would provide necessary information to users of their products. This designation system includes information on:

- the bar's producer;
- the type of fibre;
- the bar size (using the system currently used for conventional steel reinforcing bars); and,
- the strength and modulus grades (using the F# and E#.# system noted above).

11.8   Concrete Cover

CHBDC (2006) indicates that the minimum clear cover should be 35 mm with a construction tolerance of ± 10 mm. For building components the values in Table 11.1 are recommended.

CSA S806-02 provides information on concrete cover if fire rating requirements are a design criterion.

Table 11.1 — Cover of Flexural Reinforcement		
Type of Exposure	Beam	Slab
Internal	maximum (2.5 d_b, or 40 mm)	maximum (2.5 d_b, or 20 mm)
External	maximum (2.5 d_b, or 50 mm)	maximum (2.5 d_b, or 30 mm)

When selecting a concrete cover, the type of FRP reinforcement, type of member, final use of the member, and environmental conditions should be considered. Some types of GFRP expand in the transverse direction under increased temperatures, or swell in water. Since these properties depend highly on the type of matrix used for bar manufacturing, no generalization can be made in this respect. The manufacturer should be contacted if the designer is concerned.

11.9 Constructability

The following are tips for construction of FRP reinforcement cages:

- All FRP bars must be protected against UV radiation during storage.
- Always check with the manufacturer regarding storage and handling requirements, as they may differ depending on fibre type used.
- FRP reinforcement should not come into contact with steel. Therefore, cages must be tied with plastic ties.
- Due to the lightweight of FRP, the cages must be tied to the form.
- Use a plastic vibrator to compact the concrete.

Even if the bars are seated in chairs and tied, they may float up slightly, according to Rizkalla (1997).

11.10 Handling and Storage

As discussed previously, FRP reinforcing bars are comprised of high-strength fibres (typically of carbon or glass) embedded in a polymer matrix (typically vinyl ester). Because the bars are unidirectional, their strength and stiffness in the fibre (longitudinal) direction are much greater than in the transverse (off-axis) direction. Thus, while inherently durable once embedded in concrete, FRP bars are susceptible to surface damage if abused during handling and installation. Deep scoring of the bars' surface will reduce their durability and load-carrying capacity and should be avoided at all cost. Fibre-reinforced polymer bars can thus be considered similar to epoxy-coated steel reinforcing bars – caution is required during handling and application to ensure that the surface coating is not damaged. Specific storage, handling, and installation guidelines vary somewhat from manufacturer to manufacturer, and it is important to check the manufacturers' requirements for any specific FRP reinforcement which is being contemplated for use. The following are common storage and handling guidelines that should be observed in most cases. Table 11.2 provides a basic checklist of handling and storage issues for FRP reinforcing bars for concrete.

Checklist: Handling and Storage of FRP Rebars	
☑	Store bars in a clean environment
	Protect bars against:
☑	- UV radiation
☑	- High temperature
☑	- Damaging chemicals
☑	Lift bundles of bars with care
☑	Do not shear bars when cutting
SAFETY[*]	Work gloves should be worn at all times

[*] In addition to typical safety precautions and procedures

Table 11.2: Handling & Storage of FRP Rebars.

11.10.1 Gloves

The fibres contained in FRP reinforcing bars can cause splinters, cuts, and skin irritation. FRP bars should always be handled with heavy-duty work gloves.

11.10.2 On-Site Storage

FRP bars should be kept clean and free of oil, dust, chemicals, or other contaminants. They should not be stored directly on the ground, but should be placed on timber pallets to ensure cleanliness and easy handling. Access should be provided for easy inspection of materials.

11.10.3 Ultra-Violet Radiation

While FRP bars are highly corrosion resistant, most FRP polymer matrix materials are susceptible to slight degradation under prolonged exposure to ultra-violet (UV) radiation. All FRP reinforcing materials should thus be protected from exposure to UV radiation. When stored outdoors, FRP bars should be covered with opaque plastic or otherwise protected.

11.10.4 High Temperatures

FRP materials are sensitive to degradation at high temperatures and should generally not be stored in elevated temperature environments.

11.10.5 Moisture and Chemicals

Protection of FRP bars from moisture is not needed. Certain specific chemicals can damage FRP bars, however, and chemical exposure should thus be avoided. Manufacturers should be consulted in this regard.

11.10.6 Lifting and Hoisting

FRP bars are lighter (about 75 percent lighter) and more flexible that conventional reinforcing steel, and can thus be hoisted and placed with much less effort (Refer to Figures 11.1 and 11.2). Hoisting should be performed with care until operators are familiar with the behaviour of these materials upon lifting. In some cases, spreader bars are needed to prevent excessive bending due to their low-stiffness.

Figure 11.1: Large sections of preassembled formwork can be installed with ease (courtesy Vector Construction Group).

Figure11.2: Lightweight bundles of FRP bars are easily moved on site
(courtesy Vector Construction Group).

11.10.7 Cutting

FRP bars can easily be cut with high-speed diamond grinding discs or fine-blade saws. FRP bars should never be sheared as this typically causes matrix cracking and fibre damage. Appropriate safety measures should be taken when cutting FRP bars due to airborne fibre fragments. This includes the strict use of safety glasses and dust masks. Sealing of the end of the bar is not typically required.

11.11 Placement and Assembly

Placement and assembly of FRP reinforcing bar cages in formwork is performed in much the same manner as for steel reinforcement, and very little adjustment is typically required in the construction process. Manufacturers' guidelines, which may differ somewhat, should be followed at all times when placing FRP reinforcement. Typical guidelines for the placement of FRP reinforcing bars are as follows. Table 11.3 provides a basic checklist of issues in placement and assembly of FRP reinforcing bars for concrete structures.

Checklist: Placement and Assembly of FRP Rebars	
☑	Oil, grease, dirt, removed from bars
☑	Bars placed as specified by Engineer
☑	Ties type as specified by Engineer
☑	Rebar chair type as specified by Engineer
☑	No direct contact between CFRP and steel
☑	No mechanical bar splices (lap splices only)
☑	Reinforcement tied down to prevent floating
☑	Care taken during concrete vibrating
☑	No walking on bars (sometimes permitted)
☑	Bends/hooks may not be fabricated on-site
SAFETY[*]	Work gloves and eye protection must be worn at all times

[*] In addition to typical safety precautions and procedures

Table 11.3: Placement and Assembly of FRP Rebars.

11.11.1 Oil and Grease

Oil or grease on the surface of the bars will adversely affect their bond strength to concrete and should be avoided. Oil or grease on the bars' surface should be removed prior to placement by wiping or spraying with a suitable solvent.

11.11.2 Bar Placement

Unless otherwise specified by the engineer, FRP bars should be placed in accordance with tolerances set out in applicable guidelines for conventional reinforcing steel. Because FRP bars are considerably lighter than steel bars, care is needed to ensure that FRP bars are not displaced by concrete or construction workers during concrete placement operations.

Care should be taken also to ensure that FRP bars are not unnecessarily abraded by dragging or rubbing against other bars, as this may degrade their tensile strength. Figure 11.3 shows FRP bars being installed in a bridge deck using standard bar placement methods.

Figure 11.3: Placement of glass FRP bars in a bridge deck
(courtesy Vector Construction Group).

11.11.3 Contact between Steel and FRP bars

When electrically-conductive materials that have different electro-potentials come into contact with one another, a small electrical current is generated. This can lead to an undesirable phenomenon known as galvanic corrosion. Carbon fibres are highly electrically conductive and have electro-potentials that are significantly different than conventional steel reinforcement. It is thus important that carbon fibres not come into direct contact with conventional reinforcing steel in a structure, and care should be taken to ensure that these materials are electrically isolated from one another. This is not a concern for glass FRP bars.

11.11.4 Ties and Rebar Chairs

Plastic, nylon, or other non-corrosive ties and rebar chairs should be used in applications where it is desirable to completely eliminate corrosion from a structure (Refer to Figure 11.4). When carbon FRP reinforcement is used, plastic or nylon ties and chairs should be used in all cases to prevent galvanic corrosion.

Glass bars may be tied using conventional steel ties if desired (Refer to Figure 11.5). The type of chairs and ties to be used should be clearly stated in the project specifications.

Figure 11.4: Glass FRP rebars tied with nylon zip-ties and glass FRP chairs to eliminate all corrosion (courtesy Vector Construction Group).

Figure 11.5: Glass FRP rebars tied with standard steel ties and using plastic chairs (courtesy Vector Construction Group).

11.11.5 Splices

Neither mechanically-connected nor welded splices are possible when using FRP reinforcement. Lapped bar splices should be used when continuity of reinforcement is required in a structure. Applicable design guidelines and manufacturer specifications should be consulted when designing splices. Glass FRP bars can be spliced to steel reinforcement, provided that mechanical splices are not used (which might damage the FRP bars). Carbon FRP bars should not be spliced to steel reinforcement because of the potential for galvanic corrosion.

11.11.6 Reinforcement Cage "Floating"

FRP reinforcement is light and must be adequately tied to formwork to prevent it from "floating" during concrete placing and vibrating operations (Refer to Figure 11.6).

Figure 11.6: Glass FRP rebars tied down with plastic-coated steel ties (courtesy Vector Construction Group).

11.11.7 Vibrating

Care must be taken when vibrating FRP-reinforced concrete to ensure that the FRP reinforcement is not damaged (plastic protected vibrators should be used where possible).

11.11.8 Bends and Hooks

Currently-available FRP reinforcing bars are fabricated using thermosetting resin matrices and consequently cannot be bent on site. Bends and hooks, when required, must be produced by the bars' manufacturer during the fabrication process. It is possible to obtain bends and hooks in virtually any geometry from current FRP rebar manufacturers (Refer to Figure 11.7), although minimum bend radii are typically larger than for steel bars due to significant weakening of FRP bars around tight corners. Typical minimum allowable bend radii for FRP bars are 3.5 to 4 times the bars' diameter, and these bends are accompanied by up to 50 percent reduction in the tensile strength of the bar at the bend.
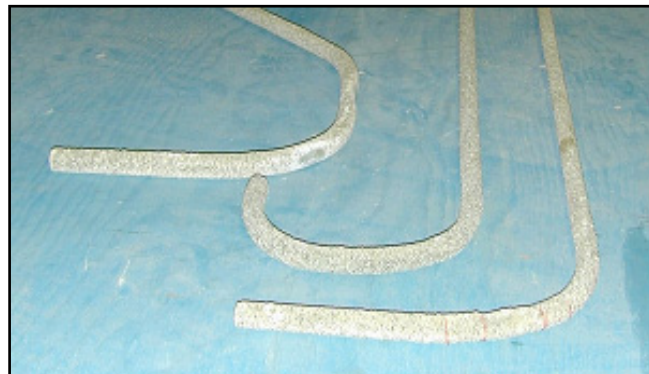
Figure 11.7: Bends in Glass FRP rebars for concrete barrier wall reinforcement (courtesy Vector Construction Group).

11.11.9 Walking on FRP Bars

Some existing design codes and guidelines state that workers should not be permitted to walk on FRP bars prior to placement of the concrete. This is only a precaution, however, which may not be necessary provided that the workers are aware of damage mechanisms for FRP reinforcing bars (Refer to Figure 11.8).

Figure 11.8: A construction worker stands on glass FRP bars while tying them together (courtesy Vector Construction Group).

11.12 Quality Control and Quality Assurance

Quality control and quality assurance are critically-important at each step of the construction process, particularly when using materials with which there is historically less experience.

Prior to construction, the engineer and owner shall decide if the manufacturer-specified properties of the FRP reinforcement are sufficient and acceptable or if independent tests are required. When required, tests should be conducted according to recommended procedures (ACI 2004).

Commonly-available FRP bars are manufactured under strict conditions, and routine sampling, inspection, and quality control tests are conducted by all manufacturers. Some FRP bar manufacturers colour-code their production runs to allow for easy tracing of individual bars' properties, and most bar manufacturers will provide certification of their materials upon request. Typical properties that are of interest to the engineer may include:

- dimensional tolerances;

- mechanical properties including tensile strength, tensile elastic modulus, fatigue strength, and ultimate strain;
- bond strength in concrete;
- fibre-volume fraction;
- hardness, die wicking properties, shear properties in flexure and in direct shear; and durability in alkaline environments.

Curing ratio, a fully cured resin system (96 percent and above) will enable the resin to develop its full resistance to chemical attack and avoid moisture absorption. Figure 11.9 shows a relationship between heat flow and temperature with 99.9 percent cure.
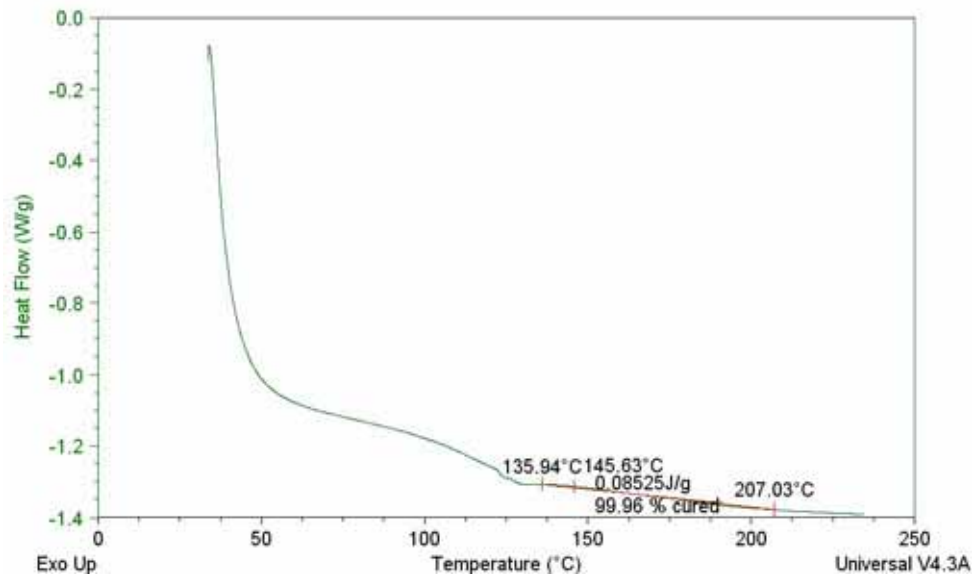
Figure 11.9: Heat flow-temperature curve with 99.9 percent cure.

11.12.1 Prior to Construction

It is important that all parties involved in a particular construction project are educated as to the specific handling and application requirements for a particular FRP reinforcing product, particularly with respect to new and/or unusual construction procedures and design innovations. All uncertainties should be resolved before construction begins.

11.12.2 During Construction

It is important that all interested parties work together to ensure the proper and adequate transport, storage, handling, and placement of materials and assemblies. Regular inspections should be conducted by trained and certified engineers who are knowledgeable in the use of FRP materials (in addition to standard construction practices and tolerances).

11.12.3 Common Safety Precautions

Because the use of FRP reinforcing bars is similar to the use of conventional steel reinforcement, few safety precautions are required in addition to common precautions that are typically observed when using conventional steel reinforcement. In most cases, the only additional precautions that are necessary are:

- **heavy-duty work gloves** should be worn at all times when handling FRP bars; and,
- **dust masks and eye protection** should be worn when cutting FRP bars.

12.1 Crowchild Trail Bridge, Alberta

Many of Canada's bridges require upgrading because they were not built to handle the weight of today's increased traffic loads. Calgary's Crowchild Bridge is one such case. The 90-m long, 11-m wide, new bridge carries two lanes of traffic over its three continuous spans. While the deck slab itself is free of reinforcing, it is supported by five steel girders and external steel straps. GFRP C-bars were used to provide the continuity and to minimize the transverse cracks of the steel-free deck over the intermediate bridge piers.

Figure 12.1: Crowchild Trail Bridge, Alberta.

Based on the results of a full-scale model test at the University of Manitoba, GFRP C-bars were also used to reinforce the cantilever slabs of the bridge. On a tendered basis, it proved to be the least costly option.

The deck has cantilevers on either side, reinforced with GFRP rods. In order to reduce surface cracks, the bridge deck concrete contains short random polypropylene fibres. The completed bridge is stronger, more resistant to corrosion, and less expensive to maintain than if it had been constructed using traditional methods and materials.

The bridge is also outfitted with remote monitoring technology: 81 strain gauges, 19 embedded gauges, five thermisters, three smart glass rebars and two fibre-optic gauges.

12.2   Hall's Harbor Wharf, Nova Scotia

Hall's Harbor Wharf is Canada's first wharf utilizing lightweight, non-corroding GFRP V-Rod bars and a steel-free deck.

Following the failure of a 40-metre section of wharf timber piles, the need to rehabilitate the 1904 structure took on an even higher level of urgency than had already been allotted. Like many east coast communities, Hall's Harbor had assumed responsibility for its marine infrastructure from the federal government.

Figure 12.2: Hall's Harbor Wharf, Nova Scotia.

In preliminary design work with Vaughan Engineering, ISIS Canada's team in Halifax showed that the cost of using innovative materials and technologies was only slightly more than the cost associated with conventional methods. The additional cost of the GFRP reinforcements and steel-free deck over conventional steel reinforced concrete was $20,000 or 4.5 percent.

The long-term benefits, however, were substantially more attractive because the absence of steel reinforcements extends the life of the wharf from approximately 30 years to between 60 and 80 years with minimal maintenance. This is a critical factor given that communities like Hall's Harbor are solely responsible for maintaining their wharfs. The inclusion of fibre-optic monitoring technology embedded in glass rods (a newly patented Canadian technology) adds solid data to support the application of FRPs in other marine environment structures.

The wharf incorporates several innovative technologies. It is constructed with concrete deck panels on deep concrete beams or pile caps spaced at approximately four-metre intervals. The transverse beams are supported on steel piles at both the front face and back. The pile caps contain a unique design where an outer layer of GFRP V-Rod reinforcement under low stress protects an inner layer of minimum steel reinforcement. The deck panels contain synthetic fibre-reinforced concrete and utilize an internal compressive arching technology. The panels also contain GFRP rods to reinforce against uplift force created by wave action during severe storms.

12.3   Joffre Bridge, Québec

Early in August of 1997, the province of Québec decided to construct a bridge using carbon FRP reinforcement. The Joffre Bridge, spanning the Saint Francois River, was another contribution to the increasing number of FRP-reinforced bridges in Canada. A portion of the Joffre Bridge concrete deck slab is reinforced with carbon FRP, as are portions of the traffic barrier wall and the sidewalk.

The bridge is outfitted extensively with various kinds of monitoring instruments including fibre-optic sensors embedded within the FRP reinforcement (these are referred to as smart reinforcements). Over 180 monitoring instruments are installed at critical locations in the concrete deck slab and on the steel girders, to monitor the behaviour of the FRP reinforcement under service conditions. The instrumentation is also providing valuable information on long-term performance of the concrete deck slab reinforced with FRP materials.

Figure 12.3: Aerial view of Joffre Bridge during construction.

12.4   Taylor Bridge, Manitoba

A significant research milestone was achieved on October 8, 1998, when Manitoba's Department of Highways and Transportation opened the Taylor Bridge in Headingley, Manitoba. The two-lane, 165.1-metre-long structure has four out of 40 precast concrete girders reinforced with carbon FRP stirrups. These girders are also prestressed with carbon FRP cables and bars. Glass FRP reinforcement has been used in portions of the barrier walls.

Figure 12.4: The Taylor Bridge, in Headingley, Manitoba, during construction.

As a demonstration project, it was vital the materials be tested under the same conditions as conventional steel reinforcement. Thus only a portion of the bridge was designed using FRPs.

Two types of carbon FRP reinforcements were used in the Taylor Bridge. Carbon fibre composite cables produced by Tokyo Rope, Japan, were used to pretension two girders, while the other two girders were pretensioned using Leadline bars produced by Mitsubishi Chemical Corporation, Japan.

Two of the four FRP-reinforced girders were reinforced for shear using carbon FRP stirrups and Leadline bars in a rectangular cross section. The other two beams were reinforced for shear using epoxy-coated steel reinforcement.

The deck slab was reinforced by indented Leadline bars similar to the reinforcement used for prestressing. GFRP reinforcement produced by Marshall Industries Composites Inc. was used to reinforce a portion of the Jersey-type barrier wall. Double-headed, stainless steel tension bars were used for the connection between the barrier wall and the deck slab.

The bridge incorporates a complex, embedded fibre-optic structural sensing system that will allow engineers to compare the long-term behaviour of the various materials. This remote monitoring is an important factor in acquiring long-term data on FRPs that is required for widespread acceptance of these materials through national and international codes of practice.

Using 64 single FOSs to monitor the bridge is not, in itself, a new procedure. What is new and significant in the Taylor Bridge is the use of two experimental, multiplexed, FOSs called Bragg Gratings that measure strain, loading and temperature. The sensors are not only immune to electromagnetic interference, they also have long-term stability in advanced materials.

12.5   Centre Street Bridge, Alberta

In 2000, the Centre Street Bridge in Calgary underwent a major rehabilitation to remove deteriorated concrete and upgrade the structure, originally built in 1903, to modern design standards. Beneath the main arches, the old deck structure was removed and a new reinforced concrete deck constructed. The design of this deck incorporated a hybrid reinforcement design concept that will produce more durable deck slabs.

It has been shown that top reinforcement does not contribute significantly to the strength of a concrete slab on girder bridge deck and that it can be removed entirely from the deck. The current isotropic steel reinforcement approach has two major drawbacks. Non-essential reinforcement is responsible for most of the costly maintenance deterioration problems and the protection of this same reinforcement leads to higher initial construction costs.

Although this top layer may not be essential for strength, it is desirable for reasons of serviceability and continuity to have secondary reinforcement in the upper portion of a deck slab. The Centre Street Bridge lower deck utilizes a hybrid design concept with GFRP reinforcement for the top layer and steel reinforcement for the bottom layer. Based on an improved understanding of

concrete bridge deck slab behaviour, the bottom layer of steel reinforcement is designed for strength based on arching principles and the top layer of non-corrodible fibre-reinforced polymer (FRP) reinforcement is provided as secondary reinforcement.

The lower deck is constructed with a 200-mm-thick reinforced concrete deck slab supported by four steel stringers at a spacing of 1870 mm across the width of the deck. Steel transverse floor beams support the deck and stringers at 4510 mm intervals. The floor beams are suspended from hanger rods that are attached to the heavy concrete arches forming the main support system for the entire structure. The bottom reinforcement is 15M steel bars at 300 mm in both directions, satisfying the 0.3 percent reinforcement criteria of the empirical design method. The top layer was a GFRP grid made from 10 x 13 mm grid element at 250 mm in the transverse direction and 10 x 10 mm elements in the longitudinal direction. The properties of the grid are an ultimate strength of 600 MPa and a modulus of 30 MPa. As required by CHBDC provisions, this amount of GFRP provides the equivalent strength to the steel layer it replaces.

Figure 12.5: Lower Deck of Centre Street Bridge, Calgary, Alberta.

12.6 Brookside Cemetery Marker Mountings, Manitoba

In the fall of 2001, Veterans Affairs Canada (VAC) and Heritage Conservation Services Canada (HCS) initiated a study on marker mountings that are rapidly deteriorating at Brookside Cemetery in Winnipeg, Manitoba. This research project addresses two conditions believed to be deleterious to the anchor assembly for the marker: mechanical (i.e., service load) and environmental (i.e., frost action and exposure to moisture) conditions. The investigation focuses on the mechanism of degradation of the anchor assembly system and GFRP reinforcement concrete support beams under synergetic effect of chemical and mechanical processes and harsh environmental conditions.

Five variables were considered in the laboratory investigation:

- marker mounting methods;
- concrete type used for the supporting beams;

- reinforcement/rod type;
- adhesive type; and,
- method of support beam emplacement.

The testing program focuses on three structural anchor assembly types: pinning, pocket and bumper. The anchor marker assembly is subjected to an accelerated aging regime that represents the long-term exposure to the actual environment. The bond degradation is quantified with a direct pull-out test, and deterioration of the reinforced concrete supporting beams is quantified by monitoring the changes in the mechanical properties with lateral loading, shear and bending tests. The marker field performance is being monitored by ISIS Canada.

Figure 12.6: GFRP-Reinforced Cemetery Marker, Brookside Cemetery, Winnipeg, Manitoba.

12.7   Université de Sherbrooke Pedestrian Bridge, Québec

A student design competition for a pedestrian bridge enabled the use of new-generation structural technologies. Set up by ISIS, the aim of this competition was to design a pedestrian bridge with a six-metre covering with access to a new entrance to the Faculty of Engineering at the Université de Sherbrooke. The objective of this project was to provide the opportunity for ISIS Canada students to participate in the design of a construction project incorporating composite materials with the integration of new fibre-optic monitoring technologies. For this project, V-ROD GFRP and CFRP bars have been used as reinforcement for the deck slab and the beams, respectively.

The composite materials for the structures and the monitoring of fibre optics are two main research goals of ISIS Canada. The winning team from Queen's University was invited to participate in the final design of the project with the engineering firm responsible for the project.

Figure 12.7: Université de Sherbrooke Pedestrian Bridge.

12.8   Laurier Taché Parking Garage, Gatineau (Québec)

Glass FRP V-Rod bars have been used in the structural slabs of the largest PWGSC's parking structure in Canada, Laurier-Taché Parking garage, Gatineau, Quebec, Canada (Benmokrane et al., 2004; Benmokrane et al., 2006). The design with GFRP bars was made to satisfy the serviceability and strength requirements as well as the two-hours fire rating required by the CAN/CSA-S806-02. The GFRP bars have been instrumented with fibre-optic sensors for remote and long-term monitoring over an extended period of time. The rehabilitation of this parking garage included the complete replacement of all structural slabs, while maintaining the other structural components such as beams, girders, columns and foundation walls.

Figure 12.8: Placement of GFRP bars in Laurier Taché Parking Garage.

12.9   Val-Alain Bridge on Highway 20 East (Québec)

The Val-Alain Bridge is located in the Municipality of Val-Alain on Highway 20 East, and crosses over Henri River in Québec, Canada. The bridge is a slab-on-girder type with a skew angle of 20º over a single span of 49.89 m and a total width of 12.57 m. The bridge has four simply supported steel girders spaced at 3145 mm. The deck slab is a 225-mm thickness concrete slab, with semi-integral abutments, continuous over the steel girders with an overhang of 1570 mm on each side. The concrete deck slab and the bridge barriers were reinforced with sand-coated V-Rod GFRP composite bars utilizing high-performance concrete.

The deck slab was designed based on serviceability criteria. The crack width and allowable stress limits were the controlling design factors. The MTQ has selected to limit the maximum allowable crack width to 0.5 mm and the stresses in the GFRP bars to 30 and 15 percent of the ultimate strength of the material under service and sustained loads, respectively. Based on this design approach, the bridge deck slab was entirely reinforced with two identical reinforcement mats using No. 19 GFRP bars. For each reinforcement mat, No. 19 GFRP bars spaced at 125 and 185 mm in the transverse and longitudinal directions, respectively, were used. A 40 and 35 mm top and bottom clear concrete cover, respectively, was used. Additional No.19 GFRP bars spaced at 250 mm were placed in the top transverse layer at the two cantilevers, as well as in the top longitudinal layer at the ends of the deck slab.

The bridge was constructed in 2004 and was well-instrumented at critical locations to record internal temperature and strain data. The bridge was tested for service performance as specified by the CHBDC using two four-axle calibrated trucks (Benmokrane et al., 2005).

The Val-Alain bridge is the Canada's first concrete bridge deck totally reinforced with GFRP bars with an expected service life of more than 75 years.

Figure 12.9: Reinforcement of the bridge deck slab and barrier walls, Val-Alain Bridge.

12.10   Continuous Reinforced Concrete Pavement with GFRP bars on Highway 40 East-Montreal

In 2006, the Ministry of Transportation of Québec used the GFRP bars as reinforcement for the continuous reinforced concrete pavement on Highway 40 East in Montreal. The concept of the CRCP is adopted when using GFRP V-Rod bars instead of steel reinforcement to eliminate any chances of deleterious effects of steel corrosion. This is a world-wide pioneer application of the GFRP reinforcement for continuously-reinforced concrete pavements.

Figure 12.10: Continuous Reinforced Concrete Pavement with GFRP bars on Highway 40 East-Montreal.

12.11   Deck Rehabilitation of Glendale Avenue Bridge (Region of Niagara, Ontario)

A new parapet wall was constructed on the existing bridge deck using GFRP V-Rod reinforcement. The design was completed following current codes and design standards outlined in the ACI 318, ACI 440, and Canadian Highway Bridge Design Code (CHBDC). The design was supported by lab and field pull-out tests. It was determined that the use of GFRP provided the Region with the best reinforcement solution considering long-term sustainable benefits and non-corrosive properties of GFRP. The durability of GFRP was the driving factor in using GFRP reinforcement. The actual costing also proved to be very favorable in comparison with conventional epoxy-coated reinforcement. The region of Niagara has accepted the design and use of GFRP in certain components of bridge structures, with consideration for future use in other bridge structures.

Figure 12.11: Deck Rehabilitation of Glendale Avenue Bridge.

13 NOTATION

13.1 Notation

A	effective tension area of concrete surrounding the flexural tension reinforcement and bearing the same centroid as that reinforcement, divided by the number of rebars, mm^2
A_{frp}	area of FRP reinforcement, mm^2
A_{frpb}	area of FRP reinforcement for balanced conditions, mm^2
A_{frpmin}	minimum area of FRP reinforcement, mm^2
A_{frpv}	area of shear reinforcement perpendicular to the axis of a member within a distance s, mm^2
b	width of compression face of member, mm
b_w	minimum effective web width within depth d, mm
c	depth of neutral axis, mm
C	resultant of compressive stresses in concrete, N
c_b	depth of neutral axis at balanced failure conditions, mm
C_n	nominal resultant of stresses in concrete, N
d	effective depth or distance from the extreme compression fibre to the centroid of the reinforcement, mm
d_b	bar diameter, mm
d_c	concrete cover measured from the centroid of tension reinforcement to the extreme tension surface, mm
d_e	effective diameter $d_e = \sqrt{4A_b/\pi}$, mm
d_v	Effective depth of section in shear taken as 0.9d, mm
E_c	modulus of elasticity of concrete, MPa
E_{frp}	modulus of elasticity of flexural FRP reinforcement, MPa
E_{frpv}	modulus of elasticity of FRP stirrup, MPa
E_s	modulus of elasticity of steel, 200×10^3 MPa
F_{SLS}	Service stress limit factor
f'_c	specified compressive strength of concrete, MPa
f_r	modulus of rupture of concrete, MPa
f_{frp}	stress in FRP reinforcement, MPa
f_{frps}	stress in FRP at service load, MPa
f_{frpu}	ultimate tensile strength of FRP, MPa
f_{frpvu}	ultimate strength of FRP stirrup, MPa
h	member thickness, mm
h_1	distance from the centroid of tension reinforcement to the neutral axis, mm
h_2	distance from the extreme tension surface to the neutral axis, mm
I_{cr}	moment of inertia of cracked section, mm^4
I_e	effective moment of inertia, mm^4
I_g	gross moment of inertia, mm^4
I_t	moment of inertia of uncracked section transformed to concrete, mm^4
k	stress decay factor
k_b	bond dependent coefficient
ℓ	length of member, mm
l_d^*	tail length, mm
ℓ_{frpd}	development length, mm
ℓ_{frpdh}	development length of a hooked bar, mm
ℓ_n	clear span, m

M_a	applied moment, N·mm
M_{cr}	cracking moment, N·mm
M_f	moment due to factored loads, N·mm
M_r	moment resistance, N·mm
M_s	service load moment, N·mm
M_u	ultimate moment, N·mm
n	curve fitting factor
n_{frp}	modular ratio
r_b	radius of bend, mm
R_n	nominal resistance
s	spacing of shear reinforcement measured parallel to the longitudinal axis of the member, mm
S_n	nominal load effect
T	internal force due to tension in FRP reinforcement, N
T_g	glass transition temperature
T_n	nominal internal force due to tension in FRP reinforcement, N
V_c	factored shear resistance attributed to concrete, N
V_d	factored shear resistance, N
V_{frp}	factored shear resistance attributed to shear reinforcement, N
V_{ser}	shear force at service load level, N
w	load per unit length, N/mm
w	crack width, mm
α	load factor
α_b	bond dependent coefficient
α_d	coefficient equal to 0.55 for T-section and 0.40 for rectangular section
α, β	stress-block factors for concrete
α_1, β_1	stress-block factors based on CSA A23.3-94
β_b	bond reduction coefficient
γ	importance factor
γ_c	density of concrete, kg/m³
δ	deflection, mm
Δ_{eu}	ultimate deflection calculated using uncracked section (I_g), mm
Δ_u	ultimate deflection, mm
ε_c	strain in concrete
ε_{cu}	ultimate strain in concrete
ε_{frp}	strain in FRP
ε_{frps}	strain in FRP at service load
$\varepsilon_{frpvser}$	strain in FRP stirrup at service load level
ε_o	strain in concrete at peak stress
ε_v	limiting strain in FRP stirrup to be used in design
ε_s	strain in steel
λ	modification factor for density of concrete
μ_{frp}	bond strength, MPa
ρ_{frp}	reinforcement ratio
ρ_{frpb}	balanced reinforcement ratio

ρ_{frpmin}	minimum reinforcement ratio required to ensure that failure occurs only when the moment exceeds the cracking moment with a sufficient margin
ρ_{frpv}	reinforcement ratio for FRP stirrups
ϕ	resistance factor
ϕ_c	material resistance for concrete
ϕ_{frp}, ϕ_f	material resistance for FRP
ϕ_s	material resistance for steel
η	Dimensionless coefficient used in deflection calculation (Refer to Section 7.5.3)
Ψ	curvature
Ψ_u	curvature at ultimate with FRP or ultimate curvature (ε_c/c)
θ	angle of inclination of shear plane

14 GLOSSARY

A

Aggregate, Low Density
: Aggregate conforming to the requirements of ASTM Standard C330.

Alkaline
: Containing hydroxyl (OH-) ions

Aramid
: Highly-oriented organic material derived from polyamide incorporating an aromatic ring structure. Used primarily as high-strength, high-modulus fibre.

B

Bar, Braided
: Bar with surface prepared by intertwining fibres in an organized fashion.

Bar, FRP
: Resin-bound reinforcing bar, made mostly of continuous fibres and resin, used to reinforce concrete uniaxially.

Bridge
: Structure which provides a roadway or walkway for passage of vehicles and pedestrians across an obstruction, gap or facility and which is greater than three metres in span.

C

Coefficient of Thermal Expansion, Longitudinal
: Linear dimension change along the longitudinal axis of the bar, per unit length per degree of temperature change. Expansion is positive, and contraction is negative.

Coefficient of Thermal Expansion, Transverse
: Linear dimension change perpendicular to the longitudinal axis of the bar, per unit length per degree of temperature change.

Composite
: A combination of one or more materials differing in form or composition on a macroscale. The constituents retain their identities; that is, they do not dissolve or merge completely into one another, although they act in concert. Normally, the components can be physically identified and exhibit an interface between one another.

Concrete Cover
: Distance from the concrete surface to the nearest surface of reinforcement.

Continuous Fibre
: Fibre that is made by spinning or drawing into one long continuous entity.

D Deformability

> The ratio of energy absorption (area under the moment-curvature diagram) at ultimate to the energy absorption at service level.

Development Length

> Length of embedded reinforcement required to develop the design strength of reinforcement.

Durability

> The ability of a system to maintain its properties with time.

E Effective Depth of a Section

> Distance measured from the extreme fibre in compression to the centroid of tension reinforcement.

E-Glass

> A family of glass with a calcium alumina borosilicate composition and a maximum alkali content of 2.0 percent. A general purpose fibre that is used in reinforced polymers.

Embedment Length

> Length of embedded reinforcement provided beyond a critical section.

Epoxy Resin

> A resin formed by chemical reaction of epoxide groups with amines, alcohols, phenols, and others.

F Fabric

> An arrangement of fibres held together in two dimensions. The fabric can be woven, non-woven, or stitched.

Fabric, Non-Woven

> A material formed from fibres or yarns without interlacing. This can be stitched, knit or bonded.

Fabric, Woven

> A material constructed of interlaced yarns, fibres, or filaments.

Factored Resistance

> The product of the unfactored resistance and the applicable resistance factor.

Failure

A state in which rupture, severe distortion, or loss of strength has occurred as a result of the load-carrying capacity of a component or connection having been exceeded.

Fibre, Aramid

Highly-oriented organic fibre derived from polyamide incorporating an aromatic ring structure.

Fibre, Carbon

Fibre produced by the heating of organic precursor materials containing a substantial amount of carbon, such as rayon, polyacrylonitrile (PAN), or pitch, in an inert environment.

Fibre Content

The amount of fibre present in a composite, usually expressed as a percentage volume fraction or weight fraction of the composite.

Fibre, Glass

Fibre drawn from an inorganic product of fusion that has cooled without crystallizing.

Fibre-Reinforced Polymer (FRP)

Composite material formed from continuous fibres impregnated with a fibre binding polymer, then hardened and molded in many forms (bars-round, rectangular; sheets; plates; grids, and shapes).

Fibre-volume Fraction

The ratio of the volume of fibres to the volume of the composite.

Filament

Smallest unit of a fibrous material.

G **Grid**

A two-dimensional or three-dimensional rigid array of interconnected FRP bars that form a continuous lattice that can be used to reinforce concrete. The lattice may be manufactured with integrally connected bars or may be made of mechanically connected individual bars.

I **Impregnate**

To saturate fibres with resin.

L   Limit States

Those conditions of a structure in which it ceases to fulfil the function for which it was designed.

Load, Dead

Specified dead load as defined in the National Building Code of Canada.

Load Factor

Factor applied to a specified load which, for the limit state under consideration, takes into account the variability of the loads and load patterns and analysis of their effects.

Load, Factored

Product of a specified load and its load factor.

Load, Live

Specified live load as defined in the National Building Code of Canada.

Load, Specified

Load specified by the National Building Code of Canada.

Load, Sustained

Specified dead load plus that portion of the specified live load expected to act over a period of time sufficient to cause significant long-time deflection.

M   Matrix

Material which serves to bind the fibres together, transfer loads to the fibres, and protect them against environmental attack and damage due to handling.

Member

An element or group of elements, which may or may not require individual design.

Modular Ratio

Ratio of modulus of elasticity of reinforcing material to that of concrete.

P   PAN Carbon Fibre

Carbon fibre made from polyacrylonitrile fibre.

Pitch

A residue of distillation of petroleum.

Polymer

High molecular weight organic compound, natural or synthetic, containing repeating units.

Precursor

Rayon, pitch or PAN fibres from which carbon fibres are derived.

Pultrusion

A continuous process for manufacturing composites that have a uniform cross-sectional shape. The process consists of pulling a fibre reinforcing material through a resin impregnation bath then through a shaping die, where the resin is subsequently cured.

R   **Resin**

Polymeric material that is rigid or semi-rigid at room temperature, usually with a melting point or glass transition temperature above room temperature.

Resistance Factor

Factor applied to a specified material property for the limit state under consideration, which takes into account the variability of dimensions, material properties, workmanship, and uncertainty in prediction of resistance.

Resistance, Factored

Resistance of a member, connection, or cross-section calculated in accordance with the provisions and assumptions of this Design Guide including the application of appropriate resistance factors.

Resistance, Nominal

Resistance of a member, connection, or cross-section calculated in accordance with the provisions and assumptions of this Design Guide, without the inclusion of any resistance factors.

S   **Serviceability Limit States**

Those limit states that restrict the intended use of a structure, including vibration, permanent deformation and cracking.

Span

The horizontal distance on a longitudinal bridge centre line between the bearing centre lines of individual piers or abutments of an articulated superstructure, or the horizontal distance between centre lines of individual column bents or individual columns of a framed structure.

Splitting Tensile Strength

Tensile strength of concrete determined by a splitting test.

Stirrup
> Reinforcement used to resist shear stresses in a structural member.

Strength of Concrete, Specified
> Compressive strength of concrete used in the design.

Stress Concentration
> On a macromechanical level, the magnification of the level of an applied stress in the region of a bend, notch, void, hole, or inclusion.

T Thermoplastic
> Resin that is not cross-linked, and which can generally be re-melted and recycled.

Thermosetting
> Resin that is cross-linked which cannot be re-melted and recycled because the polymer chains form a three-dimensional network.

U Ultimate Limit States
> Those limit states which concern structural safety including failure, overturning, sliding and other instability.

V Vinyl Ester
> Thermosetting resin containing ester of acrylic and/or methacrylic acids, many of which have been made from epoxy resin.

Y Yarn
> A group of fibres held together to form a string or rope.

15 REFERENCES

Abdelrahman, A.A. (1995). *"Serviceability of Concrete Beams Prestressed by Fibre Reinforced Plastic Tendons,"* Ph.D. Dissertation Thesis, Department of Civil and Geological Engineering, University of Manitoba, Winnipeg, Manitoba, 331 p.

Abdelrahman, A.A., Tadros, G., and Rizkalla, S.H. (1995). *"Test Model for the First Canadian Smart Highway Bridge,"* ACI Structural Journal, V. 92, No. 4, pp. 451-458.

Almusallam, T.H.; Al-Salloum, Y.; Alsayed, S.; and Amjad, M. (1997). *"Behaviour of Concrete Beams Doubly Reinforced by FRP Bars,"* Proceedings of the Third International Symposium on Non-metallic (FRP) Reinforcement for Concrete Structures (FRPRCS-3), Japan Concrete Institute, Sapporo, Japan, Vol.2, pp. 471-478.

Aly, A., Bakht, B. and Schaeffer, J. (1997). Design and Construction of Steel-fee Deck Slab in Ontario. Annual Conference of Canadian Society for Civil Engineering, Montreal, Que., V. 6, pp. 81-90.

Banthia N. and MacDonald, R. (1996). *"Durability of Fiber-Reinforced Plastics and Concretes, Part 1:Durability of Components,"* ACMBS Network of Canada, 25 p.

Bedard, C. (1992). *"Composite Reinforcing Bars: Assessing their Use in Construction,"* Concrete International, January 1992, pp. 55-59.

Benmokrane, B., et al., (1998). *"Standard Test Methods for FRP Rod and Sheet,"* Intelligent Sensing for Innovative Structures (ISIS Canada), University of Manitoba, Winnipeg, Canada, 61 pp.

Benmokrane, B., Chaallal O., and Masmoudi, R. (1996). *"Flexural Response of Concrete Beams Reinforced with FRP Reinforcing Bars,"* ACI Structural Journal, V.93, No. 1 May-June 1996, pp. 46-55.

Benmokrane, B., El-Salakawy, E.F., Cherrak, Z., and Wiseman, A. (2004). *"FRP Composite Bars for the Structural Concrete Slabs of a PWGSC Parking Garage,"* Canadian Journal of Civil Engineering, Vol. 31, No. 5, pp. 732-748.

Benmokrane, B., El-Salakawy, E., El-Ragaby, A., and Wiseman, A. (2006). *"Rehabilitation of the Structural Slabs of Laurier-Taché Parking Garage (Gatineau-Quebec) using GFRP Bar,."* Proceedings of the 34th Canadian Society of Civil Engineering Annual Conference, Calgary, Alberta, Canada, May, 9 p.

Benmokrane, B., El-Salakawy, E., Goulet, S., and Nadeau, D. (2005). *"Design, Construction, and Testing of Innovative Concrete Bridge Decks Using Glass FRP Composite Bars,"* Proceedings of the 3rd International Conference on Composites in Construction (CCC-2005), Lyon, July, Vol. 2, pp. 873-880.

Benmokrane, B., and Rahman, H.(Editors) (1998). *"Durability of Fibre Reinforced Polymer (FRP) Composites for Construction,"* Proceedings of the First International Conference on Composites for Construction (CDCC'98), 5-7 August 1998, Sherbrooke, Québec, Canada, 692p.

Benmokrane, B., Tighiouart, B., and Thériault, M. (1997). *"Bond Strength of FRP Rebar Splices,"* Proceedings of The Third International Symposium on Non-metallic (FRP) Reinforcement for Concrete Structures (FRPRCS-3). Edited by Japan Concrete Institute, Sapporo, Japan, pp. 405-412.

Chaallal, O. and Benmokrane, B. (1993). *"Physical and Mechanical Performance of an Innovative Glass-Fibre-Reinforced Plastic Rod,"* Canadian Journal of Civil Engineering, Vol.20, No.2, pp. 254-268.

Collins, M.P. and Mitchell, D. (1997). *Prestressed Concrete Structures,* Response Publications, Canada, 766 p.

Coomarasamy, A. and Goodman, S. (1997). Investigation of the Durability Characteristics of Fiber Reinforced Polymer (FRP) Materials in Concrete Environment, American Society for Composites-Twelfth Technical Conference, Dearborn, Michigan.

Debaiky, A.S., Nkurunziza, G., Benmokrane, B., and Cousins, P. (2006*).* *"Residual Tensile Properties of GFRP Reinforcing Bars after Loading in Severe Environments,"* ASCE Journal of Composites for Construction, Vol 10(5):1-11.

Ehsani, M.R., Saadatmanesh, H., and Tao, S. (1995). *"Bond of Hooked Glass Fiber Reinforced Plastic (GFRP) Reinforcing Bars to Concrete,"* Materials Journal, American Concrete Institute, Vol. 92, No. 4, pp. 391-400.

Erki, M.-A., and Rizkalla, S.H. (1993). *"FRP Reinforcements for Concrete Structures: A Sample of International Production,"* Concrete International, V. 15, No. 6, June 1993, pp. 48-53.

El-Badry, M.M. and Ghali, A. (1989)*.* *"Serviceability Design of Continuous Prestressed Concrete Structures,"* Journal of Prestressed Concrete Institute, PCI, Vol. 34, No. 1, Jan.-Feb., pp. 54-91.

Faza, S.S. (1991). *"Bending and Bond Behavior and Design of Concrete Beams Reinforced with Fiber Reinforced Plastic Rebars,"* Ph.D. Dissertation, West Virginia University, Morgantown, West Virginia.

Gao, D., Benmokrane, B., and Masmoudi, R. (1998-2). *"A Calculating Method of Flexural Properties of FRP-Reinforced Concrete Beam: Part 1: Crack Width and Deflection,"* Technical Report, Department of Civil Engineering, University of Sherbrooke, Sherbrooke, Québec, 24 pp.

Gergely, P. and Lutz, L.A. (1968). *"Maximum Crack Width in Reinforced Flexural Members,"* Causes, Mechanism and Control of Cracking in Concrete, SP-20, American Concrete Institute, Detroit, pp. 87-117.

Gerritse, A. (1992). *"Durability Criteria for Non-Metallic Tendons in an Alkaline Environment,"* Proceedings of the First International Conference on Advance Composite Materials in Bridges and Structures *(ACMBS-I),* Canadian Society of Civil Engineers, Sherbrooke, Québec, pp. 129-137.

Ghali, A. and Azarnejad, A. (1999). *"Deflection Prediction of Members of Any Concrete Strength,"* ACI Structural Journal, Vol.96, N0.5, Sept.-Oct., pp. 807-816

Ghali, A. and Favre, R. (1994). *"Concrete Structures: Stresses and Deformations",* 2nd Edition, E&FN Spon (Chapman and Hall), 459 pp.

Hall, T.S. (2000). *"Deflections of Concrete Members Reinforced with Fibre Reinforced Polymer (FRP) Bars,"* M.Sc. Thesis, Department of Civil Engineering, University of Calgary, Calgary, Alberta.

Hall, T.S., and Ghali, A., (2000*). "Minimum Thickness of Concrete Members Reinforced with Fibre Reinforced (FRP) Bars,"* Canadian Journal of Civil Engineering, Vol. 28, pp. 583-592.

Hall T.S., and Ghali A., (2000*). "Long-term Deflection Prediction of Concrete Members Reinforced with Glass Fibre Reinforced Polymer (GFRP) Bars,"* Canadian Journal of Civil Engineering, Vol. 27, No. 5, pp. 890-898.

Jaeger, L.G., Tadros, G., and Mufti, A.A. (1995). *Balanced Section, Ductility and Deformability in Concrete with FRP Reinforcement,* Research Report No. 2-1995, The Nova Scotia CAD-CAM Centre, 29 p.

JSCE (1993). *"State-of-the-Art Report on Continuous Fiber Reinforcing Materials,"* Research Committee on Continuous Fiber Reinforcing Materials, Japan Society of Civil Engineers, Tokyo.

Katz, A., Berman, N., and Bank, L.C. (1998). *"Effect of Cyclic Loading and Elevated Temperature on the Bond Properties of FRP Rebars,"* International Conference on the Durability of Fiber Reinforced Polymer (FRP) Composites for Construction, Sherbrooke, Québec, pp. 403-413.

Katz, A., Berman, N., and Bank, L.C. (1999*). "Effect of High Temperature on the Bond Strength of FRP Rebars,"* Journal of Composites for Construction, May 1999.

Kobayashi, K. and Fujisaki, T. (1995). *"Compressive Behaviour of FRP Reinforcement in Non-prestressed Concrete Members,"* Proceedings of the Second International Symposium on Non-metallic (FRP) Reinforcement for Concrete Structures (FRPRCS-2). Edited by Taerwe, RILEM proceedings 29, Ghent, Belgium 1995, pp. 267-274.

Morphy, R.D. (1999). *"Behaviour of Fibre Reinforced Polymer (FRP) Stirrups as Shear Reinforcement for Concrete Structures,"* M.Sc. thesis, Department of Civil Engineering, University of Manitoba, Winnipeg, Manitoba.

Morphy, R., Shehata, E., and Rizkalla, S.H. (1997). *"Bent Effect on Strength of CFRP Stirrups,"* Proceedings of the Third International Symposium on Non-metallic (FRP) Reinforcement for Concrete Structures (FRPRCS-3). Edited by Japan Concrete Institute, Sapporo, Japan, pp. 19-26

Mota, C., Alminar, S., and Svecova D. (2006). *"Critical Review of Deflection Formulas for FRP Reinforced Concrete,"* ASCE Journal of Composites for Construction, pp. 183-194

Nanni, A., Nenninger, J., Ash, K., and Liu, J. (1997). *"Experimental Bond Behaviour of Hybrid Rods for Concrete Reinforcement,"* Structural Engineering and Mechanics, V.5, No.4, pp. 339-354.

Newhook, J., Ghali, A., and Tadros, G. (2000). *"Concrete Flexural Members Reinforced with FRP: Design for Serviceability and Deformability,"* 31 pp, submitted for publication.

Parkyn, B. (1970). *Glass Reinforced Plastics,* Iliffe, London.

Phillips, L.N. (1989). Design with Advanced Composite Materials, Springer-Verlag.

Porter, M.L., Mehus, J., Young, K.A., O'Neil, E.F., and Barnes, B.A. (1997). *"Aging of Fiber Reinforcement in Concrete,"* Proceedings of the Third International Symposium on Non-Metallic (FRP) Reinforcement for Concrete Structures (FRPRCS-3), Japan Concrete Institute, Sapporo, Japan, V. 2, pp. 59-66.

Porter, M.L., and Barnes, B.A., (1998). *"Accelerated Durability of FRP Reinforcement for Concrete Structures,"* Proceedings of the First International Conference on Composites for Construction (CDCC 1998), Sherbrooke, Québec, pp. 191-198.

Sayed-Ahmed E.Y., and Shrive N.G. (1998). *"CFRP Post-tensioned Masonry Diaphragm Walls,"* Proceedings of the Annual CSCE Conference, 2nd Structural Specialty Conference, Halifax, Nova Scotia, pp. 571-582.

Sayed-Ahmed E.Y., and Shrive N.G. (1999). *"Smart FRP Prestressing Tendons: Properties and Prospects,"* Proceedings of the Second Middle East Symposium on Structural Composites for
Infrastructure Applications, Edited by Hosny, Mahfouz and Sarkani, pp. 80-93.

Shehata, E.F.G. (1999). *"Fibre-Reinforced Polymer (FRP) for Shear Reinforcement in Concrete Structures,"* Ph.D. Thesis, Department of Civil and Geological Engineering, University of Manitoba, Winnipeg, Manitoba.

Svecova, D. (1999). *"Behaviour of Concrete Beams Reinforced with FRP Prestressed Concrete Prisms,"* Ph.D. Thesis, Department of Civil and Environmental Engineering, Carleton University, Ottawa, Ontario, 304 p.

Tadros, G., Tromposch, E. and Mufti, A. A. (1998). Superstructure Replacement of Crowchild Trail Bridge. 5th International Conference on Short and Medium Span Bridges, edited by L. Dunaszegi, Canadian Society for Civil Engineering, Montreal, Que., pp. 499-506.
Tanigaki, M., Okamoto, T., Tamura, T., Matsubara, S., and Nomura, S. (1989). *"Study of Braided Aramid Fiber Rods for Reinforcing Concrete,"* Braided Aramid Rods for Reinforcing Concrete, FiBRA.

Thériault, M. (1998). *"Flexion, ductilité et design de poutres et de dalles en béton armé de barres en composites," Ph.D. Thesis,* Université de Sherbrooke, Québec.

Vijay, P.V., GangaRao, H.V.S., and Kalluri, R. (1998). "*Hygrothermal Response of GFRP Bars under Different Conditioning Schemes,*" Proceedings of the First International Conference on Composites for Construction (CDCC 1998), Sherbrooke, Québec, pp. 243-252.

Yagi, K., Hoshijima, T., Ando, T., Tanaka, T. (1997). "*The Durability Tests of Carbon Fiber Reinforced Plastics Rod Produced by Pultrusion Method,*" Proceedings, International Conference on Engineering Materials, Edited by Al-Manaseer, Nagataki and Joshi, CSCE/JSCE, Ottawa, Ontario, Volume 2, pp 327-340.

 RESOURCES

A.1 FRP Suppliers

Autocon Composites Inc.
203 Toryork Drive, Weston, Ontario, Canada M9L 1Y2
Ph: (416) 746-5002   Fax: (416) 743-6383
NEFMAC Distributor

Hughes Brothers, Inc.
210 North 13th Street, Seward, Nebraska, USA 68434
Ph: (402) 643-2991   Fax: (402) 643-2149   Web: www.hughesbros.com
Hughes Brothers Bars Distributor

Pultrall Inc.
700, 9e Rue Nord , Thetford Mines, Québec, Canada G6G 6Z5
Ph. (418) 335-3202   Fax. (418) 335-5117   web: www.pultrall.com
V-ROD Manufacturer and Distributor

A.2 Commercially Available Reinforcing Bars

A.2.1 Glass Fibre-Reinforced Polymer Products

ASLAN - Aslan 100 bars are manufactured by Hughes Brothers, Inc. The manufacturer provided the following mechanical properties of their product, as shown in Tables A.1 and A.2. Other product properties are available from licensed suppliers.

Table A.1 – Geometric/Mechanical Properties of Bars Manufactured by Hughes Brothers									
Bar Designation		Nominal Diameter		Effective Area		Guaranteed Tensile Strength		Tensile Modulus of Elasticity	
SI	US Customary	[mm]	[in.]	[mm^2]	[in.^{2}]	[MPa]	[ksi]	[GPa]	[ksi]
6	#2	6.35	0.250	38.84	0.054	825	130	40.8	5920
9	#3	9.53	0.375	84.52	0.131	760	110	40.8	5920
12	#4	12.70	0.500	150.32	0.233	690	110	40.8	5920
16	#5	15.88	0.625	220.64	0.342	655	95	40.8	5920
19	#6	19.05	0.750	308.39	0.478	620	95	40.8	5920
22	#7	22.23	0.875	389.67	0.604	586	95	40.8	5920
25	#8	25.40	1.000	562.58	0.872	550	85	40.8	5920
32	#10	31.75	1.250	830.32	1.287	517	75	40.8	5920

Table A.2 — Other Material Properties of Bars Manufactured by Hughes Brothers				
Specific Gravity	Coefficient of Thermal Expansion			
	Transverse		Longitudinal	
	[x10^{-6}/°C]	[x10^{-6}/°F]	[x10^{-6}/°C]	[x10^{-6}/°F]
2.0 (per ASTM D792)	33.7	18.7	6.6	3.7

V-ROD – V-ROD bars are manufactured by Pultrall. They are composite bars specially designed for concrete reinforcement. The manufacturer provided the following mechanical properties of their product, as shown in Table A.3. Other product properties are available from licensed suppliers.

Table A.3 – Geometric/Mechanical Properties of V-ROD Manufactured by Pultrall									
Bar Designation		Nominal Diameter		Effective Area		Guaranteed Tensile Strength		Tensile Modulus of Elasticity	
SI	US Customary	[mm]	[in.]	[mm^2]	[in.^{2}]	[MPa]	[ksi]	[GPa]	[Msi]
6	#2	6.35	0.250	38.97	0.054	786	114.0	46.1	6.68
9	#3	9.53	0.375	78.00	0.131	765	110.9	46.2	6.69
13	#4	12.70	0.500	136.70	0.233	710	103.0	46.4	6.72
16	#5	15.88	0.625	224.36	0.342	683	99.0	48.2	6.98
19	#6	19.05	0.750	292.57	0.478	656	95.1	47.6	6.89
25	#8	25.40	1.000	527.34	0.872	614	89.0	51.0	7.39

Table A.4 — Other Material Properties of V-Rod Bars				
Specific Gravity	Coefficient of Thermal Expansion			
	Transverse		Longitudinal	
	[x10^{-6}/°C]	[x10^{-6}/°F]	[x10^{-6}/°C]	[x10^{-6}/°F]
3.0 (per ASTM D792)	27.3	15.2	5.9	3.1

NEFMAC Glass Reinforcing Grid - NEFMAC is a non-corrosive, lightweight material made of FRP that is formed in a two- or three-dimensional grid shape by using impregnated high-performance continuous fibres (Refer to Figure A.1). The product is manufactured in North America by Autocon Composites INC.
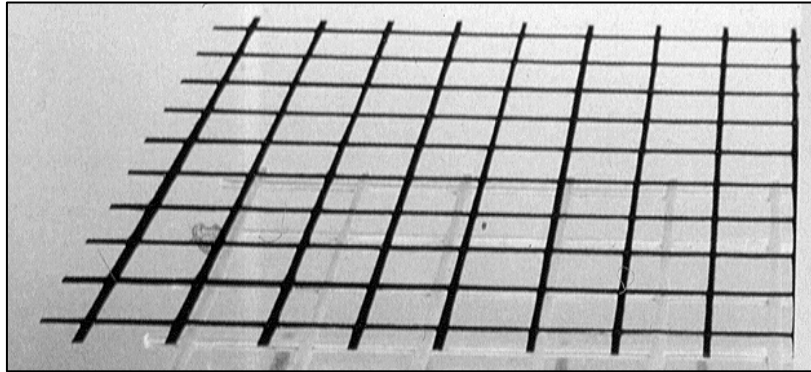
Figure A.1: NEFMAC Grid.

The manufacturer provided the following mechanical properties of their product, as shown in Table A.5.

Table A.5 — Material Properties of NEFMAC (Glass)					
GLASS FIBRE					
Bar No.	Area [mm²]	Max. Tensile Load [kN]	Tensile Strength [MPa]	Modulus of Elasticity [GPa]	Mass [g/m]
G2	4.4	2.6			7.5
G3	8.7	5.2			15
G4	13.1	7.8			22
G6	35.0	21	600	30	60
G10	78.7	47			130
G13	131.0	78			220
G16	201.0	120			342
G19	297.0	177			510

A.2.2 Carbon Fibre-Reinforced Polymer Products

LEADLINE™ - LEADLINE™ is made by Mitsubishi Corporation of Japan. Examples of the product are shown in Figure A.2. The manufacturer provided the following mechanical properties of their product, as shown in Tables A.6 and A.7.

Figure A.2: LEADLINE™ products.

Table A.6 — Geometric/Mechanical Properties of LEADLINE™				
Diameter [mm]	Area [mm²]	Tensile Strength [MPa]	Modulus of Elasticity [GPa]	Mass [g/m]
ROUND				
5	19.6	2245	147	32
8	49.0	2265	147	80
12	113.1	2255	147	184
INDENTED SPIRAL				
5	17.8	2247	147	30
8	46.1	2255	147	77
12	108.6	2255	147	177
INDENTED CONCENTRIC				
5	18.1	2265	147	30
8	46.5	2258	147	76
12	109.3	2250	147	178

TABLE A.7 — PHYSICAL PROPERTIES OF LEADLINE™	
Diameter [mm]	8
Matrix	Epoxy resin
Fibre-volume fraction	65
Tensile strength	2550
Modulus of elasticity	147
Elongation [%]	1.8
Unit weight [g/m]	77
Specific gravity	1.6
Relaxation ratio (at 20ºC)	2-3
Thermal expansion	0.7×10^{-6} / ºC

V-ROD Carbon-Vinyl Ester Reinforcing Bar - The manufacturer provided the following mechanical properties of their product, as shown in Table A.8.

Table A.8 — Geometric Properties of V-ROD – Carbon – Vinyl Ester Reinforcing Bars							
Bar Designation		Area		Diameter		Mass	Weight
SI	US Customary	[mm^2]	[in.^{2}]	[mm]	[in.]	[kg/m]	[lbs/ft]
#10	#3	71	0.11	9.3	0.366	0.142	0.100
#13	#4	129	0.20	12.3	0.484	0.266	0.179
#16	#5	198	0.31	15.9	0.625	0.415	0.279

NEFMAC Carbon Reinforcing Grid - The manufacturer provided the following mechanical properties of their product, as shown in Table A.9.

Table A.9 — Material Properties of NEFMAC (Carbon)					
CARBON FIBRE					
Bar No.	Area [mm^2]	Maximum Tensile Load [kN]	Tensile Strength [MPa]	Modulus of Elasticity [GPa]	Mass [g/m]
C6	17.5	21			25
C10	39.2	47			56
C13	65.0	78	1200	100	92
C16	100.0	120			142
C19	148.0	177			210
C22	195.0	234			277

A.2.3   Aramid Fibre-Reinforced Polymer Products

NEFMAC Aramid Reinforcing Grid - The manufacturer provided the following mechanical properties of their product, as shown in Table A.10.

Table A.10 — Material Properties of NEFMAC (Aramid)					
ARAMID FIBRES					
Bar No.	Area [mm^2]	Max. Tensile Load [kN]	Tensile Strength [MPa]	Modulus of Elasticity [GPa]	Mass [g/m]
A6	16.2	21			21
A10	36.2	47			46
A13	60.0	78	1300	54	77
A16	92.3	120			118
A19	136.0	177			174

B DESIGN TABLES

B.1 Design Tables

$\varepsilon_c/\varepsilon_0$	$f'_c=20$ MPa			$f'_c=25$ MPa			$f'_c=30$ MPa		
	α	β	$\alpha\beta$	α	β	$\alpha\beta$	α	β	$\alpha\beta$
0.1	0.184	0.602	0.111	0.163	0.600	0.098	0.150	0.600	0.090
0.2	0.325	0.639	0.208	0.293	0.636	0.186	0.271	0.634	0.172
0.3	0.455	0.657	0.299	0.418	0.650	0.272	0.390	0.647	0.252
0.4	0.569	0.672	0.382	0.533	0.661	0.353	0.503	0.656	0.330
0.5	0.666	0.686	0.457	0.636	0.672	0.428	0.609	0.664	0.404
0.6	0.746	0.700	0.522	0.724	0.684	0.495	0.702	0.674	0.473
0.7	0.810	0.714	0.578	0.796	0.697	0.555	0.781	0.685	0.535
0.8	0.860	0.728	0.626	0.853	0.711	0.606	0.844	0.698	0.589
0.9	0.897	0.743	0.666	0.894	0.726	0.649	0.890	0.713	0.635
1.0	0.923	0.757	0.699	0.923	0.742	0.685	0.921	0.729	0.671
1.1	0.941	0.772	0.726	0.940	0.758	0.713	0.938	0.747	0.700
1.2	0.952	0.786	0.748	0.948	0.775	0.734	0.942	0.766	0.722
1.3	0.958	0.800	0.766	0.949	0.791	0.751	0.938	0.785	0.736
1.4	0.959	0.813	0.780	0.943	0.808	0.762	0.926	0.805	0.745
1.5	0.956	0.827	0.791	0.934	0.825	0.770	0.909	0.825	0.750
1.6	0.951	0.840	0.798	0.921	0.841	0.774	0.887	0.846	0.750
1.7	0.944	0.852	0.804	0.905	0.857	0.776	0.864	0.866	0.748
1.8	0.935	0.864	0.807	0.888	0.873	0.775	0.839	0.885	0.743
1.9	0.924	0.876	0.809	0.870	0.888	0.773	0.813	0.905	0.736
2.0	0.913	0.887	0.810	0.851	0.903	0.769	0.787	0.924	0.727

Table B.1 — Stress-Block Factors for 20 to 30 MPa Concrete

$\varepsilon_c/\varepsilon_0$	Table B.2 - Stress-Block Factors for 35 to 45 MPa Concrete								
	$f'_c = 35$ MPa			$f'_c = 40$ MPa			$f'_c = 45$ MPa		
	α	β	$\alpha\beta$	α	β	$\alpha\beta$	α	β	$\alpha\beta$
0.1	0.141	0.600	0.085	0.134	0.600	0.080	0.129	0.600	0.077
0.2	0.255	0.634	0.161	0.243	0.633	0.154	0.23	0.633	0.148
0.3	0.368	0.645	0.238	0.352	0.645	0.227	0.339	0.645	0.218
0.4	0.479	0.653	0.313	0.459	0.651	0.299	0.443	0.651	0.288
0.5	0.584	0.660	0.385	0.564	0.657	0.370	0.546	0.655	0.358
0.6	0.681	0.667	0.454	0.662	0.663	0.438	0.644	0.660	0.425
0.7	0.765	0.676	0.518	0.750	0.670	0.503	0.735	0.666	0.489
0.8	0.834	0.688	0.574	0.823	0.680	0.560	0.812	0.675	0.548
0.9	0.885	0.702	0.621	0.879	0.694	0.610	0.872	0.687	0.599
1.0	0.918	0.719	0.660	0.915	0.710	0.650	0.911	0.703	0.641
1.1	0.934	0.738	0.689	0.931	0.730	0.679	0.926	0.724	0.671
1.2	0.936	0.759	0.710	0.929	0.753	0.699	0.920	0.749	0.689
1.3	0.926	0.781	0.723	0.912	0.778	0.710	0.898	0.777	0.697
1.4	0.907	0.804	0.729	0.885	0.805	0.713	0.863	0.808	0.697
1.5	0.881	0.828	0.730	0.852	0.833	0.710	0.821	0.840	0.690
1.6	0.852	0.853	0.726	0.814	0.862	0.702	0.776	0.874	0.678
1.7	0.820	0.877	0.719	0.775	0.891	0.691	0.730	0.907	0.662
1.8	0.788	0.901	0.710	0.736	0.920	0.677	0.686	0.940	0.645
1.9	0.755	0.925	0.699	0.698	0.948	0.662	0.643	0.973	0.626
2.0	0.723	0.948	0.686	0.662	0.976	0.646	0.604	1.005	0.607

Table B.3 - Stress-Block Factors for 50 to 60 MPa Concrete								
$\varepsilon_c/\varepsilon_0$	$f'_c = 50$ MPa			$f'_c = 55$ MPa			$f'_c = 60$ MPa		
	α	β	$\alpha\beta$	α	β	$\alpha\beta$	α	β	$\alpha\beta$
0.1	0.125	0.600	0.075	0.122	0.600	0.073	0.119	0.600	0.071
0.2	0.226	0.633	0.143	0.220	0.633	0.141	0.216	0.633	0.136
0.3	0.328	0.644	0.211	0.320	0.644	0.206	0.313	0.644	0.202
0.4	0.430	0.650	0.280	0.419	0.650	0.272	0.410	0.650	0.266
0.5	0.531	0.654	0.347	0.518	0.654	0.339	0.507	0.654	0.331
0.6	0.629	0.658	0.414	0.615	0.657	0.404	0.603	0.656	0.396
0.7	0.721	0.663	0.478	0.708	0.661	0.468	0.696	0.660	0.459
0.8	0.802	0.670	0.537	0.791	0.667	0.528	0.781	0.665	0.519
0.9	0.866	0.682	0.590	0.859	0.677	0.581	0.852	0.674	0.574
1.0	0.907	0.697	0.632	0.902	0.693	0.625	0.898	0.688	0.618
1.1	0.921	0.719	0.662	0.917	0.715	0.655	0.912	0.711	0.648
1.2	0.912	0.746	0.680	0.902	0.744	0.671	0.892	0.742	0.662
1.3	0.882	0.777	0.685	0.865	0.779	0.673	0.847	0.781	0.662
1.4	0.839	0.812	0.681	0.813	0.818	0.665	0.788	0.825	0.650
1.5	0.789	0.849	0.670	0.756	0.860	0.650	0.723	0.871	0.630
1.6	0.737	0.887	0.654	0.698	0.902	0.630	0.661	0.918	0.607
1.7	0.686	0.925	0.634	0.643	0.945	0.608	0.603	0.965	0.582
1.8	0.637	0.963	0.614	0.593	0.986	0.584	0.552	1.009	0.557
1.9	0.593	0.999	0.592	0.547	1.026	0.561	0.507	1.052	0.533
2.0	0.552	1.035	0.571	0.506	1.064	0.539	0.467	1.092	0.510

Table B.4 – Coefficient K for Calculation of Cracked Moment of Inertia of Rectangular Section $I_{cr} = K \times bd^3$						
	n					
ρ	1	1.5	2	2.5	3	3.5
0.0001	0.0001	0.0001	0.0002	0.0002	0.0003	0.0003
0.0005	0.0005	0.0007	0.0009	0.0012	0.0014	0.0016
0.0010	0.0009	0.0014	0.0018	0.0023	0.0027	0.0031
0.0020	0.0018	0.0027	0.0036	0.0044	0.0052	0.0060
0.0030	0.0027	0.0040	0.0052	0.0064	0.0075	0.0087
0.0040	0.0036	0.0052	0.0068	0.0083	0.0098	0.0112
0.0050	0.0044	0.0064	0.0083	0.0102	0.0119	0.0137
0.0060	0.0052	0.0075	0.0098	0.0119	0.0140	0.0161
0.0070	0.0060	0.0087	0.0112	0.0137	0.0161	0.0183
0.0080	0.0068	0.0098	0.0127	0.0154	0.0180	0.0206
0.0090	0.0075	0.0109	0.0140	0.0170	0.0199	0.0227
0.0100	0.0083	0.0119	0.0154	0.0187	0.0218	0.0248
0.0110	0.0090	0.0130	0.0167	0.0202	0.0236	0.0268
0.0120	0.0098	0.0140	0.0180	0.0218	0.0254	0.0288
0.0130	0.0105	0.0151	0.0193	0.0233	0.0271	0.0308
0.0140	0.0112	0.0161	0.0206	0.0248	0.0288	0.0327
0.0150	0.0119	0.0170	0.0218	0.0263	0.0305	0.0345
0.0160	0.0127	0.0180	0.0230	0.0277	0.0321	0.0363
0.0170	0.0133	0.0190	0.0242	0.0291	0.0337	0.0381
0.0180	0.0140	0.0199	0.0254	0.0305	0.0353	0.0399
0.0190	0.0147	0.0209	0.0266	0.0319	0.0369	0.0416
0.0200	0.0154	0.0218	0.0277	0.0332	0.0384	0.0433
0.0210	0.0161	0.0227	0.0288	0.0345	0.0399	0.0449
0.0220	0.0167	0.0236	0.0299	0.0358	0.0413	0.0465
0.0230	0.0174	0.0245	0.0310	0.0371	0.0428	0.0481
0.0240	0.0180	0.0254	0.0321	0.0384	0.0442	0.0497
0.0250	0.0187	0.0263	0.0332	0.0396	0.0456	0.0512
0.0260	0.0193	0.0271	0.0343	0.0408	0.0470	0.0527
0.0270	0.0199	0.0280	0.0353	0.0421	0.0483	0.0542
0.0280	0.0206	0.0288	0.0363	0.0433	0.0497	0.0557
0.0290	0.0212	0.0297	0.0374	0.0444	0.0510	0.0571
0.0300	0.0218	0.0305	0.0384	0.0456	0.0523	0.0585
0.0310	0.0224	0.0313	0.0394	0.0468	0.0536	0.0599
0.0320	0.0230	0.0321	0.0404	0.0479	0.0548	0.0613
0.0330	0.0236	0.0329	0.0413	0.0490	0.0561	0.0627
0.0340	0.0242	0.0337	0.0423	0.0501	0.0573	0.0640
0.0350	0.0248	0.0345	0.0433	0.0512	0.0585	0.0654
0.0360	0.0254	0.0353	0.0442	0.0523	0.0597	0.0667
0.0370	0.0260	0.0361	0.0451	0.0534	0.0609	0.0679
0.0380	0.0266	0.0369	0.0461	0.0544	0.0621	0.0692
0.0390	0.0271	0.0376	0.0470	0.0555	0.0633	0.0705
0.0400	0.0277	0.0384	0.0479	0.0565	0.0644	0.0717

Table B.4 - Continued						
				n		
ρ	4	4.5	5	5.5	6	6.5
0.0001	0.0004	0.0004	0.0005	0.0005	0.0006	0.0006
0.0005	0.0018	0.0021	0.0023	0.0025	0.0027	0.0029
0.0010	0.0036	0.0040	0.0044	0.0048	0.0052	0.0056
0.0020	0.0068	0.0075	0.0083	0.0090	0.0098	0.0105
0.0030	0.0098	0.0109	0.0119	0.0130	0.0140	0.0151
0.0040	0.0127	0.0140	0.0154	0.0167	0.0180	0.0193
0.0050	0.0154	0.0170	0.0187	0.0202	0.0218	0.0233
0.0060	0.0180	0.0199	0.0218	0.0236	0.0254	0.0271
0.0070	0.0206	0.0227	0.0248	0.0268	0.0288	0.0308
0.0080	0.0230	0.0254	0.0277	0.0299	0.0321	0.0343
0.0090	0.0254	0.0280	0.0305	0.0329	0.0353	0.0376
0.0100	0.0277	0.0305	0.0332	0.0358	0.0384	0.0408
0.0110	0.0299	0.0329	0.0358	0.0386	0.0413	0.0440
0.0120	0.0321	0.0353	0.0384	0.0413	0.0442	0.0470
0.0130	0.0343	0.0376	0.0408	0.0440	0.0470	0.0499
0.0140	0.0363	0.0399	0.0433	0.0465	0.0497	0.0527
0.0150	0.0384	0.0421	0.0456	0.0490	0.0523	0.0555
0.0160	0.0404	0.0442	0.0479	0.0514	0.0548	0.0581
0.0170	0.0423	0.0463	0.0501	0.0538	0.0573	0.0607
0.0180	0.0442	0.0483	0.0523	0.0561	0.0597	0.0633
0.0190	0.0461	0.0503	0.0544	0.0583	0.0621	0.0657
0.0200	0.0479	0.0523	0.0565	0.0605	0.0644	0.0681
0.0210	0.0497	0.0542	0.0585	0.0627	0.0667	0.0705
0.0220	0.0514	0.0561	0.0605	0.0648	0.0689	0.0728
0.0230	0.0532	0.0579	0.0625	0.0668	0.0710	0.0750
0.0240	0.0548	0.0597	0.0644	0.0689	0.0731	0.0772
0.0250	0.0565	0.0615	0.0663	0.0708	0.0752	0.0793
0.0260	0.0581	0.0633	0.0681	0.0728	0.0772	0.0814
0.0270	0.0597	0.0650	0.0699	0.0746	0.0791	0.0834
0.0280	0.0613	0.0667	0.0717	0.0765	0.0811	0.0854
0.0290	0.0629	0.0683	0.0734	0.0783	0.0830	0.0874
0.0300	0.0644	0.0699	0.0752	0.0801	0.0848	0.0893
0.0310	0.0659	0.0715	0.0768	0.0819	0.0866	0.0912
0.0320	0.0674	0.0731	0.0785	0.0836	0.0884	0.0930
0.0330	0.0689	0.0746	0.0801	0.0853	0.0902	0.0948
0.0340	0.0703	0.0762	0.0817	0.0869	0.0919	0.0966
0.0350	0.0717	0.0777	0.0833	0.0886	0.0936	0.0984
0.0360	0.0731	0.0791	0.0848	0.0902	0.0953	0.1001
0.0370	0.0745	0.0806	0.0863	0.0918	0.0969	0.1018
0.0380	0.0758	0.0820	0.0878	0.0933	0.0985	0.1034
0.0390	0.0772	0.0834	0.0893	0.0948	0.1001	0.1050
0.0400	0.0785	0.0848	0.0908	0.0964	0.1016	0.1066

C

ISIS Canada Analysis Software for FRP-Reinforced Concrete

Dr. Gamil Tadros has developed software to conduct the flexural analysis of FRP-reinforced concrete sections based on the theory and formulas presented in this manual. The program is available for free download from the ISIS Canada website (www.isiscanada.com). An executable file and a PowerPoint demonstration of the use of the program are provided.

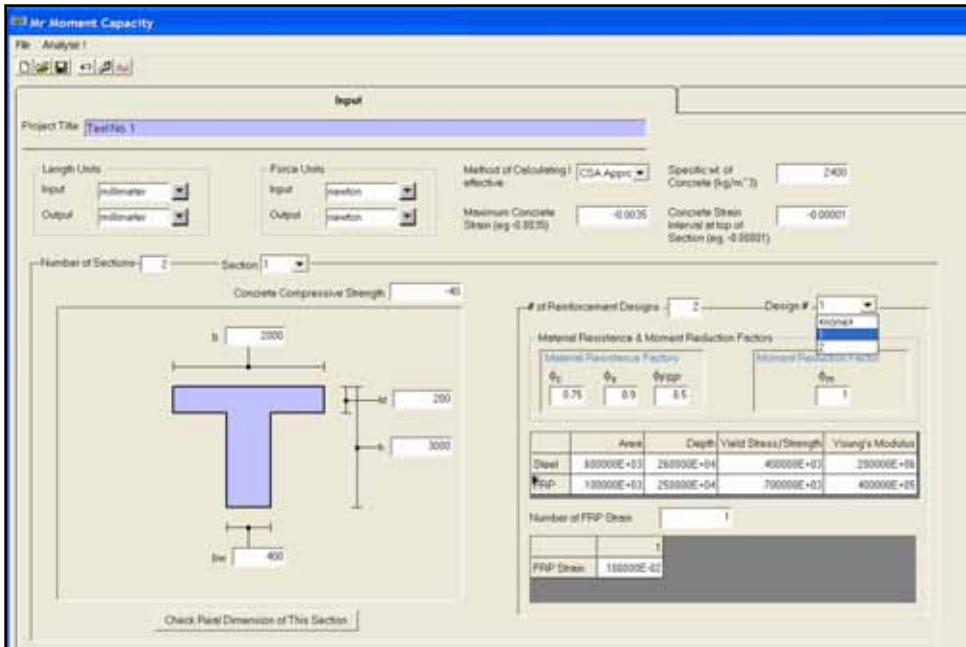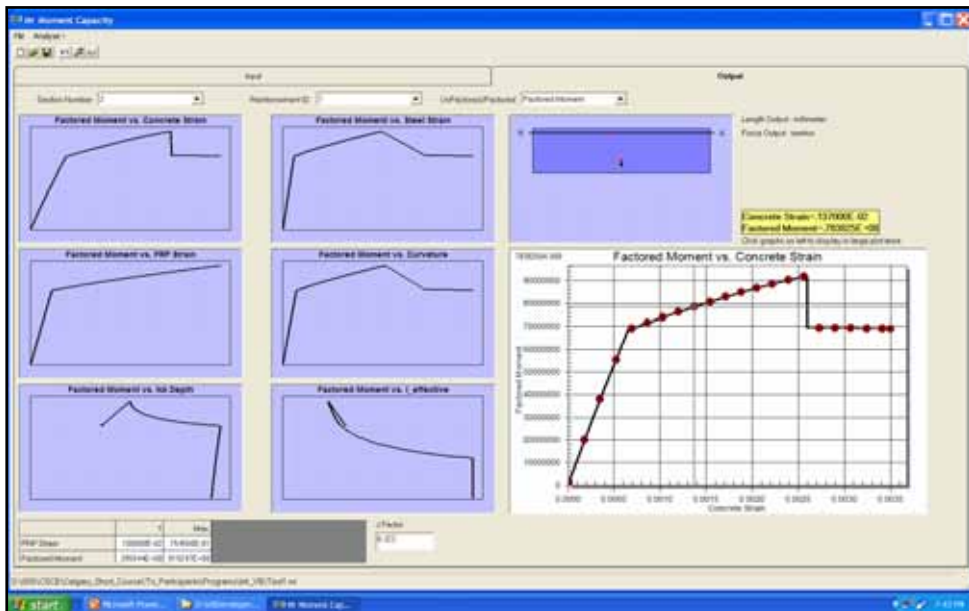Sample input and output pages are shown below.

Figure C.1: Representative Input Page.

Figure C.2: Representative Output Page.